DISSERTATION

Titel der Dissertation

Characterization of a Knockout of the Non-coding Y RNA in the Nematode *Caenorhabditis elegans*

angestrebter akademischer Grad

Doktor der Naturwissenschaften (Dr. rer.nat.)

Verfasser:	Mag. Michael Matthias Müller
Matrikel-Nummer:	a9601604
Dissertationsgebiet (lt. Studienblatt):	091 441 Genetik – Mikrobiologie (Stzw)
Betreuer:	ao.Univ.-Prof. Dr. Günter Steiner
	ao.Univ.-Prof. Dr.Michael Jantsch

Wien, im April 2009

1 Introduction

1.1 Ro RNPs

Ro ribonucleoprotein complexes (RNPs) are small mainly cytoplasmic structures, which are assumed to be present in all animal cells and some eubacteria, but have not been found in archaea or yeasts. The core structure of Ro RNPs is composed of one molecule of Y RNA to which the 60kDa Ro protein (Ro60) is stably bound. In a large fraction of Ro RNPs also the La protein is present. Ro RNPs are present at a number of 10^5 copies in human cells or about 1/100 of the abundance of ribosomes (Hendrick et al. 1981). Y RNAs are RNA polymerase III (pol III) transcripts, about 100 nucleotides on average in size, and the number of Y RNA family members varies from one in *C. elegans* and two in mice to four in *Xenopus laevis* and humans (Kato et al. 1982; Wolin and Steitz 1983; Wolin and Steitz 1984; O'Brien et al. 1993; Van Horn et al. 1995). While Ro60 and Y RNAs are present in equal amounts in the cell, La is about fifty times more abundant and it has been shown to bind nearly all nascent RNA pol III transcripts independently of Ro RNPs (reviewed in Wolin and Cedervall 2002). In contrast to other RNA pol III transcripts, Y RNAs have been found to keep their 3'-oligo-Uridine tail also in their mature forms (Mamula et al. 1989b; Boire and Craft 1990). The 3' oligo-(U) tail was identified as the binding site for the La protein and accordingly the majority of Ro RNPs contain La in addition to Ro60. Ro RNPs are mainly found in the cytoplasm, and there is some evidence that most nuclear Y RNAs are not bound to Ro60 and possibly Ro RNPs are only assembled before being exported to the cytoplasm (Simons et al. 1994; Simons et al. 1996a; Pruijn et al. 1997). Functions that have been suggested for Ro RNPs include UV damage response (Chen et al. 2000; Chen et al. 2003; Xue et al. 2003), regulation of ribosomal protein mRNA translation (Pellizzoni et al. 1998), ribosomal RNA (rRNA) processing (Chen et al. 2007), and non-coding RNA quality control, as the Ro protein has been shown to bind mutant 5S rRNAs and U2 small nuclear RNAs (snRNAs) (O'Brien and Wolin 1994; Shi et al. 1996; Chen et al. 2003).

1.1.1 The discovery of Ro RNPs

Patients suffering from systemic rheumatic diseases often show autoantibodies against prevalent intracellular antigens, such as dsDNA and ssDNA, histones or centromeres in their sera. Antibody profiles – an analysis of the different kinds of antibodies present in a patient's sera – can be characteristic for specific syndromes, but also facilitate a diagnosis of the severity or stage of the disease and thus may be helpful in determining the appropriate therapy. Remarkably, the majority of antibodies in these patient's sera are directed against some classes of highly conserved DNA-protein or RNA-protein complexes such as nucleosomes or spliceosomes (reviewed in von Muhlen and Tan 1995). Noteworthy, such sera derived antibodies led for instance to the discovery of the Smith (Sm) antigen and U snRNAs. Another class of antibodies that are frequently found in sera of patients suffering from Sjögren's syndrome (SS) or systemic lupus erythematosus (SLE) are targeting the Ro60 protein – otherwise known as Sjögren's autoantigen A (SS-A) – and the La (or SS-B) autoantigen, which are stable components of Ro RNPs (Hendrick et al. 1981; Lerner et al. 1981).

1.1.2 Clinical relevance of Ro RNPs as targets in auto-immune diseases

Antibodies against Ro60/SS-A and La/SS-B are commonly produced by patients suffering from Sjögren's Syndrome (88%-96% SS-A antibodies; 71%-86% SS-B antibodies) or SLE (24%-60% SS-A antibodies; 9-35% SS-B antibodies) and are indicative for those diseases as they only appear with a prevalence of 5% -10% in patient's sera suffering from other systemic autoimmune diseases. In SLE patients Ro60 antibodies are an indication for subacute cutaneous lupus leading to photosensitive lesions, where these antibodies appear in 70% - 90% of cases; complement deficiency syndromes (90% of cases) and neonatal lupus (>90% of cases); La antibodies are prevalent in sera of neonatal lupus patients where they appear in 75% of cases. The risk of a child being born with neonatal lupus is higher, if the mother's serum has both antibodies to Ro60 and La.

In Sjögren's Syndrome the appearance of Ro60 and La autoantibodies is associated with symptoms such as purpura (skin discolorations), elevated levels of gamma globulin, salivary gland dysfunction, swelling of the parotid glands, reduced levels of lymphocytes and leukocytes and the presence of rheumatoid factor. In Sjögren's

syndrome patients the immune reaction against Ro60 and against La, respectively, seems to be strongly linked, since both antibodies frequently co-occur in the same serum, while in sera of SLE patients Ro60 antibodies are often present alone (reviewed in von Muhlen and Tan 1995; Stinton and Fritzler 2007).

1.1.3   Components of human Ro RNPs

Ribonucleoprotein complexes containing the Ro60 protein and one of the four human Y RNAs (hY1, hY3, hY4 or hY5) were termed Ro RNPs and it could be shown that most Ro RNPs contain the La protein as well. Binding to Ro RNPs *in vitro* was previously also suggested for the autoantigen Ro52 (Ben-Chetrit et al. 1988), but Ro52 binding was either found to be a Ro60/Ro52 protein-protein interaction (Slobbe et al. 1992) or could not be verified at all (Boire et al. 1995) or may occur only marginally in a small subset of Ro RNPs (Fabini et al. 2000). Accordingly it has remained controversial, if Ro52 is indeed a part of Ro RNPs. Other proteins that were found to bind Ro RNPs *in vitro* are Calreticulin, a calcium-binding molecular chaperone (McCauliffe et al. 1990) and pp75/rip11/gaf-1 (Wang et al. 1999), which is associated with endosomal vesicular trafficking and recycling and was also shown to be involved with insulin-stimulated glucose uptake (Kamath et al. 2003; Welsh et al. 2007). But data concerning Ro RNP interaction with these candidates and their relevance for the *in vivo* situation remain controversial, as clear evidence is missing. For binding of additional proteins such as RoBPI/Puf60/FIR (Bouffard et al. 2000), hnRNP I/PTB, hnRNP K (Fabini et al. 2001) and Nucleolin (Fouraux et al. 2002) more supporting data is available. Some of these interactions have been established *in vivo* and/or binding sites on the Y RNA have been mapped. Using tagged Y RNAs, ribosomal protein L5 was recently shown to interact with hY5 RNPs *in vivo* (Hogg and Collins 2007).

1.1.3.1 SS-B/La

The SS-B/La autoantigen, an abundant mainly nuclear phosphorprotein, acts in 3'-end protection, chaperoning and possibly unwinding from their DNA template of nascent RNA pol III (and some other) small, non-coding transcripts such as Y RNA, pre-5S rRNA, pre-tRNA, snRNA, RNAse P and RNAse MRP. La binds the precursor

rather than the mature RNA as an important binding site for the La protein is the oligo-Uridine stretch at the 3'-end of most newly synthesized RNA pol III transcripts. This 3' oligo-(U) is usually removed in the process of RNA maturation, which leads to dissociation of the La protein (Stefano 1984; reviewed in Wolin and Cedervall 2002). Mature human Y RNAs however are not processed at their 3' end and thus retain their oligo-(U) stretch and the La binding site (Mamula et al. 1989b; Boire and Craft 1990). Binding of La to Y RNAs was found to be responsible for nuclear retention of Y RNAs and accordingly it was proposed that dissociation of La is necessary for export and assembly of cytoplasmic Ro RNPs (Simons et al. 1994; Simons et al. 1996b; Grimm et al. 1997). However, La was also found in cytoplasmic Ro RNPs (Fabini et al. 2000).

La contains a phosphorylation site at the serine residue 366 and while the bulk of La is located in its phosphorylated form in the nucleus to bind nascent non-coding transcripts, non-phosphorylated La was found in the cytoplasm and in nucleoli (Intine et al. 2003; Intine et al. 2004). In the cytoplasm non-phosphorylated La was shown to play a role in the translation of some viral RNAs and was also found associated with the small ribosomal subunit (Meerovitch et al. 1993; Svitkin et al. 1994; Peek et al. 1996). La might additionally regulate the translation of mRNAs encoding proteins that are involved in the translational machinery – most notably ribosomal protein mRNAs – which contain a 5' terminal oligopyrimidine (TOP) sequence (Pellizzoni et al. 1996; Pellizzoni et al. 1998; Crosio et al. 2000; Cardinali et al. 2003). Another involvement with ribosome biogenesis was suggested for non-phosphorylated La, a fraction of which resides in nucleoli and was shown to co-localize with nascent RNA polymerase I transcripts, such as the 35S pre-rRNA, and with nucleolar proteins nucleolin and fibrillarin, which bind pre-rRNAs, during early rRNA maturation (Intine et al. 2004).

1.1.3.2 RoBPI/Puf60/FIR

Association of the evolutionarily conserved Ro RNP-binding protein (RoBPI) to Ro RNPs was demonstrated in a yeast-three-hybrid screen and RoBPI was shown to associate with hY5 Ro RNPs but not with Ro RNPs containing other Y RNA species (Bouffard et al. 1999; Bouffard et al. 2000). However in a different study, employing tagged Y RNAs, binding of RoBPI to hY1 and hY3 was also found, while strongest binding to hY5 RNAs was confirmed *in vivo* (Hogg and Collins 2007). RoBPI was

characterized as a polypyrimidine binding splicing factor under its alternative name 60kDa poly-U binding splicing factor (PUF60) and was demonstrated to assist U2 snRNP in binding pre-mRNA (Page-McCaw et al. 1999). In further studies PUF60 was shown to promote weak 3'-splice site intron splicing (Hastings et al. 2007). Under the alias FarUpStream Element Binding Protein Interactor (FIR) RoBPI was shown to be essential for c-myc expression control (Liu et al. 2006).

1.1.3.3 hnRNP I/PTB

Heterogeneous nuclear ribonucleoprotein I (hnRNP I) otherwise known as polypyrimidine-tract binding protein (PTB) was identified as a hY1 RNA and hY3 RNA interactor *in vivo* and *in vitro* and was shown to bind a minor Ro RNP subfraction of about 10-20% (Fabini et al. 2000; Fabini et al. 2001). The presence of an intact La binding site is important for hnRNP I binding, which raised speculations that La might be responsible for correct Y RNA folding, as a requirement for hnRNP I binding. The internal oligopyrimidine tract of hY1 RNA and hY3 RNA – a feature shared with the *C. elegans* Y RNA – was identified as the hnRNP I binding site. Interestingly, hnRNP I localizes to the perinucleolar compartments (Ghetti et al. 1992) as it was also shown for human Y RNAs 1, 3 and 5 (Matera et al. 1995). hnRNP I was characterized as an RNA binding shuttling protein required in RNA processing and export, but it also seems to act in mRNA translation and stability (Pinol-Roma and Dreyfuss 1992; Bomsztyk et al. 1997; Kim et al. 2000). Interestingly PTB has been found to play a role in the stabilization and glucose-induced increase of preproinsulin mRNA (Tillmar and Welsh 2002).

1.1.3.4 hnRNP K

Heterogeneous nuclear ribonucleoprotein K (hnRNP K) was found in the same study as hnRNP I to interact with hY1 RNA and hY3 RNA, yet evidence was only provided *in vitro*. As with hnRNP I the internal oligopyrimidine tract was shown to be essential for binding. An unmutated La binding site seems to play a role as well (Fabini et al. 2000; Fabini et al. 2001). hnRNP K has been connected to chromatin remodeling (Ostrowski et al. 2003), RNA splicing (Expert-Bezancon et al. 2002) and nuclear-cytoplasmic shuttling (Michael et al. 1997).

1.1.3.5 Nucleolin

Nucleolin is a nucleo-cytoplasmic shuttling protein that interacts with ribosomal proteins and was suggested to be involved in their transport from the cytoplasm to the nucleolus (Borer et al. 1989; Bouvet et al. 1998). Additionally it was associated with rRNA processing, ribosome maturation, internal ribosome entry site translation and histone chaperoning especially in RNA polymerase I transcription (Erard et al. 1988; Ginisty et al. 1998; Izumi et al. 2001; Angelov et al. 2006; Rickards et al. 2007). Nucleolin was found to associate with a subset of Ro RNPs in a large scale immunoprecipitation (IP) using monoclonal anti-Ro60 and anti-La antibodies. It was shown to bind hY1 RNA and hY3 RNA, but not hY4 RNA or hY5 RNA containing Ro RNPs. As the co-IP occurred in an RNA dependent manner, the Y RNA was assumed as binding partner for nucleolin I*n vitro* experiments showed the single stranded oligopyrimidine tract in the loop of hY1 RNA to be required for binding of nucleolin. Nucleolin is able to bind hY1 RNA simultaneously with hnRNP I but not hnRNP K *in vitro.* As Y RNAs as well as hnRNP I were found in perinucleolar compartments, binding of nucleolin was suggested to provide a signal for further transport of newly transcribed Y RNAs to either the nucleolus or the nuclear envelope and - subsequent to Ro60 binding -further to the cytoplasm (Fouraux et al. 2002).

1.1.3.6 L5

Using affinity purification of tagged hY RNAs *in vivo* a recent study proposed binding of large ribosomal subunit protein L5 to hY5 RNAs (Hogg and Collins 2007). L5 protein was previously identified as a 5S rRNA binding protein and involvement in 5S rRNA stabilization, transport to the nucleolus and incorporation into the ribosome was shown. L5 was found to bind the majority of non-ribosome bound 5S rRNA in the cell. Processing at the 3'-end of L5 bound 5S rRNAs indicates that this association occurs after 5S rRNA has been released from the La protein (Steitz et al. 1988) L5-hY5 RNA complexes were shown to bind co-expressed mutant 5S rRNAs with a higher affinity than endogenously expressed native 5S rRNAs in these experiments. The internal loop of hY5 RNA was shown to be essential for co-purification of 5S rRNAs. Accordingly a suggested 5S rRNA quality control function of Ro60 (O'Brien and Wolin 1994; Shi et al. 1996) was proposed to take place in the context of Ro RNPs by interaction of hY5 RNA and L5 protein (Hogg and Collins 2007). These results remain

controversial as they disagree with a previous model, which suggested Ro60 to act on its own in RNA quality control, after the release from Y RNA (Stein et al. 2005; Fuchs et al. 2006).

1.1.4   Ro RNP localization

The localization of mammalian Ro RNPs has been studied extensively and while many of the early studies found Ro RNPs in differing locations, such as the nucleus (Harmon et al. 1984; Lopez-Robles et al. 1986; Xia et al. 1987; Mamula et al. 1989a), the cytoplasm (Alspaugh et al. 1978; Hendrick et al. 1981) or in both nucleus and cytoplasm (Ben-Chetrit et al. 1988; Slobbe et al. 1992), it is commonly believed today that most Ro RNPs are mainly cytoplasmic, while there is evidence that uncomplexed Ro60 may reside in the nucleus. (O'Brien et al. 1993; Peek et al. 1993; Simons et al. 1994) There is, however, the notable exception of hY5 containing Ro RNPs, which were also detected in the nucleus (Gendron et al. 2001). Mouse Ro60 as well as mY3 RNA were shown to accumulate in the nucleus after UV irradiation (Chen et al. 2003) and the same was demonstrated for human Ro60 in human tissue culture cells after UV treatment as well as after exposure to oxidizing reagents (Sim et al. 2009).

HY1 RNA injected into *Xenopus laevis* oocyte nuclei requires the native Ro60 binding site for its export to the cytoplasm, while La binding is not necessary and rather promotes nuclear retention (Simons et al. 1996b). Thus it is believed that Ro60 and La are translated and actively transported to the nucleus, where Y RNAs are bound to La. Only after the binding of Ro60, as the essential step, Ro RNPs are swiftly exported to the cytoplasm (Simons et al. 1994). As an alternative model, it was suggested, that binding of La upholds retention of hY1 RNAs in the nucleus and only after release or modification of the La protein and after Ro60 binding, translocation to the cytoplasm takes place, a process requiring RanGTP and exportin-5 (Simons et al. 1996b; Rutjes et al. 2001; Gwizdek et al. 2003).

Another study employing fluorescence in situ hybridization (FISH) to analyze the subcellular distribution of hY RNA in HeLa cells a mainly cytoplasmic localization was observed. However a small amount of hY1, hY3 and hY5 but not hY4 RNA anti-sense probes hybridized to structures in the vicinity of nucleoli that were termed perinucleolar compartments (PNC). These structures could be distinguished from

coiled bodies, fibrillar centers and are also not identical with Y RNA or 5S rRNA gene loci. Additionally it was shown that hnRNP I/PTB (Ghetti et al. 1992) and two RNA pol III transcripts co-localize to PNCs: RNAse P – a ribozyme involved in processing the 5' leader sequence of precursor tRNAs – as well as RNAse MRP, an rRNA processing ribozyme (Lygerou et al. 1996; Reiner et al. 2006; reviewed in Altman 2007).

1.2 The Ro60 protein

1.2.1 Ro60 in pro- and eukaryotic systems

Apart from human cells Ro60 orthologues were found or bioinformatically predicted in all other animal genomes analyzed as well as in some unicellular eukaryotes as the green algae *Chlamydomonas reinhardtii*, in several Eubacteria and bacteriophages. To date no Ro RNPs were found in Spermatophytes, yeasts and archaea. In *Deinococcus radiodurans* the Ro60 orthologue RSR has been characterized and also its structure was solved (Chen et al. 2000; Ramesh et al. 2007). Ro60 orthologues were also predicted by bioinformatic analysis in eubacterial phyla including planctomycetes (for instance *Pirellula, Planctomyces*), Enterobacteria (*Salmonella*), Proteobacteria (including *Pseudomonas, Rhizobium* and *Agrobacterium*) Actinobacteria (*Streptomyces*) and Cyanobacteria (*Nostoc punctiforme*) and in several Mycobacterial phages (for instance *Bxz1*). It is very likely that eubacterial Ro60 orthologues were derived from lateral transfer. A Ro60 orthologue characterized in the nematode *C. elegans* and bioinformatic annotation of the fly and the bee genome also predicted the presence of Ro60 orthologues in insect genomes. Interestingly, a recent report also predicted the finding of a Y RNA related non-coding RNA in *Anopheles gambiae*, while Y RNAs previously had not been identified in insects. Ro60 orthologues were additionally predicted *in silico* in the phylum of chordates from lancets to sea urchins and vertebrates from bony fish to mammals (Chen and Wolin 2004; Perreault et al. 2007).

Biochemical evidence for the presence of Ro RNPs composed from Ro60 protein and Y RNAs is available from species including humans (Lerner et al. 1981), mice (Wolin and Steitz 1983), *Xenopus laevis* (O'Brien et al. 1993), *C. elegans* (Van Horn et al. 1995) *and Deinococcus radiodurans* (Chen et al. 2000)*.*

1.2.2 The structure of Ro60 and binding to RNA

Even before the publication of the *Xenopus laevis* Ro60 crystal structure (Stein et al. 2005) there was evidence that Y RNAs and misfolded non-coding RNAs are competing for Ro60 binding. The binding sites of the Ro60 protein for Y RNAs and for misfolded non-coding RNAs, respectively, are either identical or partially overlapping (Green et al. 1998). The crystal structure (Figure 1, page 26) finally showed that Ro60 contains a C-terminal von Willebrandt factor A domain (vWFA) and an N-terminal HEAT-repeat domain. RNA is exclusively bound by the HEAT-repeat domain which is nearly entirely helical and forms a loop with a central cavity and thus is reminiscent of importin-β. The vWFA domain closes this loop and contains an acidic surface that includes a metal-ion-dependent-adhesion-site (MIDAS) known from integrins, where it is important for ligand binding. The vWFA domain might also interact with RNA quality control proteins. Ro60 is related in its general structure to telomerase associated protein TEP1, which is binding small non-coding vault RNAs similar in size to Y RNAs. A conserved region of the outer surface of the HEAT-repeat domain of Ro60 binds double stranded RNA such as the stem of Y RNAs. Single stranded RNAs such as 3'-extensions of mutant 5S rRNA are bound by the central tunnel of the N-terminal HEAT domain. Mutagenesis assays showed that exclusively the outer surface of the N-terminal HEAT domain is responsible for Y RNA binding, while the outer surface as well as the central cavity are binding mutant 5S rRNAs. Since the binding domains for the Y RNAs and mutant 5S RNAs respectively are overlapping, a negative regulatory role for the Y RNAs in 5S rRNA quality control was suggested (Stein et al. 2005; Fuchs et al. 2006).

The general structure of the *Deinococcus radiodurans* Ro60 orthologue RSR is very similar to *Xenopus laevis* Ro60. Interestingly, multimers of about 12 molecules of RSR/Y RNA are formed *in vitro*, which are independent of metal ions at the vWFA domain. Similar multimers have not been observed with Ro RNP of other organisms (Ramesh et al. 2007).

1.2.3 Functions of the Ro60 protein

Two major functions have been suggested for the Ro60 protein: Quality control of small non-coding RNAs (O'Brien and Wolin 1994; Shi et al. 1996; Chen et al. 2003) and a role in cellular protection after UV irradiation (Chen et al. 2000; Chen et al.

2003; Xue et al. 2003). It has been suggested that these two functions may actually be connected (Chen et al. 2003). For both functions Ro60 was proposed to act alone after the release from Y RNA (Green et al. 1998; Chen et al. 2003). For the role of Ro60 in the protection from effects of UV irradiation this hypothesis is mainly based on data, showing that Ro60 translocates to the nucleus in absence of Y RNA as well as after cell stress. These results indicate a regulatory role for Y RNA on the subcellular distribution of Ro60 (Sim et al. 2009). Ro60 is believed to act in non-coding RNA quality control as free protein since the protein's crystal structure showed a partial overlap of the binding site for Y RNAs and the one for misfolded RNAs (Stein et al. 2005). Thus a role for the Y RNA in regulating access for other RNAs to Ro60 was proposed (Fuchs et al. 2006). However, a recent study using tagged hY5 RNAs indicated that intact Ro RNPs interact with misfolded 5S rRNAs (Hogg and Collins 2007).

Additionally Ro60 has been suggested to play a role in La guided ribosomal protein translation control (Pellizzoni et al. 1997; Pellizzoni et al. 1998) As Ro60 functions in an RNA dependent manner in this ill-defined process, a role of Y RNA was suggested. While quality control and UV-damage response or ribosomal protein translation control may be more general functions of all Ro60 proteins, an additional function was recently reported especially for RSR, the R060 orthologue in *Deinococcus radiodurans*. RSR has been shown to play a role in large subunit 23S rRNA processing of *Deinococcus radiodurans* (Chen et al. 2007). But it is not known, if Ro60 orthologues other than RSR might fulfill a similar function.

Remarkably, the *C. elegans* Ro60 orthologue ROP-1 was shown to play a role in the nematode specific process of the formation of stress-resistant non-breeding *dauer* larvae (Labbe et al. 2000), which will be discussed in a later chapter.

1.2.3.1 Ro60 and its role in non-coding RNA quality control

Studies of Ro RNPs in *Xenopus laevis* revealed that the Ro60 orthologue in this organism is not exclusively complexed to one of the four *Xenopus laevis* Y RNAs (xYα, xY3, xY4, xY5), but that it also binds mutant 5S rRNA precursor (O'Brien and Wolin 1994). These molecules feature about 8 additional nucleotides at the 3'-end, which is caused by a failure of RNA pol III to halt at the first transcription termination

signal. These elongated 5S rRNA precursors (5S+ rRNAs) additionally are mutated at one or several positions compared to the canonic 5S rRNA sequence and are believed to fold in an alternative secondary structure. Mutations found *in vivo* in 5S+ rRNA precursors are believed to inhibit correct processing to form mature 5S rRNAs. Artificially modified human 5S rRNAs that had been shaped based on Xenopus 5S+ RNAs were shown to bind Ro60 *in vivo* in human tissue culture cells (Hogg and Collins 2007). The latter observation was, however, based on the assumption that Y RNAs are not stable in the absence of Ro60, because only the binding of hY5 RNA to ribosomal protein L5 and 5S rRNAs simultaneously was shown, but no direct evidence for Ro60 binding could be obtained.

Elevated levels of mutant 5S rRNAs incorporated in ribosomes were detected in *C. elegans* when the Ro60 orthologue ROP-1 is deficient. This was taken as evidence for a role of ROP-1 in a quality control step for 5S rRNAs (Labbe et al. 1999b).

In cultured mouse embryonic stem (ES) cells Ro60 was shown to bind mutant U2 snRNAs that are believed to be misfolded. Mutant U2 snRNA encoding genes are as abundant in the mouse genome as mutant 5S rRNA genes are in the *Xenopus laevis* genome. Therefore it was speculated that the kind of non-coding RNA bound by Ro60 in a particular species may be determined by the abundance of misfolded copies of this RNA in that species (Chen et al. 2003).

The fate of mutant 5S+ rRNAs in *Xenopus laevis* and *C. elegans* as well as misfolded U2 snRNAs in mice, bound by Ro60, remains unclear: It could involve recruitment of exonucleases and subsequent degradation of the misfolded RNA molecule (Wolin and Wurtmann 2006). On the other hand the function of an RNA chaperone was suggested for the Ro60 protein. (Shi et al. 1996). RNA chaperoning was defined as an activity that either keeps RNAs from settling into a variant secondary structure or the assistance in loosening and re-folding of RNA structures. However, recent data obtained with Ro60 in several RNA chaperoning assays found no activity for Ro60 in cis- and transsplicing assays *in vitro* and only modest chaperoning activity *in vivo*. However, Ro60 was active in an RNA annealing *assay in vitro*. Interestingly, Y RNA binding proteins as La, hnRNP I and hnRNP K showed strong activity in the *in vitro* assays, which could be completely inhibited by the addition of Y RNA. Accordingly, a recruitment of RNA chaperones by Ro60 in non-coding RNA quality control appears

to be more likely than an RNA chaperoning function of Ro60 itself (Belisova et al. 2005; Rajkowitsch et al. 2007).

1.2.3.2 The role of Ro60 in the cellular response to UV radiation

Evidence for the function of Ro60 in facilitating cell survival after UV irradiation first became evident in the multi-radiation resistant eubacterium *Deinococcus radiodurans* and was later confirmed in Ro60$^{-/-}$ mice and thereof derived ES cells. In *Deinococcus radiodurans* deletion of the Ro60 orthologue RSR leads to a significantly reduced resistance to UV irradiation. Notably also an increase of RSR expression in *Deinococcus radiodurans* wild-type cells could be observed after UV treatment and RSR was shown to bind RNAs structurally resembling Y RNA under these conditions. Interestingly, viability of ΔRSR is not divergent from WT after DNA double-strand-break inducing X-ray irradiation (Chen et al. 2000).

Ro60 knockout mice also show a higher sensitivity to UV irradiation. The formation of apoptotic keratinocytes in these RO$^{-/-}$ mice was doubled compared to WT mice after treatment with 1000J/m2 UVB irradiation (Xue et al. 2003). These results were confirmed in Ro60$^{-/-}$ ES cells, which showed a 3- to 8-fold increase of lethality after 10J/m2 UVC irradiation. Also a massive translocation of Ro60 from the cytoplasm to the nucleus occurred after UV irradiation (Chen et al. 2003). This process was suggested to be regulated by Y RNA dissociation and also occurs under oxidative stress (Sim et al. 2009).

The role for Ro60 in RNA quality control might be related to its role in UV stress response. UV irradiation causes pyrimidine dimer formation in DNA but is also known to induce RNA:protein as well as RNA:RNA crosslinking. Newly transcribed RNA that has not yet settled in its default secondary and tertiary structure might be particularly susceptible to UV induced crosslinking. Ro60 might bind these RNAs and would either assist in their refolding or degradation (Chen et al. 2003). An additional function of Ro60 might be the orchestration of cell responses to stress conditions such as UV radiation. In accordance with this model Ro60 was proposed to function as a cellular beacon that senses cell damage through increased binding of misfolded RNAs. This would lead to the induction of responses on the cellular level or even

trigger a developmental adaptation of the whole organism, such as the formation of stress-resistant *dauer* larvae in *C. elegans* (Labbe et al. 2000).

1.2.3.3 RSR plays a role in 23S rRNA processing

A function for the *Deinococcus radiodurans* Ro60 orthologue RSR in large ribosomal subunit 23S rRNA maturation has recently been discovered. There is to date no evidence for a related role for Ro60 proteins in other organisms, which however due to the high conservation of these proteins cannot be excluded. *Deinococcus radiodurans* RSR cooperates with 3' to 5' exonucleases RNase PH and RNase II in the maturation of 23S rRNA at elevated temperatures. During normal growth at 30°C 23S rRNA processing is inefficient, resulting in accumulation of precursors containing 5' and 3' extensions. At 37°C 23S rRNA maturation is dependent on RSR and efficient in wild-type. While in the absence of RSR unprocessed 23S rRNA precursors accumulate. Interestingly, 23S rRNA maturation is efficient at all temperatures if *Deinococcus radiodurans* Y RNA is depleted, indicating an inhibitory role for the Y RNA on RSR function (Chen et al. 2007).

1.2.3.4 A possible link between Ro RNPs and translation of ribosomal proteins

The 5'-untranslated regions (UTRs) of vertebrate ribosomal protein mRNAs feature conserved structural cis-elements that have been associated with translational regulation of these mRNAs – a process involving their redistribution between translationally active polysomes and inactive sub-polysomes. In amphibia and mammals a polypyrimidine tract in the 5'-UTR has been shown to be essential for translational regulation and mRNAs featuring this element are classified as terminal oligo-pyrimidine (TOP) RNAs. Interestingly not only ribosomal protein mRNAs but also mRNAs of other proteins involved in the translational machinery were found to contain the 5'-TOP-element (reviewed in Hamilton et al. 2006). The La protein has been shown to bind the 5'-TOP *in vitro*. Together with the cellular nucleic acid binding protein (CNBP), which binds a region downstream of the 5'-UTR, it was found to be important for translational control of 5'-TOP-mRNAs. Mutations in the 5'-TOP element lead to loss of translational repression and also prevent La from binding *in vitro*. (Pellizzoni et al. 1997). Ro60 has been shown to assist La and CNBP in binding 5'-

UTR of ribosomal protein L4 mRNA. There is evidence that RNA is playing a role in this function and Y RNAs have been suggested as possible candidates. (Pellizzoni et al. 1998).

1.3 Y RNAs

1.3.1 The evolution of Y RNAs

RNAs of the Y family vary in their length from 70 to 115 nucleotides. They are transcribed by RNA pol III and do not seem to contain modified nucleotides. Four Y RNAs were characterized in human cells: hY1, hY3, hY4 and hY5 – while hY2 was shown to be a degradation product of hY1 RNA. In mouse cells two Y RNAs (mY1 and mY2) are present, in *C. elegans* only one but none was found in *Drosophila melanogaster* (reviewed in Chen and Wolin 2004). Varying numbers of Y RNAs were additionally predicted in many other animal genomes (Farris et al. 1999; Teunissen et al. 2000; Mosig et al. 2007; Perreault et al. 2007) and Y RNAs were characterized in the eubacterium *Deinococcus radiodurans* (Chen et al. 2000).

However, not each Y RNA encoded in a genome will be expressed in every tissue: Human erythrocytes are expressing just hY1 and hY4 RNA while in human thrombocytes only hY3 and hY4 RNA were found, while all 4 species were detected in other cell types(Rader et al. 1989; O'Brien and Harley 1990; Itoh and Reichlin 1991). This is of interest as these two blood cell types are anucleate and Ro RNPs containing hY5 have been found in the nucleus whereas other Ro RNPs are mainly cytoplasmic (Gendron et al. 2001).

hY5 RNA was initially detected exclusively in primates and was suggested to be an evolutionary new development derived from retrotransposition (Maraia et al. 1996). However, recent reports predict that Y5 RNAs arose in a common vertebrate ancestor (Mosig et al. 2007; Perreault et al. 2007). An exception is *Xenopus laevis*, where Y RNAs belonging to vertebrate classes Y1, Y4 and Y5 were found and a *Xenopus laevis* specific Yα RNA. In non-vertebrate species a single Y RNA in *C. elegans* was detected, which cannot be classified into one of the vertebrate Y RNA categories (Figure 2, page 26). Recently *in silico* a second Y RNA in *C. elegans* was predicted as well as a Y RNA in *Anopholes gambiae*, which would be the first Y RNA

in insects. Four Y RNAs have been found in *Deinococcus radiodurans*, which also pose a class on their own (Mosig et al. 2007; Perreault et al. 2007).

Interestingly, mutated Y RNAs were shown to be able to retrotranspose via the L1 retrotransposition machinery in *trans*. More than 1,000 Y RNA derived pseudogenes were found in the human genome, while Y RNA pseudogenes in the mouse genome are very rare (Perreault et al. 2005).

1.3.2   The structure of Y RNAs and the relevance for protein binding

The most stable and also conserved structural element of Y RNAs is a double stranded helix, formed by base-pairing of the 5'- and 3'-ends (Figure 2, page 26). This has been established as the binding site of the Ro60 protein. The binding of Ro60 to this conserved helix requires a characteristic bulged cytidine residue in its middle portion in position 8 or 9 (Wolin and Steitz 1984; Stein et al. 2005). Mature vertebrate Y RNAs – unlike other RNA pol III transcripts - preserve their 3' oligo(U) tail, which allows sustained La binding (Mamula et al. 1989b; Boire and Craft 1990). However, La binding to 3' truncated hY RNAs was also observed and it is not entirely clear if La may not be able to weakly bind an internal oligo(U) stretch in the Y RNA loop (Pruijn et al. 1991). Presence of a 3' oligo(U) tail was not demonstrated for the *C. elegans* Y RNA and thus La binding remains questionable in *C. elegans* (Van Horn et al. 1995; Labbe et al. 1999a).

Binding of Y RNA to Ro60 was suggested to regulate Ro60 functions in non-coding RNA quality control and UV damage response. Structural and biochemical studies have indicated that a role of Y RNAs is to control access of other RNAs to Ro60. The crystal structure of *Xenopus laevis* Ro60 showed that the binding site of the Y RNA and the one for misfolded non-coding RNAs are partially overlapping. This makes a model likely in which the Y RNA has to dissociate from Ro60 to allow Ro60 binding to misfolded non-coding RNAs. A recent study also showed that Ro60 translocation from the cytoplasm to the nucleus after UV irradiation or oxidative stress, depends on Y RNA dissociation from Ro60 and therefore a regulatory role of Y RNAs for the cellular localization of Ro60 was proposed (Stein et al. 2005; Fuchs et al. 2006; Sim et al. 2009).

1.3.3 A role for Y RNAs in human chromosomal DNA replication and cancer

Human Y RNAs have been shown to act as essential factors for chromosomal DNA replication in template nuclei from late G1-phase human cells. RNAse A treatment can inhibit establishment of chromosomal DNA replication forks in human cell free systems. This inhibition can be abrogated by addition of hY RNAs. As this is also the case for mutated Y RNAs lacking the bulged-cytidine essential for Ro60 binding, this function of hY RNAs is thought to be independent of Ro60 binding. The results also indicate that hY RNAs play a role in chromosomal DNA replication *in vivo,* as treatment with small interfering RNAs (siRNAs) specific for hY1 RNA significantly inhibited entrance of tissue culture cells into S-Phase (Christov et al. 2006). Consistent with these results a recent report finds all four hY RNAs overexpressed in solid human tumors. Depletion by RNA interference (RNAi) of hY1 and hY3 also led to a significant cytostatic effect in cell lines derived from these tumors (Christov et al. 2008). Another study finds a structural motif, conserved in vertebrate Y RNAs, to be essential for chromosomal DNA replication and shows that the *C. elegans* Y RNA, which does not contain this motif, is not able to reconstitute DNA replication in human cell free systems (Gardiner et al. - in press). Interestingly, however, this motif was detected *in silico* in the novel class of nematode sbRNAs, which are predicted to be more related to human Y RNAs than to the *C. elegans* Y RNA found to be bound by ROP-1 (Deng et al. 2006 and Stadler P.F., personal communication).

1.3.4 Y RNA degradation during apoptosis

In human tissue culture cells immediate, specific degradation of Y RNAs during apoptosis can be observed, which takes place in a nucleolytic manner and can be induced by a variety of stimuli in a large range of cell types. Degradation of Y RNAs seems to be selective, as other non-coding RNAs in the same size range, such as 5S rRNA, 7SL RNA or U snRNAs are not degraded during apoptosis. This process seems to be caspase dependent, as caspase inhibitors are able to repress Y RNA degradation after the induction of apoptosis. Interestingly also the Ro60 protein is not affected during apoptosis, while there is evidence for phosphorylation and even proteolytic cleavage of a subset of La protein (Rutjes et al. 1999).

1.4 Caenorhabditis elegans

The soil-living nematode *Caenorhabditis elegans* was suggested as a genetic model organism (Brenner 1974) for several reasons. The worm is small (~1 mm in size), features a large brood size (up to 300 progeny), but a short life cycle (Figure 3, page 27). *C. elegans* can be grown at temperatures between 14°C and 25°C on agar plates or in liquid culture respectively with E. coli bacteria as food - the higher temperature range leading to an accelerated life cycle. *C. elegans* exists as two sexes: hermaphrodites (XX) that are able to self fertilize and males (X0) that only emerge at a low rate of about 0.2% in natural populations. Males are able to mate with hermaphrodites and thus permit cross-breeding. A complete lineage for each somatic cell of the mature animal (facilitated by determinate spiral cell cleavage in nematodes) as well as the completely sequenced genome (containing about 19.000 genes on five pairs of autosomes and one pair of sex chromosomes) are available in online databases (www.wormatlas.org; www.wormbase.org). A rich pool of characterized mutants and easily applied reverse genetic approaches, such as RNAi by feeding, soaking or injection, make *C. elegans* an attractive model organism in cell biological and genetic research.

1.4.1   The *dauer* diapause in *C. elegans*

In *C. elegans dauer* diapause a non-feeding larval stage, in which the worms are arrested in their development, presents an alternative form of larval stage three (reviewed in Fielenbach and Antebi 2008). Under favorable environments *C. elegans* will reproductively develop from embryo through four larval stages to adult in 90 hours at 20°C (Figure 3, page 27). When worms hatch in an environment without any food, they will arrest at the larval stage 1 (L1), and fail to continue larval development (Baugh and Sternberg 2006) *Dauer* larvae however will form in an unfavorable environment, if the worms are exposed to overcrowded populations with scarce food during early larval development (Cassada and Russell 1975). Prior to the *dauer* larvae formation, worms store carbohydrate and fat. During the molting they undergo a massive remodeling of various tissues. Throughout the *dauer* diapause, aerobic respiration is inhibited in favor of fermentative metabolism and glycolysis while food intake is suppressed. *Dauer* larvae are immobile, but they can move swiftly when stimulated by contact. All orifices are sealed and a thickened cuticle resists

desiccation and protects the animal from oxidative and thermal stress. *Dauer* larvae are able to endure for months under adverse conditions and live by far longer compared to a maximum of 30 days of non-*dauer* worms. After return to favorable conditions, *dauer* larvae quickly recover to post-L3 stages and reproductive adults. Interestingly, time spent as *dauer* larvae does not affect average life span after exit from the *dauer* state.

A pheromone constitutively expressed by the worms leads to *dauer* formation at high concentrations. However, temperature and bacterial food supply also play a role in this developmental decision. Thus, low temperatures and sufficient food, combined with a low pheromone level result in the normal replicative life cycle, which leads to gametogenesis and reproduction of the adult worm. Whereas, at high concentrations of the pheromone in combination with higher temperatures and little or no food, *dauer* formation is induced or *dauer* arrest is maintained (Golden and Riddle 1982; and reviewed in Hu 2007).

Mutations in more than 30 *dauer*-formation-abnormal (*daf*) genes (Figure 4, page 27) were characterized and their depletion either results in a *dauer* defective (*daf-d*) phenotype with inhibited or reduced *dauer* formation or otherwise in a *dauer* constitutive (*daf-c*) phenotype. The *daf-c* phenotype is characterized by *dauer* formation in the presence of sufficient food and/or a disability to exit the *dauer* stage under these conditions. While *dauer* formation affected by daf-c alleles is independent of pheromone concentration or the presence of food, temperature still plays an important role in most cases (reviewed in Riddle and Albert 1997). Genetic interactions that lead to entry into the *dauer* stage are complex, but two main pathways have been identified: On the one hand the insulin/IGF-1 signaling pathway via insulin receptor DAF-2 *(daf-c) and* Forkhead Box transcription factor DAF-16 *(daf-d)*; on the other hand the TGFβ mediated pathway via transforming growth factor DAF-7 *(daf-c)*, its DAF-1/DAF-4 receptor complex (daf-c) and the nuclear SMAD effectors DAF-3 and DAF-5 (both *daf-d*). DAF-12 *(daf-d)* a steroid hormone receptor regulates *dauer* formation downstream of the TGFβ- and insulin signaling pathways and is able to fully suppress the *daf-c* phenotype of upstream mutations in both branches. (reviewed in Riddle and Albert 1997; Fielenbach and Antebi 2008).

1.4.2　Ro RNPs in *C. elegans*

Previous studies found that the *C. elegans* open reading frame (ORF) C12D8.11 encodes the orthologue of the human Ro60 autoantigen, ROP-1 (Labbe et al. 1995; Van Horn et al. 1995). The *rop-1* gene is located on chromosome V at position 2.42 ±0.003cM. The actual size of ROP-1 remains controversial: Different reports agree that the predicted size would be 72.8kDa. However, an actual size of about 69kDa was reported for ROP-1 in adult worm extracts by van Horn et al. (1995). Another study using a different antibody found a 65kDa form by *in vitro* translation and in young worm larvae, which is processed by additional 3,5kDa during development (Labbe et al. 1995; Labbe et al. 2000). ROP-1 was also found to be diverging from its human orthologue, Ro60, especially by a 6- and a 19-amino acid insert in its RNA recognition motif (Van Horn et al. 1995).

An anti-ROP-1 antibody was used to co-immunoprecipitate RNA from worm extracts. By sequencing these RNAs, it could be shown that only a single Y RNA species is bound by the ROP-1 protein *in vivo* (Van Horn et al. 1995). This *C. elegans* Y RNA is encoded by the gene *yrn-1* (locus F55G1.16) on chromosome IV at position 3.34cM. *Yrn-1* is located on the minus strand of the second intron of the ORF F55G1.15 coding for the uncharacterized nematode-specific protein WP:CE35980 (Figure 6, page 44). Although the *C. elegans* Y RNA was found to share some features with human Y3 RNA, it cannot be categorized to any of the vertebrate Y RNA classes (Perreault et al. 2007). Interestingly the ROP-1 protein is not able to bind human Y3 RNAs *in vitro*, while the human Ro60 protein shows an even higher affinity to the *C. elegans* Y RNA than to hY3 RNAs (Van Horn et al. 1995). Additionally the *C. elegans* Y RNA is also not able to substitute for the role of human Y RNAs in chromosomal DNA replication, a function which was shown to be independent of a native Ro60 binding site (Gardiner et al. - in press). In contrast to vertebrate Y RNAs, mature *C. elegans* Y RNAs are possibly not bound by La: a 3'oligo-(U) tail was not reported for the *C. elegans* Y RNA (Van Horn et al. 1995) and *C. elegans* Ro RNPs did not show any other protein, but ROP-1 stably bound to the Y RNA (Labbe et al. 1999a).

A mutant line of *rop-1* was created by transposon insertion and described in two studies (Labbe et al. 1999b; Labbe et al. 2000). Labbe et al. (1999b) do not report a specific phenotype in *rop-1* mutants under laboratory conditions, but find the expression levels of the *C. elegans* Y RNA dramatically reduced in the absence of

ROP-1. This observation was later confirmed in RSR depleted *Deinococcus radiodurans* cells and in a Ro60 knockout mouse (Chen et al. 2000; Xue et al. 2003). The presence of ROP-1 was suggested to be essential for the stability of the Y RNA.

Additionally, elevated levels mutant 5S rRNAs were found incorporated in ribosomes in worms mutant for *rop-1*. In fact the levels were similar to those found in total RNA in both wild-type and *rop-1* mutants (about 7.5%). However in ribosomes from wild-type worms the levels of mutant 5S rRNA were nearly fivefold reduced (1.6%). Labbe et al (1999b) consider this as confirmation for a previously proposed role of Ro60/ROP-1 in an ill-defined quality control pathway for non-coding RNAs (O'Brien and Wolin 1994; Shi et al. 1996).

Rop-1 mutants do not form *dauer* larvae under starved and crowded conditions. This indicates a role for ROP-1 in the *dauer* formation pathway. Analysis of *dauer* formation in *rop-1* mutants in genetic backgrounds of various *daf-c* alleles suggests that *rop-1* genetically interacts with *daf-2.* All characterized alleles of *daf-2* were previously classified into two different but overlapping classes, depending on their phenotype in *dauer* formation and severity of pleiotropy (Gems et al. 1998). Interestingly, the influence of the *rop-1* mutation onto the phenotype of different *daf-2* alleles does not follow this classification, as it enhances *dauer* formation together with class-II *daf-2* alleles *e1370* and *m579*, but reduces *dauer* formation in combination with class-I allele *m41* but also class-II allele *m596*. The *e1370* mutation is located in the *daf-2* tyrosine kinase domain residing in the cell lumen, while the other three mutations map to ligand binding domains located on the outer cell membrane - potentially interacting with insulin ligands (Figure 4B; page 27). *Rop-1* was additionally shown to genetically interact with *daf-7* and to function upstream of *daf-16.* Therefore it seems to interact with both branches of the *dauer* formation pathway - the insulin and the TGFβ branch, respectively. Proteolytic processing of ROP-1 at the larval transition from L2 to L3 by an undefined aspartic proteinase was found and d*af-2* was shown to be essential for this process. Thus in L3 and older animals only the processed ROP-1 is prevalent, while in *dauer* and post-*dauer* animals both forms, unprocessed and processed respectively can be detected (Labbe et al. 2000).

C. elegans dauer larvae formation allows worms to survive in unfavorable environmental conditions and to return to the regular life cycle, in order to multiply,

when conditions have improved. In order to combine their observations of the role of ROP-1 in 5S rRNA quality control as well as in the *dauer* formation pathway, Labbé et al (2000) hypothesize that ROP-1 might "sense" cellular damage by screening quality of non-coding RNAs. Cellular damage and RNA misfolding, for instance after UV irradiation, would therefore lead to induction of non-breeding *dauer* larvae formation. This would facilitate the repair of accumulated cell damage prior to replication of the adult animal. This model remains controversial, as induction of the *dauer* formation pathway by intracellular factors, such as molecular damage accumulation, has not been demonstrated.

1.5 Aim of this study

We wanted to benefit from the fact that the *C. elegans* genome harbors only a single Y RNA encoding gene, *yrn-1,* and that a characterized disruption mutant of the Y RNA binding protein ROP-1 is available. In the *rop-1* mutant Y RNA levels are massively reduced, but Y RNA is still detectable, which does not allow distinguishing between effects caused by the *rop-1* deficiency or by Y RNA reduction. We therefore decided to create a knockout line of *yrn-1* in *C. elegans* with the aim to study the effects of a total absence of Y RNAs on viability, reproduction or development. Ro RNPs had previously been associated with processes such as UV damage response or in *C. elegans* the formation of stress-resistant *dauer* larvae. The creation of a strain mutant for *yrn-1,* would allow us to study a potential role, the Y RNA might play in these processes. We also planned to analyze the consequence of Y RNA deficiency for the ROP-1 protein on the molecular level. Finally a knockout would also give us a tool to detect genetic interactions of the Y RNA *in vivo*. This would help to identify cellular pathways the Y RNAs might be involved in and allow to focus further research accordingly.
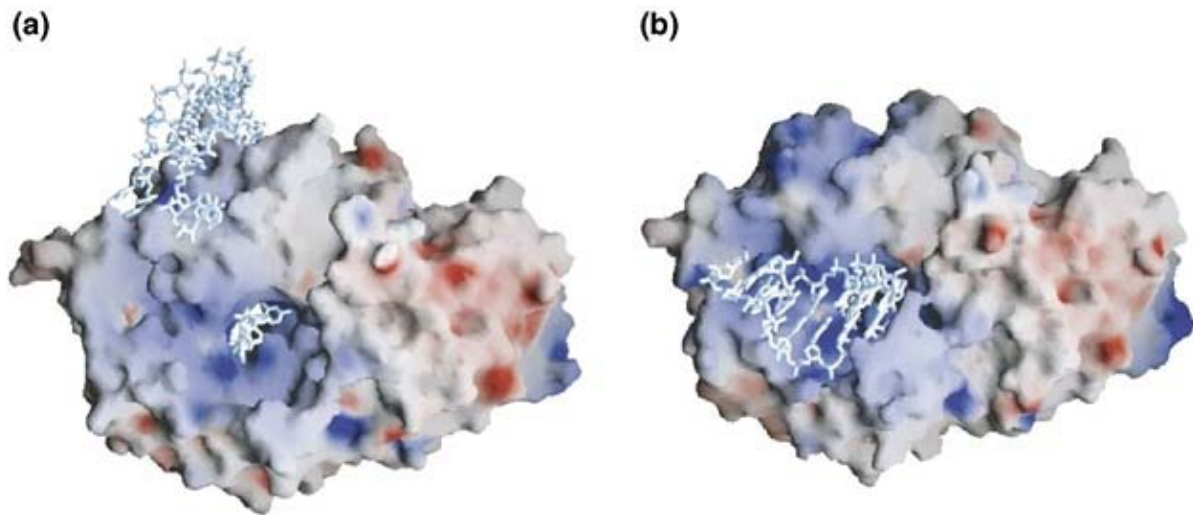
Figure 1: Crystal structure of the *Xenopus laevis* Ro60 protein a) A fragment of the Y RNA binds the outer surface of the N-terminal HEAT repeat domain. b) A fragment of a misfolded 5S rRNA binds toRo60's central cavity (structure published by Stein et al. 2005; picture taken from Reinisch and Wolin 2007).
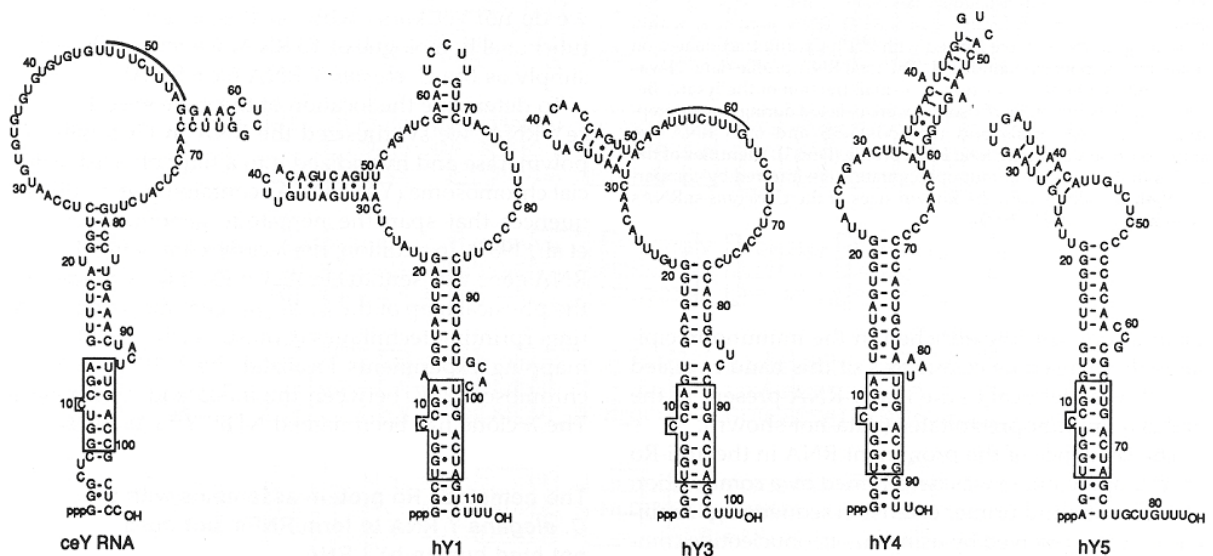

Figure 2: Proposed structure of the single *C. elegans* Y RNA and the four human Y RNAs (hY1, hY3, hY4 and hY5). The Ro binding site – a conserved helix with a single bulged Cytidine is indicated as well as a conserved sequence in the loop of the *C. elegans* Y RNA, the human Y3 and also the *Xenopus laevis* Y3 RNA (picture taken from Van Horn et al. 1995)
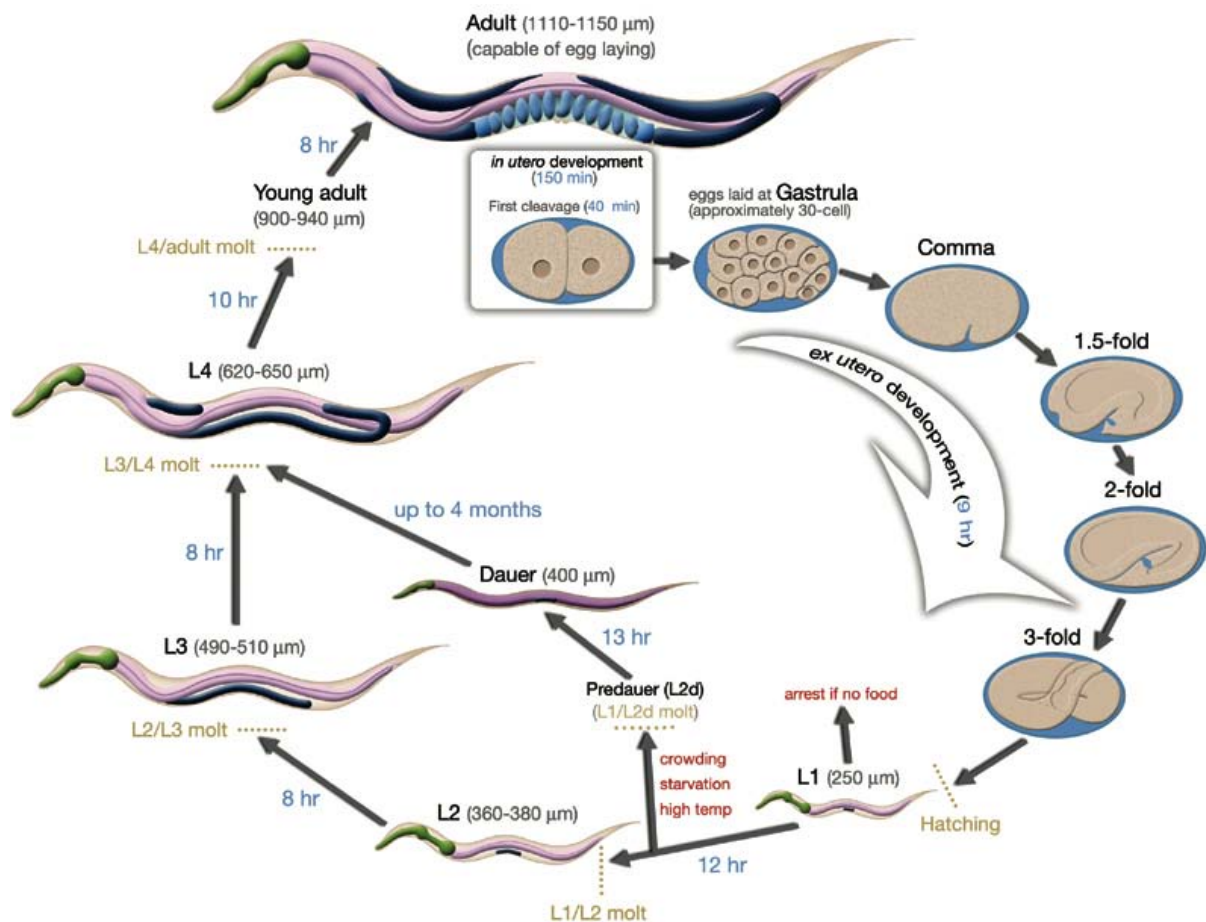
Figure 3: Life cycle of *C. elegans* at 22°C. Fertilization at 0min. Time span spent at a certain stage are indicated in blue along the arrows (taken from www.wormatlas.org).

Figure 4 on the following page: A) Under favorable conditions, the DAF-28 insulin-like molecule – the antagonist of human insulin orthologue INS-1 - activates the DAF-2 insulin receptor initiating a signal transduction pathway, which blocks the translocation of the DAF-16 Forkhead transcription factor to the nucleus and prevents *dauer* larvae formation. In a parallel pathway, DAF-7/TGF-β triggers the DAF-1/DAF-4 receptor complex to block the SMAD complex DAF-3/DAF-5 This prevents *dauer* larvae formation and facilitates reproductive growth. The guanylyl cyclase DAF-11 positively regulates the expression of DAF-28 and DAF-7 and thus supports reproductive growth via both pathways. During favorable conditions, the CYP2 cytochrome P450 enzyme DAF-9 is activated and catalyzes the DAF-12 ligand dafachronic acid. In the absence of its ligand DAF-12 initiates *dauer* formation, while it promotes reproductive development with the ligand bound. (Von Stetina et al. 2007)

B) Structural representation of homology models of DAF-2 domains constructed in orientation to the human insulin receptor crystal structure (Hubbard et al. 1994). The location of mutations of different *daf-2* alleles is indicated. Green, are class-I mutations; red are class-II mutations; black are nonconditional mutations. Class-II alleles *e1370, m579, m596* as well as class-I allele *m41* were studied by Labbé et al (2000) in the *rop-1* background (indicated in blue letters), while *e1370* and *m41* were analyzed in this project in both the *rop-1* and the *yrn-1* background, respectively. The regions L1 and CR are thought to interact with human IGF-1 and /or Insulin (homologous to worm DAF-28 and INS-1), while the tyrosine kinase signals via the PI 3-kinase pathway. (Figure taken from Patel et al. 2008)
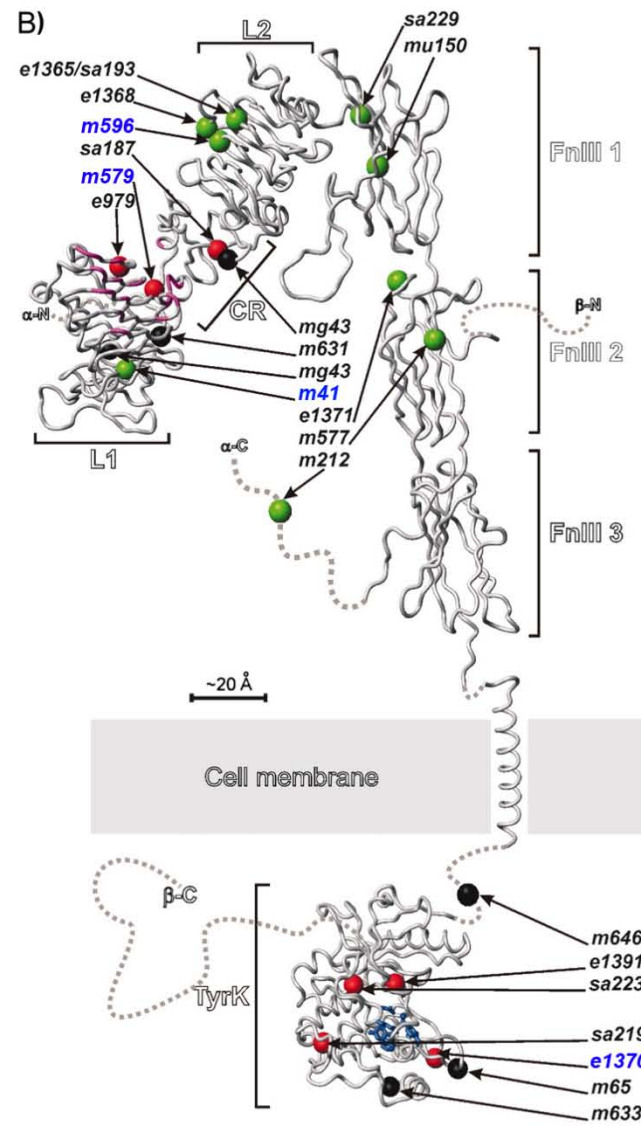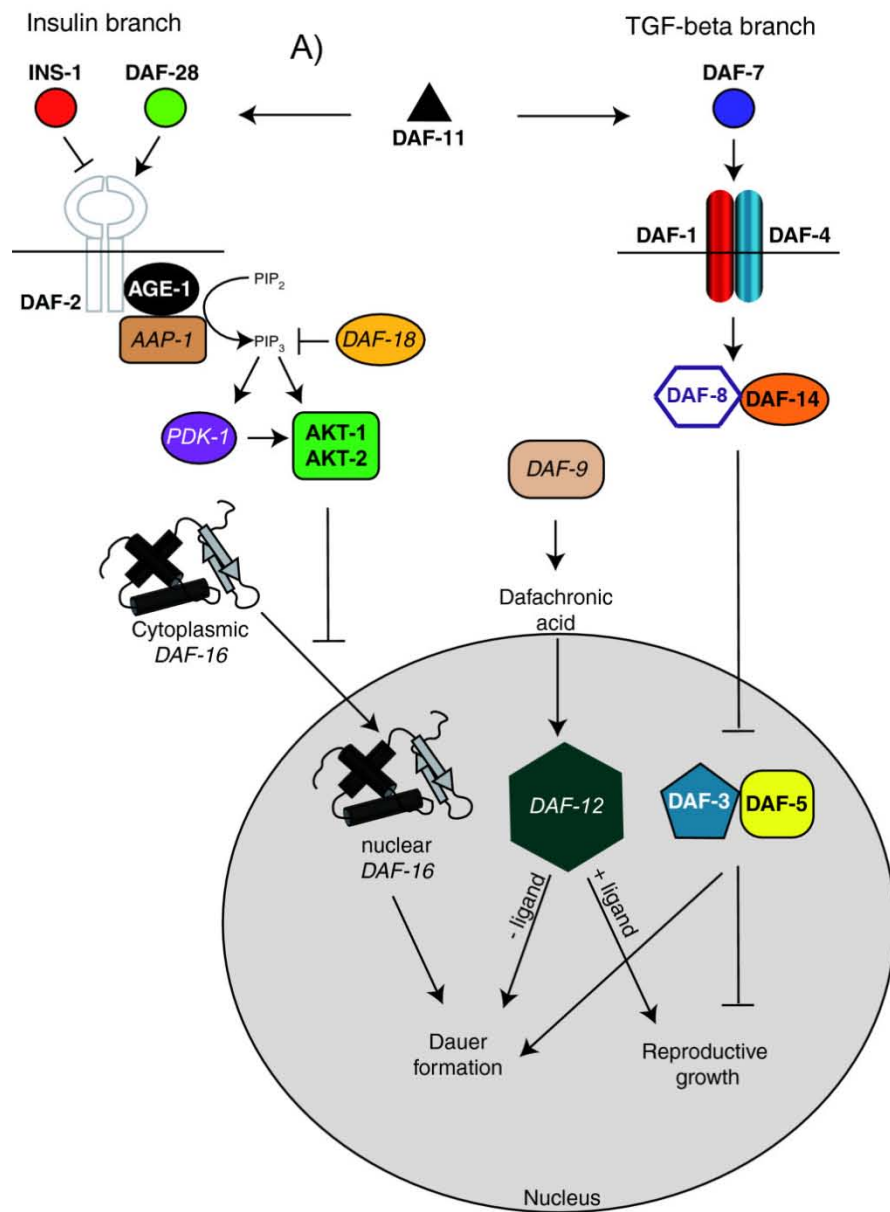
2 Material & Methods

2.1 Strains and oligonucleotides used in this study

All *C. elegans* strains were cultured using standard techniques (Brenner, 1974). The wild-type (N2 Bristol), DP38 *unc-119(ed3)*, MQ470 *rop-1(pk93)*, DR1564 *daf-2(m41)* and CB1370 *daf-2(e1370)* strains were obtained from the *Caenorhabditis* Genetics Center (University of Minnesota, St. Paul, Minn.). The *yrn-1(tm2634)* mutant was obtained from Dr. Shohei Mitani of the *National Bioresource Project for the nematode* at Tokyo Women's Medical University School of Medicine, Japan. This strain *yrn-1(tm2634)* was out-crossed three times and termed *yrn-1(YJA)* for this work, MQ470 *rop-1(pk93)* was also three times out-crossed and will be referred to simply as *rop-1* mutant in this study.

The *yrn-1* knockout strain Y5B was created according to chapter 2.3. The strains *yrn-1(Y5B);rop-1(pk93), daf-2(e1370);yrn-1(YJA), daf-2(e1370);rop-1(pk93), daf-2(m41);yrn-1(YJA) and daf-2(m41);rop-1(pk93)* were created by crossing and analysis of the genotype by PCR using primers indicated below.

Primers used for characterization of the genotype during this work: For *yrn-1(Y5B)* primer pairs ext1/unc1, x1/z1 and y1/z1 were used (for sequences see chapter 2.3). For identification of *yrn-1(YJA)* deletion, primer pair 2226 5'-AAT CCT TAT CCG AAA GGG CT-3' and 2227 5'-TGA GGT TGG AAC CGA GGT TC-3' yielding a 550nt product in the case of *yrn-1(tm2634)* mutation, but a 750nt product in wild-type. Primers used for *rop-1(pk93)* genotype verification: 1562 5'-CGT CAA ATG GAG AAA GTC AAG G-3' and 1563 5'-ATT TTG TGA ACA CTG TGG TGA AG-3' for a ~0.9kb product in case of *rop-1* disruption, but no product in wild-type as well as 1575 5'-ATG CTC ACG GAC AAG TCC ATG-3' in combination with primer 1562 for no product in case of disruption, but a 1kb product in the wild-type situation. *Daf-2* alleles *m41* and *e1370* are single nucleotide polymorphisms and were detected by PCR and consecutive restriction digest. For *daf-2(m41)* PCR was carried out using primer pair 2557 5'-AGC TTG CGA AGA GGA TAA AGG-3' and 2558 5'-GAC ATT TAT CCG AGC AAA GGC-3' yielding a 413bp product. Digestion by RSRII restriction enzyme results in a 153nt and a 261nt fragment in wild-type but the 413bp fragment remains undigested in the presence of the *daf-2(m41)* allele. The

daf-2(e1370) genotype was determined by PCR with primer pair 33 5'-ATC AAT GCG TAC TCC TCA TCC-3' and 34 5'-TTT GTG ATG GTA TGG CGT ACC-3'. The reaction results in a 772bp product, which can be cut in wild-type by PFLM1 restriction enzyme into two fragments of 279bp and 494bp, but no digest takes place if the *daf-2(e1370)* allele is present. Strain *unc-119(ed3)* was identified by its severe *uncoordinated* phenotype.

2.2   General protocols and materials used in this study

Nematode growth media (NGM) (Brenner 1974): 3g NaCl, 2.5g peptone, 1ml cholesterol (5 mg/ml in ethanol), 975 ml H_2O. were autoclaved and: 1 ml 1M $CaCl_2$, 1ml 1M $MgSO_4$, 25ml 1M KH_2PO_4 pH6.0 was added afterwards. This liquid medium was used for the RNAi screen and ampicilin (Amp) and Isopropyl-β-D-thiogalactopyranosid (IPTG) was added as described in 2.14. For NGM plates 17g bacto-Agar were added before autoclaving and 50µg/ml streptomycin as well as 100µg/ml nystatin were added after the autoclaving. NGM plates were seeded with E. coli strain OP50, which is streptomycin resistant and uracil auxotroph.

Egg salts buffer: 0.12M NaCl, 0.05M KCl

Egg plates (Krause 1995): 10 chicken egg yolks were put into a sterile bottle and well shaken. Two volumes of 2xTY medium were added and incubated one hour at 60°C. After cooling down and adding of 40ml of overnight OP50 liquid culture, 8ml of the mix was distributed per large NGM plate and left to sediment overnight. The supernatant was removed and plates were left for drying another night.

M9-buffer (Brenner 1974): 3g KH_2PO_4, 6g NA_2HPO_4, 5g NaCl, 1ml $MgSO_4$ 1M; to pH7.4 in1 liter H_2O

2xTY: 1 liter: 10g yeast extract, 16g tryptone, 5g NaCl – for plates add 15g bacto agar

1xTE: 10mM Tris pH7.5; 1mM EDTA

Net-2: 150mM NaCl; 50mM Tris pH7.4; 0.05% NP40

20xSSC: 175.3g NaCl, 88.2g sodium citrate in 1 liter H_2O

10xTBE: 1liter: 108g Tris base; 55g boric acid; 40ml 0.5M EDTA

50xTAE: 1 liter: 242g Tris base; 57ml glacial acetic acid, 18.6g EDTA

10xTBS: 80g NaCl, 2g KCl, Tris base 30g; to pH8.0 in 1 liter.

Urea loading buffer: 8M urea; 5mM Tris pH7.5; 0.5% (w/v) bromphenol blue; 0.5% (w/v) xylene cyanol FF; 20mM EDTA, pH8.0.

10% 19:1 poly-acrylamide gel: 9.5% acrylamide (w/v); 0.5% bis-acrylamide (w/v); 14ml 10M urea; 2ml 10xTBE buffer; 0.2ml 10% ammonium persulfate; 1.8ml monoQ water

Church & Gilbert buffer (Church and Gilbert 1984): for 1 liter: 7% SDS; 1% BSA; 1mM EDTA; 500 ml 2xNaHPO$_4$ pH7.2 (1Liter 2xNaHPO$_4$: 34g Na$_2$HPO$_4$.7H$_2$O; 4 ml 85% H$_3$PO$_4$)

Single-worm-PCR lysis buffer (Barstead et al. 1991; Williams et al. 1992): 0.45% NP40, 50mM KCl, 10mM Tris pH8.3, 2.5mM MgCl$_2$, 0.01% w/v gelatin

All RNAse sensitive assays were carried out with 1:2000 DEPC treated reagents.

2.3   Cloning of the *yrn-1* targeting construct and scoring for mutants

The targeting construct for the knockout of the *yrn-1* gene was generated by inserting three genomic regions (fragment A, B and C) into pPD#MM016 (Maduro and Pilgrim 1995), a Bluescript vector containing the *unc-119* rescuing locus (of about 5.7 kb) cloned into the XbaI and HindIII sites. Additionally fragment SF, which was derived from cDNA and accordingly intron 2 of ORF F55G1.15 is missing therein, was cloned between fragment A and B (Figure 5, page 44). Fragment A was amplified with primers MJ1323 5'- AGG TAC CCC ACA AGA ACA TAT CTG C-3' and MJ1324 5'-TT AA<u>G</u>$^{(A)}$ CT<u>T</u>$^{(G)}$ GTT GGT TCA TTT TCC ATT TGT G-3' and cloned into the KpnI and HindIII sites. Fragment SF was amplfied with MJ1327 5' - AT <u>A</u>$^{(C)}$AG <u>C</u>$^{(T)}$TT AAT GAG CAA AAC CAC ACA AC-3' and MJ1328 5'-GAG CT<u>C</u>$^{(A)}$ GTT GAT GAT CAT TAT ATG-3' and cloned into the HindIII and SacI sites. Fragment B was amplfied with MJ1325 5' -AC GAG CT<u>C</u>$^{(A)}$ ATC GAA ATC TAT AAA AAA GA-3' and MJ1326 5'-GTG TCG ACT GAC CAT CAG ATT GCG-3' and cloned into the SacI and SalI sites. Fragments A, SF and B were first inserted by

T/A-cloning separately into pGEM-T easy vectors. Fragments SF and B were released by restriction digest with the corresponding enzymes mentioned above and sequentially subcloned into the pGEM-T easy vector containing fragment A. The resulting insert A/SF/B was released from the pGEM-T easy vector using restriction enzymes KpnI and SalI and subcloned into the pPD#MM016 Bluescript vector upstream from the *unc-119* rescuing locus. Fragment C was amplfied with MJ1329 5'-TTG CGG CCG CGA GCA AAC ATT CAA AAA G-3' and MJ1330 5'- AAC CGC GGC ATA AAG AGC ATT TCC ATC C-3' and cloned via the NotI and SacII sites downstream of the *unc-119* locus of the #MM016 Bluescript vector containing the fragment A/SF/B. Two artificial restriction sites HindIII and SacI were introduced into the exonic sequence of F55G1.15 in the targeting construct by the use of degenerate primers without affecting the encoded amino acid sequence, conserving a leucine and a lysine residue at the 5' end of fragment SF and a leucine residue at the 3' end. (Mutated nucleotides are underlined in the sequence of the primers; original sequence in superscript). All exonic regions of the completed construct, upstream and downstream of the *unc-119* locus, were entirely sequenced and no error affecting the encoded amino acid sequence or the splicing pattern was found.

2.4 Biolistic transformation

Biolistic transformation of *unc-119(ed3)* mutants with the *yrn-1* targeting construct was carried out according to (Berezikov et al. 2004), which is a scaled up version of earlier protocols (Wilm et al. 1999; Praitis et al. 2001): Gold particles (0.3-3 µm, Bio-Rad) were prepared as described in the PDS-1000/He (Bio-rad) user's manual: 60mg of microparticles were weighed in and soaked for 15min in 2ml 70% ethanol, washed three times in sterile monoQ water and resuspended in 1ml of a sterile 50% glycerol solution. Construct DNA was released from the vector using restriction enzymes Spe1 and BamH1 and was used directly for coating the gold particles without prior purification. For one bombardment with the Hepta adaptor, 50µl of gold particles (60mg/ml) were aliquoted, shortly spun and the supernatant was removed. Subsequently the following solutions were added to the gold particles while resuspending after each step: 50µl of DNA (10-15µg), 50µl of 2.5M CaCl$_2$ and 20µl of 0.1M spermidine. The cocktail was incubated for 30min on ice with sporadic resuspensions, shortly spun, washed in 300µl of 70% ethanol, followed by 1ml of

100% ethanol, resuspended in 170µl of 100% ethanol. 20µl of DNA-coated gold particles were distributed onto each of seven macrocarriers, which were left for drying, and bombardments were performed within 5-10 min later. Parameters for the bombardment were 4mm distance between exits of the Hepta-adaptor gas splitter and macro-carriers, 20mm distance between stopping screens and target shelf, 1350psi rupture disks and 28 inches of Hg vacuum.

Unc-119 worms were cultured on egg plates (Krause 1995) at 20°C to 25°C. Populations of 5 to 10 plates were finally washed off using egg salts buffer and washed several times and distributed onto one pre-cooled large NGM plate for each bombardment.

After the bombardment worms were washed off from each plate using 10ml egg salts buffer and left in the buffer in a 15ml Falcon tube for about 30min. Then the worms were resuspended and distributed onto 20 NGM plates (prepared with high-gel strength agar, A9799 Sigma) seeded with OP50 bacteria. These plates were left at 20°C for three to six weeks depending on population density. Scoring was carried out, when no *uncoordinated* worms were left on the plate.

2.5 Detection of homologous recombination

All non-*unc* and *dauer* worms from scored plates were singled and cultured and were subjected to diagnostic PCR. Worms were lysed in lysis buffer for 60min at 65°C; proteinase K was inactivated by incubation at 95°C for 15min. An aliquot of 0.5µl of the lysed material was added to the PCRs. Primer pair unc1 5'-GAA GTA TTG TTA AAA TTC TAG AGC G-3' and ext1 5'-CAA TTG AGC AAT GAA AAT GAC TGC-3' were designed to amplify a part of the *unc-119* locus, the 3' homology region of the construct and a piece of the chromosomal region next to the desired insertion site, which is not contained within the targeting construct. This primer pair would yield a ~4kb product in case of homologous integration of the targeting construct only. Confirmation of *yrn-1* deletion was carried out using primers x1 5'-TGC AAC ACG GAA TCG GAA AAC C-3' and z1 5'-TTC TTC AAT CAG TAC ATC GTG ATC-3' resulting in a 853bp product in wild-type and a 574bp product in case of *yrn-1* deletion and both in heterozygous worms. Additional confirmation was carried out by y1 5'-TAT GTT GGA AGA AAA TAT CTC ACA C-3' and z1 PCR

resulting in a 622bp product in wild-type and heterozygous worms and no product in homozygous Y RNA knockout worms.

2.6 Validation of the genotype by Southern blotting

Mixed stage N2 and *yrn-1* worms were washed off 4 large NGM plates and rinsed several times with M9 buffer. Worms were lysed in 500µl lysis buffer (100mM Tris pH8.5; 100mM NaCl; 50mM EDTA; 1% SDS) and 200µg Proteinase K for two hours at 65°C. 80µl 5M NaCl were added, mixed and 80µl CTAB mix (10% CTAB; 0.7M NaCl) were added and the sample was incubated for 5min at 65°C. 700µl 24:1 CHCl3/isoamylalcohol was added and mixed. After 5min centrifugation at 14,000rpm the aqueous phase was transferred to a fresh tube and the $CHCl_3$ extraction was repeated. The DNA in the aqueous phase was precipitated with an equal amount of isopropanol and centrifuged. The pellet was washed with 70% ethanol and the dried pellet was resuspended in 50µl TE and incubated with 10µg RNAse A for two hours at 42°C. The DNA content was measured and 5µg DNA were digested by EcoRI restriction enzyme, heat-inactivated at 65°C for 20min and run on a 1% agarose gel in TAE. The gel was depurinated by agitating 20min in 0.1N HCl and denatured by leaving in 0.5N NaOH/1M NaCl for 20min. DNA was capillary-blotted with 20xSSC onto a nylon membrane and UV cross-linked (modified from Southern 1975; Brown 1994b)

To generate a hybridization antisense probe, the PCR product from genomic DNA using the primer pair MJ1327/MJ1328 (chapter 2.3), was cloned into a pGEM-T easy vector. The orientation was determined by sequencing and after SPH1 restriction digest, the insert was *in vitro* transcribed from the SP6 promoter (1µg DNA, 4µl transcription buffer, 1µl DTT, 2.5µl nucleoside mix [5mM CTP, 5mM GTP, 5m MUTP, 3mM ATP], 2µCI ^{32}P ATP, 1µl RNAsin, 1µl Promega SP6 Polymerase) for 3 hours at 37°C. The probe was run through a Sephadex G-50 column, denatured at 70°C for 10 minutes and added to the Southern blot in Church&Gilbert buffer and hybridization was carried out overnight at 65°C. After two 2xSSC/0.5%SDS washes, and one wash with 1xSSC/0.5%SDS, 0.5xSSC/0.5%SDS and 0.2xSSC/0.5%SDS the blot was exposed on a Kodak storage screen (Screen-K).

2.7 Validation of the genotype by Northern blotting

Total RNA was extracted by washing off mixed stage N2 and *yrn-1(Y5B)* worms from 4 NGM plates with M9 buffer. After several times washing with M9 buffer to remove the OP50 bacteria, worms were pelleted and 500µl TRIZOL reagent (Invitrogen) and 1mM EDTA was added. About 300µl of zirconia beads and were added and lysis was carried out in a three minutes (10sec on:10sec off) cycle at 2,500rpm in a multi-beads shocker (Yasui Kikai) at 4°C. 100µl of $CHCl_3$ was added, mixed and left at ice for three minutes. Centrifugation at full speed for 10 minutes was followed by extraction of the aqueous phase with an equal amount of $CHCl_3$ and precipitation with an equal amount of isopropanol. After centrifugation at full speed for 30min, the pellet was dried and resolved in 25µl urea loading buffer. The samples were denatured for 10min at 70°C and run on a 10% 19:1 poly-acrylamide gel in 1xTBE buffer. The gel was ethidiumbromide stained (0.05%; 10 min), photographed and electro-blotted onto a nylon membrane in 1xTAE buffer overnight at 15 volt at 4°C. The blot was UV cross-linked and pre-incubated in Church & Gilbert buffer.

A *yrn-1* antisense probe was derived by PCR from genomic DNA with primer pair 982 5'-GTC GGG CAC TTT CCT ATG C-3' and 983 5'-AAG TGC AAA ACT CGG AAA TCC-3', resulting in a 185bp product (25nt upstream overhang; 54nt downstream overhang), which was cloned into a pGEM-T easy vector. After determination of the orientation by sequencing and after SPH1 restriction digest to linearize the vector, the insert was *in vitro* transcribed from the SP6 promoter (1µg DNA, 4µl transcription buffer, 1µl DTT, 2.5µl nucleoside mix [5mM CTP, 5mM GTP, 5mM UTP, 3mM ATP], 2µCl ^{32}P ATP, 1µl RNAsin, 1µl Promega SP6 polymerase) for 3 hours at 37°C. The probe was run through a Sephadex G-50 column, denatured at 70°C for 10 minutes and added to Northern blot in Church&Gilbert buffer and hybridization was carried out overnight at 65°C. After two 2xSSC/0.5%SDS washes, and one wash with 1xSSC/0.5%SDS, 0.5xSSC/0.5%SDS and 0.2xSSC/0.5%SDS the blot was exposed on a Kodak storage screen (Screen-K). This protocol and the same probe was also used for the verification of the *yrn-1(Y5B)* genotype (Figure 9 right, page 48) and in the same way for analysis of the genotype of *yrn-1(Y5B);rop-1* double mutants and *yrn-1(YJA)* deletion mutants (Figure 12, page 51). (Brown 1994a)

2.8 Validation of the genotype by RT PCR

Total RNA was prepared as described in 2.7. 75µg RNA was solved in 100µl TE and denatured for 10min at 70°C. 1mg oligo(dT)$_{25}$ magnetic dynalbeads were washed twice in solution D (20mM Tris-HCl (pH7.5), 1M LiCl, 2mM EDTA) resuspended in 100µl solution D and added to the RNA, rotated 5min on a wheel at room temperature and pelleted with a magnet. The supernatant was removed and the beads were washed twice with 200µl buffer B (10mM Tris-HCl pH7.5, 0.15M LiCl, 1mM EDTA). Poly(A)-RNA was solved by adding 2x 40µl monoQ and incubating at 80°C for 2 minutes. The beads were pelleted with a magnet and the supernatant was transferred. The DNA in the sample was digested by adding 10U DNAse I (Fermentas) and 10µl 10x reaction buffer and incubated for one hour at 37°C. 200µl TE was added and the sample was extracted once with an equal amount of phenol, once with an equal amount of 25:24:1 phenol/ chloroform/isoamylalcohol and once with an equal amount of 24:1 CHCl$_3$/ isoamylalcohol. After the precipitation with an equal volume of isopropanol and centrifugation for 30 minutes at 4°C, the pellet was resolved in 10µl monoQ and 2µl oligo(dT) primer (50µM) were added and the cocktail was incubated for 3min at 70°C. The mixture was put on ice and 2µl 10xRT buffer, 4µl 10mM dNTPs, 1ml RNAsin and 1µl Reverse Transcriptase was added and the mixture was incubated for 1 hour at 42°C. The reaction was stopped by incubation at 94°C for 10 minutes. This cDNA sample was used as a template for PCR with primers 1870 5'-AAC CGC TTA CAC ATG TCT TTG C-3'and1871 5'-TGT ATG TAG GAA CGC ATG TTC C-3'; 1866 5'-AAG CGG CTG TTA CTG CAT TCG-3' and 1867 5'-ATA CAT CTC TGA CAG GTA GTC C-3'; 1220 5'-TGG ATT TAT TAT ATG GTC AGA CGC-3' and 1221 5'-GCA TAC AAC ATA GAA GCT ACT TTG-3'; 1124 5'-GCA CTG TCT TCA CCA AGT TTA TG-3' and 1125 5'-GAT TTC AAT ACC ATG CGG ATC AG-3' (Figure 10, page 49). (Krause 1995)

2.9 Brood size and life span assays

For the determination of fecundity 20 gravid adults of N2, *yrn-1(YJA)* and *rop-1* strains grown at 20°C were left to lay eggs for about one hour and then removed. The synchronous population derived was incubated at assay temperature of 14°C or 25°C until late L4 stage. 10 worms were singled on small, seeded plates and these

worms (P0) were picked to new plates every 24 hours at 14°C or 12 hours at 25°C, respectively, until reaching the end of the reproductive period. F1 plates were inspected for the occurrence of non-hatching eggs and worms were removed and counted when reaching L3 to L4 larval stage.

For the determination of life span (according to Gems et al. 1998) P0 animals of the 25°C brood size experiment were inspected every 24 hours and death of a worm was scored as the absence of any pharyngeal movement and failure to move at all after several light pokes with a platinum wire.

2.10 UV irradiation assay

20 gravid adults of N2, *rop-1, yrn-1(Y5B)* or *yrn-1*(YJA) strains grown at 20°C were left to lay eggs for about one hour and then removed. The synchronous population derived was incubated at assay temperature of 20°C until reaching young adult larval stage. 25 worms were carefully picked onto a pre-cooled unseeded NGM plate and irradiated immediately in a Stratalinker (Stratagene UV 2400) at 254nm 1800J/m2. Worms were directly distributed to single plates with a lot of care and scored every 24 hours. Death was scored as described in chapter 2.9.

2.11 *Dauer* formation assay

Experiments were carried out as described by Gems et al. (1998): 20 gravid adults of *daf-2(e1370), daf-2(e1370);yrn-1(YJA), daf-2(e1370);rop-1* or *daf-2(m41), daf-2(m41);yrn-1(YJA), daf-2(m41);rop-1(pk93)* strains grown at 14°C were left to lay eggs for about one hour and then removed. The synchronous population derived was incubated at 14°C until late L4 stage. Ten worms were singled on small, seeded plates and shifted to the assay temperature of 20°C or 22.5°C. These worms (P0) were picked to a new plate every 24 hours until reaching the end of the reproductive period. Each F1 plate was examined daily and any L4 larvae or adults were counted and removed. The number of *dauer* progeny was scored 80 hours after the midpoint of egg laying at 22.5°C and after 96 hours at 20°C. Only uncontaminated plates were analyzed. Scoring for *dauer* larvae was carried out by visual inspection and picking of the *dauer* candidates into a 1% SDS solution. *Dauer*

larvae were scored two hours later by the ability to move after several light pokes with a platinum wire.

2.12 ROP-1 expression

ROP-1 expression was determined by picking 50 gravid adults of N2, *yrn-1(Y5B)* and *rop-1* strains onto an unseeded NGM plate, leaving them for 1 hour to get rid of the OP50 bacteria and carefully picking them into 25ml of Laemmli loading buffer (2.4ml 1M Tris pH6.8; 3ml 20% SDS; 3ml glycerol; 1.6ml β-mercapto-ethanol; 0.006g bromophenol blue) and boiling the samples for four minutes and running them on a denaturing 12% poly-acrylamide gel (2.8ml 30% 30:1 acrylamide:bisacrylamide solution; 1.5ml monoQ; 2.6ml 1M Tris pH8.8; 50µl 10% SDS; 50µl 10% APS; 15µl TEMED) in SDS running buffer (Tris base 3.03g; Glycine 14.4g; SDS 1g to 1 liter with dH_2O). Proteins were blotted onto a nitrocellulose membrane in transfer buffer (3.03 g Tris base; 14.4g glycine; 200ml methanol; water to 1 liter) for 1hour at 100 volt. The blot was blocked for one hour with 5% dry milk in 1xTBS, washed twice for 5min with 1xTBS and incubated with primary anti-ROP-1 antibody - generously provided by S. Wolin (1:1000 anti-ROP-1 and 0.5% dry milk in 1xTBS) overnight at 4°C. The blot was washed three times in TBS and incubated with a secondary antibody (1:10000 anti-rabbit horse radish peroxidase) for 30min at room temperature. Detection by *Electrochemiluminescence* (ECL by GE Healthcare) was carried out according to the manual. Exposure of 30 seconds was carried out on Kodak BioMax XAR-5 film. (Gallagher and Smith 1993)

2.13 ROP-1 Immunoprecipitation

5mg protein A sepharose beads (Invitrogen) were left for swelling in 500µl Net-2 buffer, quick-spun and the supernatant was removed. The procedure was repeated twice. 10µl of antibody stock (or monoQ for the mock control) was added to beads in 500µl Net-2 buffer and incubated over night on a rotating wheel at 4°C. After quick spin and removal of the buffer, the beads were washed three times in Net-2 buffer. N2 and *yrn-1(Y5B)* worms from dense mixed stage culture were removed from 4 large plates using M9 buffer and washed several times. The worm pellet was ground in liquid nitrogen and the powder was dissolved in 1ml Net-2 buffer. The mixture

was centrifuged at 14,000rpm for 10min at 4°C. The supernatant was transferred to a new tube and the procedure was repeated. After the second centrifugation 1/100 of the supernatant was transferred to a new tube and mixed with 300µl phenol (pH8.0) and extracted as described below for the IP samples, radioactively labeled in the same way as the IP samples and run on the gel (indicated as N2 lysate). The remaining supernatant was mixed with antibody-coupled sepharose beads and incubated at 4°C for 1 hour on the rotating wheel. After a quick spin and removal of the supernatant, the beads were washed six times with 500µl Net-2 buffer. After the last wash the supernatant was removed and the beads were resuspended in 100µl TE and 150µl Trizol reagent (Invitrogen) and 1mM EDTA. The mixture was left for 10min at 65°C with shaking and afterwards 50µl $CHCl_3$ was added, mixed, left on ice for 3min and spun at full speed for 5min at 4°C. The aqueous phase was extracted once with equal amount phenol, centrifuged and extracted with phenol/chloroform/isoamylalcohol (25:24:1), centrifuged and extracted with $CHCl_3$. The aqueous phase was precipitated with one tenth of the volume of NaAC(pH5.2) and three volumes 96% ethanol and left over night at -80°C. The RNA suspension was mixed and one third was centrifuged for 30min at full speed at 4°C. The pellet was washed twice with 70% ethanol, air-dried and dissolved in 20µl TE buffer. 2.5µl NEB buffer 3, 1µl RNAsin and 1.5µl Calf intestinal phosphatase were added and the mixture was incubated for one hour at 37°C. 275µl TE was added and phenol extraction and ethanol precipitation was carried out as described earlier. After centrifugation and 70% ethanol washing, the pellet was resolved in 40µl MonoQ water and 5µl PNK buffer, 5µCi ^{32}P γ-ATP, 1µl RNAsin and 1µl T4 Polynucleotidekinase (NEB) was added. The mixture was adjusted to 50µl with monoQ water and incubated for 30min at 37°C. After ethanol precipitation and washing with 70% ethanol, samples were dissolved in urea-loading buffer and run on a 10% 19:1 poly-acrylamide gel in 1xTBE buffer. The gel was dried and exposed on Kodak storage screen (Screen-K). (Springer 1994)

2.14 Large RNAi screen for synthetic genetic interaction in liquid culture

The RNAi library of *C. elegans* chromosome II and IV was obtained from Geneservice Ltd. and had been constructed by Julie Ahringer's group at the Wellcome CRC Institute, University of Cambridge, Cambridge, England (Fraser et

al. 2000; Kamath et al. 2003). The RNAi screen in liquid culture using 96-well plates was carried according to a published method (Lehner et al. 2006): 384-well library plates were expanded to 96 well plates. Bacteria were replicated on 2xTY-Amp plates and grown over night and replicated into 400µl liquid 2xTY-Amp in 96-well deep-well plates (Corning Costar 3961). Cultures were grown with shaking overnight at 37°C. For induction of RNAi expression IPTG was added to a total of 4mM the following morning and the cultures were left at 37°C for another hour. The cultures were pelleted by centrifugation for 5min at 3,500rpm. The supernatant was discarded by inversion. The bacterial cultures were resuspended in 400µl liquid NGM, 100µg/ml Amp and 4mM IPTG. Of each bacterial culture 40µl were pipetted into a well of a 96-well plate (flat bottom; Sarstedt 82.1581.001) for the *yrn-1* mutant and the same was done in the well in the neighboring row for N2. Thus, each row of the original 96-well plate containing the bacterial cultures was duplicated on the screening plates. Therefore two screening plates were used for each original library plate, whereby the first screening plate contained rows A to D and the second plate contained rows E to H of the library plate cultures. N2 and *yrn-1* mutant worms were grown separately on NGM plates and washed off with M9 buffer as mixed stage and washed several times in M9 buffer with centrifugation at 1,000g in between, to remove OP50 bacteria. Mixed stage worm suspension was filtered through a 10 µm mesh filter for purifying L1 worms (generously provided by Julia Tischler – then at Fraser lab, Sanger Center, Cambridge, UK). Worm suspensions were diluted to a concentration of 10 L1 larvae/10µl. 10µl L1 worm suspension was then added to each well and in doing so one row of *yrn-1* mutants was alternated with one row of N2 worms. Thus each bacterial clone was once seeded with wild-type worms and in corresponding well of neighboring row with *yrn-1* mutants to allow for direct comparison of the phenotype. The plates were left shaking at 37°C in plastic boxes to prevent evaporation of worm/bacterial suspensions. Plates were monitored on a dissecting microscope four days after seeding worms and re-scored 24 hours later. Embryonic lethality (emb) and sterility (ste) was scored semi-quantitatively on a scale from 0 (wild-type) to 3 (100% emb or ste) and N2 was directly compared to *yrn-1* mutants.

Additionally to the RNAi library of chromosome II and IV a fragment of ORF C44E4.4 encoding for the *C. elegans* La orthologue was cloned into a L4440 vector and used for RNAi feeding experiments as described above. Primers VJ132 5'-TCA

GCA CTG ACA CCC AAT TGG-3' and VJ133 5'-AGC GAA CAC AGT ACG CTT AGC-3' were used to amplify a 806bp fragment of chromosomal DNA completely covered by C44E4.4 exon 3. The fragment was cloned into pGEM-T easy vector by TA-cloning and sub-cloned via NcoI/SpeI restriction sites into a L4440 feeding vector (Timmons and Fire 1998). The insert was sequenced and retransformed into *HT115(DE3)* bacterial strain and used as described above.

2.15 Immunostaining of dissected worms

N2, *yrn-1(YJA)* and *rop-1* worms were put in 1xPBS on poly-L-lysine coated slides. An equal amount of 2% formaldehyde was added and a cover slip was put on. 5 minutes later slides were immersed in liquid nitrogen, cracked and fixed in -20°C methanol for 5 minutes. Slides were washed three times for 5 minutes in 1xPBS-Tween (0.1%) and blocked in a humid chamber with 20µl 10% horse serum in 1xPBS for 30min at room temperature. After blocking slides were washed three times for 5 minutes in 1xPBS-Tween. 10µl primary antibody (anti-human fibrillarin rabbit serum 1:1,000) was dropped on the sample, covered with a soft cover slip and incubated overnight at 4°C in a humid chamber. Slides were washed three times in 1xPBS-Tween and 10µl secondary antibody (anti-rabbit FITC 1:2,000) was dropped on the sample, covered with a soft cover slip and slides were incubated for two hours at room temperature in a humid chamber. The slides were washed three times for 5 minutes in 1xPBS-Tween and 10µl 0.1% DAPI in Vectashield (Vector Labs) solution was dropped onto the sample, glass cover slips were put on and sealed with nail polish. (Duerr, J. S. – Wormbook web site)

2.16 Ribosomal RNA processing assay

Total RNA from N2, *yrn-1(YJA) and rop-1* worms was extracted by picking 50 worms into M9 buffer. After several times washing with M9 buffer to remove OP50 bacteria, worms were pelleted and 500µl TRIZOL reagent (Invitrogen) and 1mM EDTA was added. About 300µl of zirconia beads were added and lysis was carried out in a three minutes (10sec on: 10sec off) cycle at 2,500rpm in a multi-beads shocker (Yasui Kikai) at 4°C. 100µl of $CHCl_3$ was added, mixed and left on ice for three minutes. Centrifugation at full speed for 10 minutes was followed by extraction

of the aqueous phase with an equal amount of CHCl$_3$ and precipitation with an equal amount of isopropanol. After centrifugation at full speed for 30min, the pellet was dried and resolved in 20µl formamide loading buffer (750µl formamide, 27µl 37% formaldehyde, 150µl 10xMOPS buffer; 571µl monoQ; 3µl 10mg/ml ethidiumbromide 0.375mg OrangeG). The samples were denatured for 10min at 70°C and run on a MOPS agarose gel (1g agarose boiled in 72ml water until dissolved and cooled to 60°C; 10 ml 10xMOPS running buffer, and 18ml 37% formaldehyde) in 1xMOPS running buffer (0.4 M MOPS, pH7.0; 0.1M sodium acetate; 0.01M EDTA). The gel was analyzed under UV light and capillary northern blotted overnight using 10xSSC buffer. (Brown 1994a)

The probes for the hybridization of the northern blots (Figure 20, page 71) were produced by PCR and random primed labeling (Feinberg and Vogelstein 1983): Probe 1 (5' ETS) was derived from reaction with primer pair 229 5'-CCC GCA CAC TCC TAT ATG-3' and 230 5'-TAC GCA GAC ATA TAG TCT AG-3'; Probe 2 (5' ITS1): Primer pair 241 5'-CTC TGT GCC CGT GAT ATC-3' and 242 5'-CAT CTC AAC TGG AAC GTT G-3'; Probe 3 (3' ITS1): 243 5'-AGG AAG TTA GTT GAC GAT AG-3' and 244 5'-TAT TAT CGA GAT GCA AAT CTC-3'; Probe 4 (ITS2): 233 5'-AAC TCA ATG CCT AGG CT TC-3' and 234 5'-AGC AAG ACA CGC ACC GTC-3'. The PCR products were run on a 2% agarose gel and eluted by Freeze&Squeeze columns (Bio-rad). 50ng PCR product DNA was adjusted to 14µl with monoQ water and denatured by boiling for 5 minutes and put on ice. 20µl LS (25:25:1 of 1M Hepes pH6.6, TM [25:10:0.35 of 1M Tris pH8.0; 25mM MgCl$_2$ and 2-mercaptoethanol] and OL [30U/ml random hexamers]), 6µl CTG nucleotide mix (150 µM of each dCTP, dGTP, dTTP and 2.5mg/ml BSA), 20µCi [32]P dATP and 1µl Klenow fragment (Fermentas) were mixed and added to denatured DNA. The mixture was incubated for 3 hours at 37°C. Free radioactive nucleotides were removed by centrifugation over a Sephadex G-50 column for three minutes at 1,500rpm. The activity was measured and the mixture was boiled for 5 minutes and used as a probe for the northern blots, which were pre-hybridized in Church&Gilbert buffer and reimmersed in 50ml Church&Gilbert buffer. Hybridization was carried out over night at 65°C and the blots were washed twice in 2xSSC/0.5%SDS, and once in 1xSSC/0.5%SDS, 0.5xSSC/0.5%SDS for 10min each at 65°C. Exposure was done on a Kodak storage screen (K-screen).

2.17 Ribosome fractionation

Ribosomes were isolated according to an established method (Brown et al. 1974) with some modifications: Mixed stage N2 and *yrn-1(YJA)* worms from 5 large NGM plates were washed off with M9 and rinsed several times with M9 and centrifuged at 800g in between. The worm pellet was resuspended in 1ml ribosomal buffer D (0.1M KCl; 5mM MgCl2; 1mM β-mercaptoethanol; 0.1mM EDTA; 50mM Tris pH7.8; 1% Sodium deoxycolate, 20mM vanadyl ribonucleoside-complex and Roche complete-Mini proteinase inhibitor cocktail). About 300µl of zirconia beads were added and lysis was carried out in a three minutes (10sec on:10sec off) cycle at 2,500rpm in a multi-beads shocker (Yasui Kikai) at 4°C. The lysate was centrifuged twice for 15 minutes at 14,000rpm to remove cell debris and the mitochondrial fraction and the supernatant – avoiding the fatty surface layer – was loaded onto a continuous 10%-50% (w/v) sucrose gradient prepared in ribosomal buffer E (50mM KCl; 2mM MgCl2; 1mM β-mercaptoethanol; 50mM Tris pH7.8). The gradient was ultra-centrifuged for 10 hours at 23,000g at 4°C using a SW28 rotor in a Beckman LE80 ultra-centrifuge. The gradient was fractionated from the bottom in 1ml fractions and the RNA content was determined by mixing 2µl sample with Ribogreen reagent (Molecular Probes; 1:2000 in TE) and measuring in a in a Bio-rad Versafluor fluorometer (excitation at 490 nm, emission monitored at 520 nm).

Peak fractions were pelleted (SW55; 36,000g for 6 hours at 4°C) and sent to Professor Knud Nierhaus at MPI Molecular Genetics, Berlin, Germany, where two dimensional polyacrylamide gel electrophoresis (2D-PAGE) was carried out.
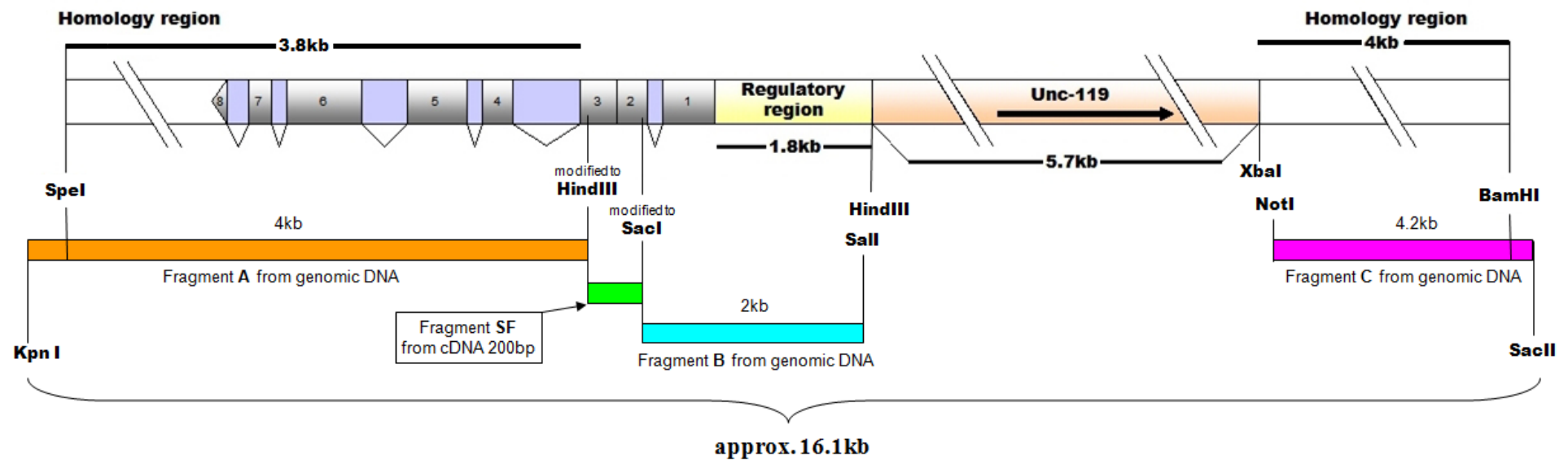
Figure 5: Cloning scheme of the *yrn-1* targeting construct, in a Bluescript vector, used for homologous transformation of *unc-119* mutants by biolistic transformation.
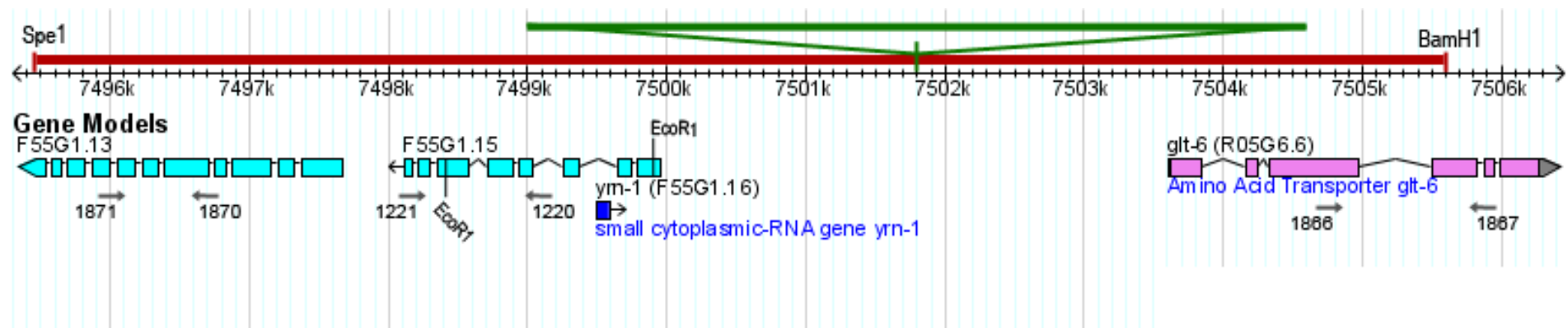

Figure 6: Genomic context of the *yrn-1* gene (modified from www.wormbase.org release WS199). The range of the *yrn-1* targeting construct is indicated in red and the insertion site of the *unc-119* locus marked in green. Charted primer pairs refer to Figure 10 and the actual positions are marked by arrow heads.
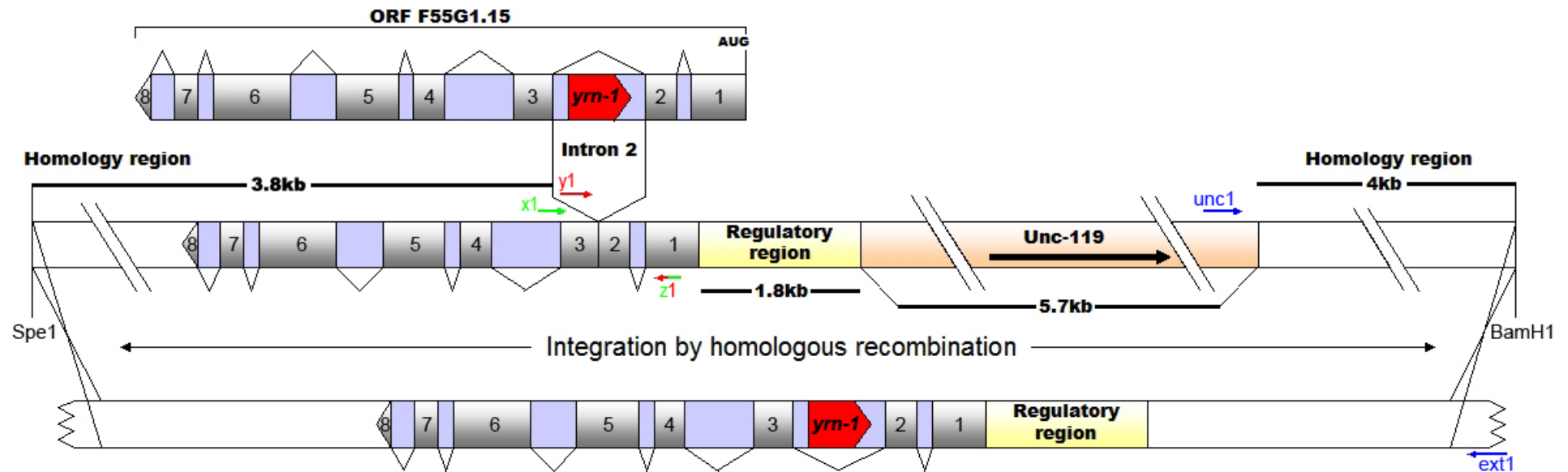
Figure 7: *Yrn-1* targeting construct: Intron 2 of ORF F55G1.15 (upper part) was removed in a construct (middle part) by merging Exon 2 an 3 without influencing the encoded amino acid sequence. Leaving 1.8kb of potential regulatory region for F55G1.15 the *unc-119* region was inserted upstream. 3.8kb of potential homology region was left 5' of the site where exon 2 was removed and 4kb respectively next to the *unc-119* region at the 3' end. Naturally occurring restriction sites Spel and BamHI (cutting uniquely) were used to release the construct for bombardment. Homologous recombination at the desired region is schematically depicted (lower part). Indicated primer pairs refer to Figure 8.
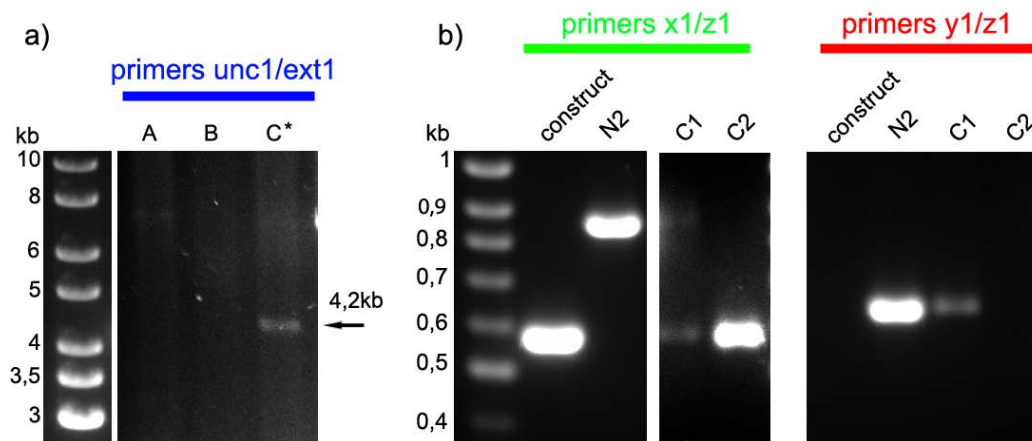

Figure 8: a) Detection of the homologous integration of the *yrn-1* targeting construct. Three transformants (*dauer* worms A, B and C) scored from bombardment 75 and singled. After growing P0 animals were lysed and PCR using primer pair unc1/ext1 (see Figure 7) was carried out. Worm C is a homologous integrant, while A and B are non-homologous. **b)** F1 generation of worm C was singled. PCR using primer pairs x1/z1 and y1/z1 was carried out. Strain C1 is heterozygous for *yrn-1*, while C2 is a homozygous *yrn-1* knockout worm.

45

3 Results

3.1 A Knockout of the *C. elegans* Y RNA encoding gene *yrn-1*

In order to investigate about the *in vivo* functions of the *C. elegans* Y RNA we generated a knockout of the *yrn-1* gene (Figure 7, page 45). We therefore employed the method of homologous gene targeting by biolistic transformation (Berezikov et al. 2004), which we modified for our purpose. This method allows transformation of *C. elegans* by microparticle bombardment that can lead to homologous recombination between the introduced DNA and the chromosomal locus. A selection marker included in the transformation-construct allows the selection of transformed animals. In this method the *unc-119* locus is used as a selection marker and *unc-119* mutant worms are used as target of the transformation. These *unc-119*(*ed3*) mutants are movement impaired due to their severe *uncoordinated* phenotype. They are also defective in the formation of *dauer* larvae in starved conditions. Thus, untransformed animals will starve and die within a few weeks after the transformation, while transformed animals can move to find food, multiply and survive after entering *dauer* stage. The original method (Berezikov et al. 2004) as well as a published implementation (Jantsch et al. 2004) had the aim to knockout conventional protein coding genes and therefore the *unc-119* marker was placed in a way to disrupt an exon of the open reading frame of the gene of interest. In the case of the *yrn-1* gene, the aimed target is embedded in intron 2 of the open reading frame F55G1.15 encoding for the nematode-specific, uncharacterized protein WP:CE35980. Accordingly the disruption of the *yrn-1* gene by the 5.7kb *unc-119* locus would also disrupt the surrounding protein coding gene WP:CE35908.

Therefore in the *yrn-1* targeting construct the complete intron 2 of F55G1.15 was deleted, thus merging exon 2 and 3. Degenerate primers for the introduction of restriction sites of PCR fragments of different sub-cloning fragments were designed in a way to prevent a change in the encoded amino acid sequence of the WP:CE35980 protein. The following orientation data are relative to the *yrn-1* gene on the plus-strand, while the F55G1.15 ORF is located on the minus-strand (as depicted in Figure 7, page 45): The targeting construct consists of a 3.8kb chromosomal homology region directly upstream of the deletion site, which ends with exon 3 of

ORF F55G1.15 at the 3'-side. Directly downstream from the deletion, 2kb of unedited genetic locus are guaranteeing that the regulatory region of F55G1.15 remains intact. This part starts with exon 2 of F55G1.15 at the 5'-side which results in a combination of exon 2 and 3 to form one single merged exon and a deletion of intron 2. The 3'-end of the potential F55G1.15 regulatory region in an intergenetic section of the chromosome is adjacent to the 5.7kb *unc-119* locus (including *unc-119* regulatory elements) further downstream from the deletion site. Downstream of the *unc-119* locus another 4kb homology region is located at the 3'-end of the construct. All sequences of exonic regions of the final construct were verified by sequencing. The construct was released from the vector using naturally occurring endogenous restriction sites SpeI (5'-end) and BamHI (3'-end), allowing that both ends were perfectly homologous to the sites of desired recombination. Using the released construct featuring the *unc-119* marker, *unc-119* mutant worms were transformed as described by Bereznikov et al (2004).

3.2   Scoring for transformants and genotyping of *yrn-1* mutants

From 75 biolistic transformations, 173 rescued non-*unc* lines were obtained, grown and analyzed for homologous integration by PCR. (A detailed description of the expected PCR products in case of homologous integration or the wild-type situation, are given in chapter 2.5 and the genomic position of detection primers are indicated in Figure 7, page 45). One internal primer (unc1) at the first possible site within the *unc-119* locus, which is not homologous to the genomic region at the desired integration site as well as one external primer (ext1) directly next to the planned recombination site in the genomic context and not contained in the construct, were used for PCR. One homologous integrant was detected by this reaction as a 4kb product was amplified - as expected in case of the construct integrated at the homologous location. Additional PCRs using primers x1/z1 and y1/z1 showed this integrant to be heterozygous - as the x1/z1 reaction resulted in both the 853bp wild-type fragment and a 574bp *ynr-1* deletion fragment - while a 622bp wild-type fragment was produced in the y1/z1 reaction (Figure 8a, page 45). The progeny were singled and analyses showed that selfing resulted in a Mendelian segregation pattern - a ratio of 1:3 *unc* offspring versus non-*unc* animals) – indicating somatic viability. Further PCR analysis of the F1 generation of the homologous integrant using primer

pair x1/z1 (yielding only the smaller 574bp fragment in the homozygous *yrn-1* knockout worm) and y1/z1 (resulting in no product in the homozygous knockout worm - as primer y1 bind the *yrn-1* gene) confirmed a Mendelian segregation pattern - a ratio of 1:2 homozygous mutants versus heterozygous animals within the non-*unc* offspring. A worm homozygous for the *yrn-1* deletion was picked and grown. This strain carrying the *yrn-1* knockout allele was out-crossed three times and was termed Y5B. Homologous integration and thus the deletion of the *yrn-1* gene was confirmed by Southern blotting of EcoR1 digested chromosomal DNA and detection using a F55G1.15 (exon 4 to 6) probe (Figure 9a, page 48). A chromosomal deletion of roughly 300nt in the F55G1.15 locus was shown, which complies with the removal of 281nt exon 2.No ectopic duplications could be detected. For further confirmation of the genotype, total RNA was northern blotted and the Y RNA was undetectable after hybridization with a labeled *yrn-1* anti-sense probe in the *yrn-1* knockout strain (Figure 9b, page 48). We therefore observe that worms carrying a *yrn-1* null allele are viable.
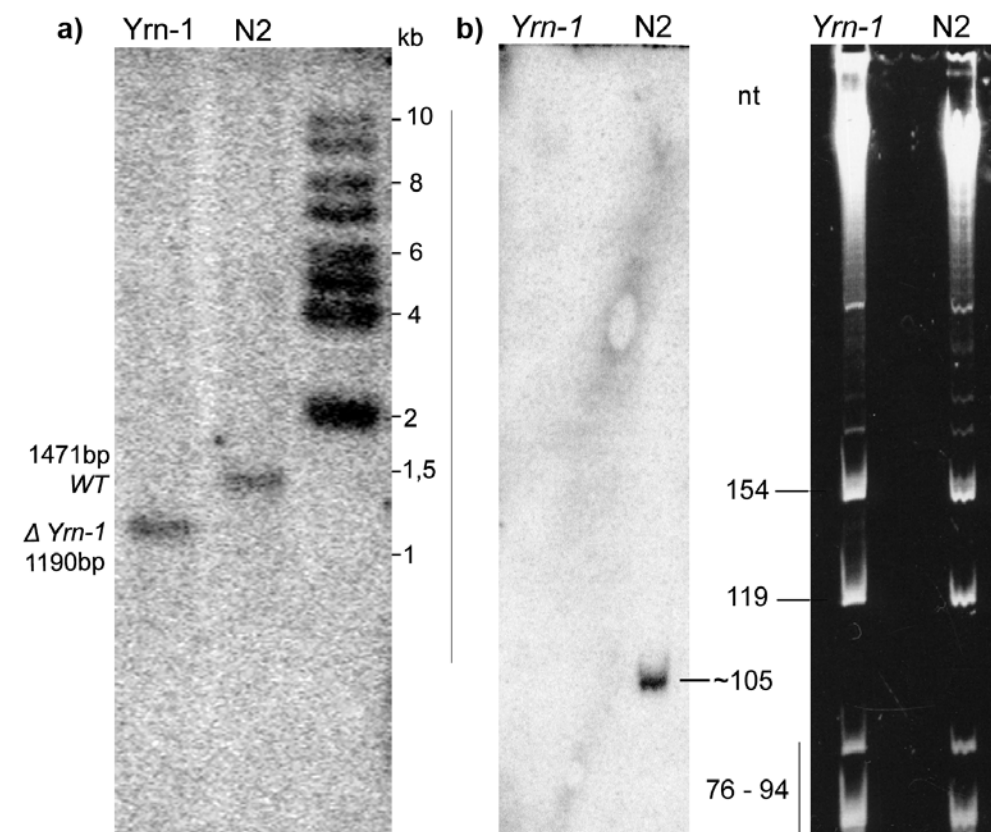

Figure 9: Verification of the genotype of the *yrn-1(Y5B)* knockout strain. a) Chromosomal DNA from strain Y5B and WT was EcoR1 digested, Southern blotted and hybridized to a F55G1.15 anti-sense probe. The fragment bound to the probe in strain Y5B is 281nt smaller than in WT corresponding to the size of the deleted intron 2. b) Northern blot from total RNA (ethidiumbromide stained gel for loading control on the right) was hybridized to a Y RNA anti-sense probe. The Y RNA is missing in Y5B worms.

3.3 Expression of *yrn-1* neighboring genes in the *yrn-1* knockout strain

In order to investigate, if the integration of the *yrn-1* targeting construct at the homologous locus affects gene expression of genes that are partially or completely covered by the construct, we carried out RT-PCR from cDNA of N2 and *yrn-1(Y5B)* worms (using primer pairs indicated in Figure 6, page 44). Expression of the gene *glt-6* (Figure 10 A, page 49) which is encoded in the 3'-homology region of the construct was analyzed using primer pair 1866/1867 A 382bp product of comparable intensity was visible in N2 cDNA and *yrn-1(Y5B)* cDNA samples, but not in RT-minus samples. For the gene product of ORF F55G1.15, primer pair 1220/1221 (Figure 10 B) was used in PCR from N2 and *yrn-1* mutant cDNA template. The expected fragment of 507bp was obtained with comparable intensities. A 738bp product derived from chromosomal DNA template containing intronic sequences is visible in PCR from N2 lysates, but not in the cDNA samples. Neither with cDNA templates from N2 worms nor from *yrn-1* mutants, did PCR of F55G1.13 ORF (primer pair 1870/1871) result in a product. However, the expected fragment was obtained in PCR from N2 genomic DNA (not shown). A control for the concentration of the cDNA template from N2 and *yrn-1* mutants was carried out using primer pair 1124/1125 (Figure 10 C), which amplifies the unrelated germline gene *spo-11*. This PCR resulted in the expected 501bp exonic product, but not in the 660bp product projected in the case of chromosomal DNA contamination. Intensities of N2 and *yrn-1* 1124/1125 products were similar and show that the concentration of cDNA samples and accordingly the expression of the genes tested, is equal
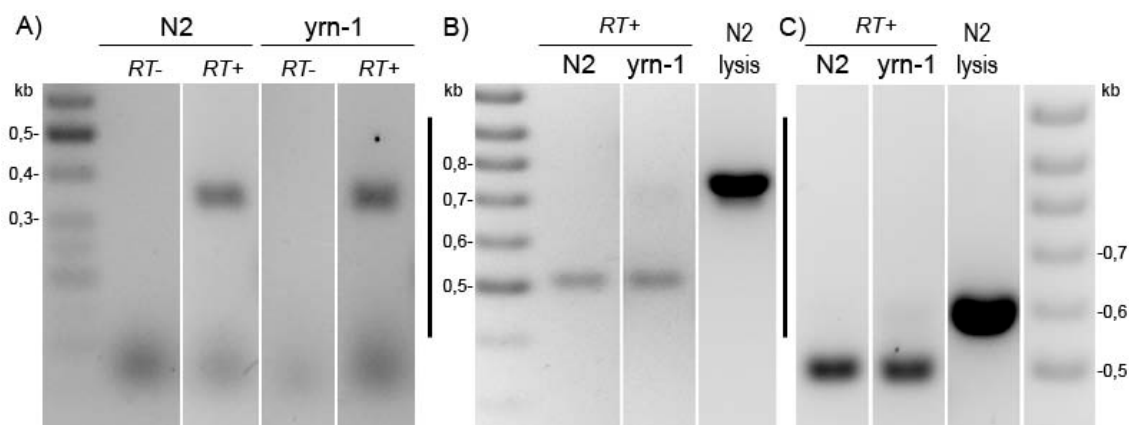

Figure 10: Analysis of the expression of genes situated within the borders of the *yrn-1* targeting construct. RT PCR from N2 and *yrn-1* samples: Primer pairs used are indicated in Figure 6 A) *glt-6* (primer pair 1866/67) yield expected 382bp product in RT+PCR but no product in RT- PCR. B) F55G1.15 (primer pair 1220/21) RT+ PCR results in expected 507bp product, obviously smaller than 738bp genomic version in PCR from lysate. C) Control of concentration of the cDNA template (used also as template in other RT+ reactions): N2 and *yrn-1* RT+ PCR using primer pair 1124/1125 to amplify the unrelated meiotic gene *spo-11* result in expected 501bp product of equal intensity, while PCR from lysate yields 660nt product.

3.4 An additional *yrn-1* deletion strain

Additionally to the *yrn-1* (Y5B) knockout strain, which was created by homologous recombination, a deletion mutant of the *yrn-1* gene was obtained from the *Japanese National Bioresource Project for the nematode*. Allele *tm2634* is a 191nt deletion that covers the 5'-part of ORF F55G1.15 exon 3 as well as the 3'-part of intron 2 (Figure 11 left side, page 50). This deletion also includes a 25nt truncation of the 5' end of *yrn-1,* encoded on the minus-strand of the F55G1.15 ORF. This deletion completely removes the 5'-end of the Y RNA and thus one strand of the helix, which forms the Y RNA stem (Figure 11 right side, page 50). The strain *yrn-1* carrying deletion allele *tm2634* was outcrossed three times and will be referred to as *YJA.* The Y RNA is not detectable on a northern blot in the strain *YJA* using a full length antisense probe (Figure 12, page 51). The deletion allele of this strain also affects the uncharacterized, nematode-specific ORF F55G1.15, which harbors *yrn-1* in its intron 2. Forty-four nucleotides of the 3' part of exon 3 of F55G1.15 open reading frame are deleted, leading to a non-sense mutation after amino acid residue 89 in the protein. This is a theoretical assumption not taking into account the effect on splicing after deletion of the 5' splice site. Expression of the F55G1.15 gene product in YJA worms was not analyzed for this study.
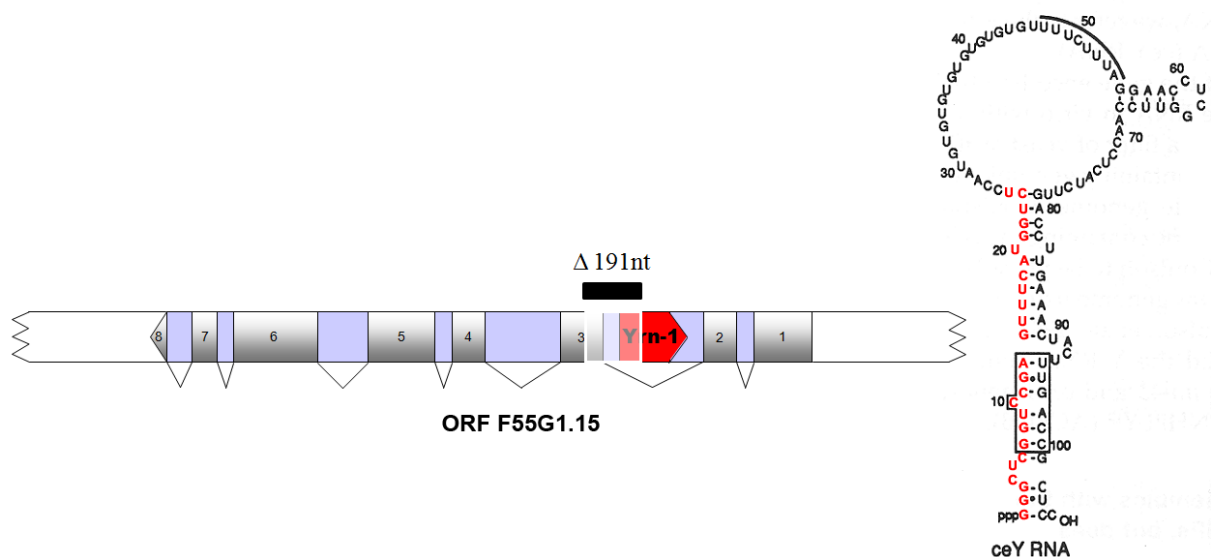

Figure 11: Genomic structure of *yrn-1* deletion strain *YJA* (left) and fold of the *C. elegans* Y RNA (right) - nucleotides in red are deleted in strain *YJA* (modified from Van Horn et al. 1995)
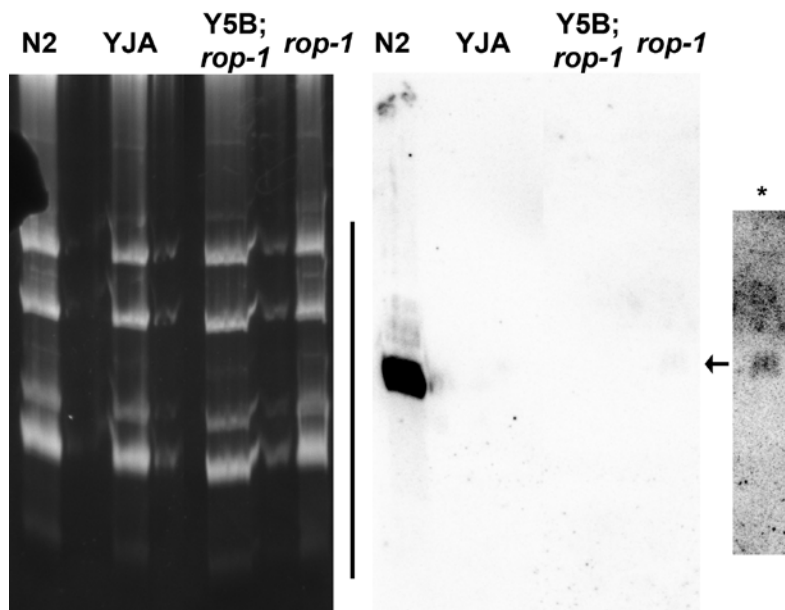
Figure 12: Northern blot confirming Y RNA deficiency in *yrn-1(YJA)* strain and in *rop-1;yrn-1(Y5B)* double mutants. Total RNA gel was ethidium-bromide stained (left) and the corresponding Northern blot (right) hybridized to a *yrn-1* anti-sense probe. The Y RNA signal is only detectable in the N2 and in *rop-1* mutants, where the intensity was calculated to be about 100 times reduced.

*Signal in the *rop-1* mutant lane highly overexposed.

3.5   Y5B versus YJA strain

Yrn-1 mutants of the homologous recombination knockout strain Y5B show a defect in chemotaxis, which became first obvious as worms tended to leave the agar and dry out on the wall of the petri-dish at a high rate. Since this phenotype did not appear in the deletion strain YJA, it seems to be caused by changes in the expression levels or rather pattern of UNC-119. The expression of UNC-119 is highly regulated and only occurs in GABA motor neurons in wild-type (Knobel et al. 2001). In the Y5B knockout strain an *unc-119* mutant is rescued by the *unc-119* locus, which is used as marker gene in the targeting construct. The *unc-119* locus includes the promoter region, however, it cannot be excluded that UNC-119 expression is also regulated by trans-elements or the chromatin structure at the native genomic position. Therefore phenotyping of *yrn-1* mutants was mainly carried out using strain YJA, which as the Y5B strain overall behaves wild-type under laboratory conditions.

3.6   Fertility and lifespan of *yrn-1* (YJA) mutants

Homozygote *yrn-1 (YJA)* as well as *Y5B* knockout worms did not show any obvious morphological phenotype. No difference in embryonic, larval or vulva development or anatomy was apparent. Y RNA deletion worms *(YJA)* showed practically wild-type fertility levels (Table 1, page 52) at both 14°C and 25°C in an average from more than five experiments. The experiments were additionally carried out with the *rop-*

1(pk93) mutant strain. A slightly stronger defect in fertility for *rop-1* worms, which only reach 87% of WT fertility at 14°C and 84% at 25°C. Fertility was analyzed by scoring progeny that reached L3/L4 larval stages. As *yrn-1* mutants did not show any obvious embryonic lethality, a rate of occurrence of embryonic lethality was not determined.

Life span at 25°C was analyzed in three independent experiments (Figure 13, page 52). The life span of N2, *yrn-1 (YJA)* and *rop-1* mutants was similar. However, on average there were more Y RNA deletion mutants dying in the early part of the experiment, while the death rate became lower compared to WT worms the longer the experiment was running. In total this trend resulted in a very similar average lifespan of 12.2 days for *yrn-1* mutants compared to 12.11 days for N2 worms. *Rop-1* mutants showed a slightly lower average life span of 11.7 days.

strain / assay temperature	14°C	25°C
N2	284.6 (±12.4; 10)	156.9 (±17.6; 7)
Yrn-1(YJA)	273.9 (±11.9; 10)	151.2 (±7.5; 6)
Rop-1	246.4 (±11.1; 9)	131.9 (±13.5; 9)

Table 1: Fertility of WT, *Yrn-1* (YJA) and *Rop-1* worms: Offspring reaching L3/L4 larval stage was scored. The average number of progeny (±SEM; number of individuals whose total progeny was scored). Only the reduction of the fertility of *rop-1* mutants at 14°C is statistically significant (paired t-test p= 0.037).
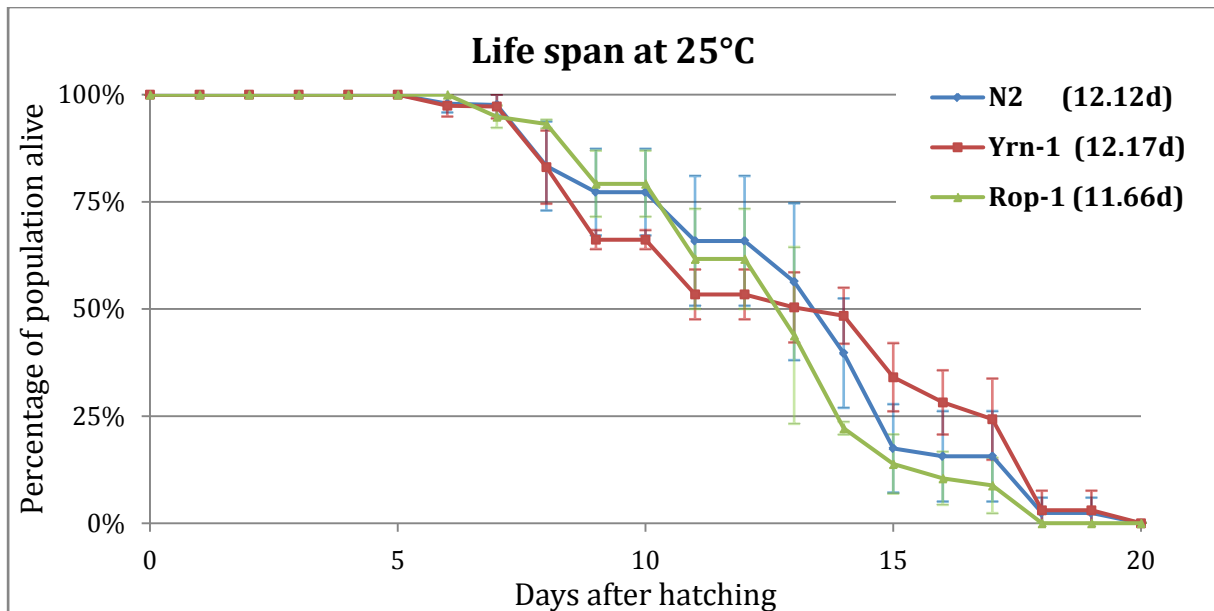

Figure 13: Life span of N2, *yrn-1 (YJA)* and *rop-1* worms at 25°C. The error bars correspond to standard errors and the average life span is indicated in parentheses. 3 independent experiments were carried out (n=20 worms per strain and experiment).

3.7 *Yrn-1* mutants show a higher resistance to UV irradiation

The Ro60 protein has been shown to play a role in facilitating cell survival upon UV irradiation. This was initially shown for *Deinococcus radiodurans*, where deletion of the Ro60 orthologue RSR leads to massive reduction of the resistance against UV irradiation and the expression of RSR is increased after UV irradiation (Chen et al. 2000). Similar observations were made in mouse embryonic stem cells, which show a lower survival rate upon UV irradiation. Also the mouse Ro60 orthologue translocates to the nucleus following UV irradiation (Chen et al. 2003). These results led us to the question, if deficiency of ROP-1 or the Y RNA, respectively, might have an influence on UV sensitivity in *C. elegans*

Young adult worms were singled and irradiated at 1.8kJ/m² by 254nm UV irradiation. After the irradiation worms were kept at 20°C and every 24 hours dead worms were counted. This assay showed a significantly lower death rate of *yrn-1(Y5B)* mutant worms and higher death rate of *rop-1* mutants compared to the wild-type (Figure 14 top, page 54). For N2 the half life of the population was calculated at 55.4 hours and for *yrn-1(Y5B)* mutants at 72.2 hours (which is 30% longer than WT, paired t-test p=0.05) The experiment was repeated with the YJA strain (Figure 14 bottom, page 54) In this set of experiments the half lives were 54.9 hours for N2; 63.1 hours for *yrn-1* (YJA) mutants; The *rop-1* mutant showed a significantly reduced resistance to UV irradiation: In a total of 10 assays from both series *rop-1* mutant populations showed an average life span of 50.1 hours (7.3% shorter than average of N2 in these 10 experiments). Thus we observe a higher sensitivity to UV irradiation in the absence of the ROP-1 protein, which has proposed to function in RNA quality control. Furthermore, we observed a higher resistance to UV irradiation in the absence of Y RNAs and the higher UV resistance was detected in both *yrn-1* (*Y5B* and *YJA*) strains.
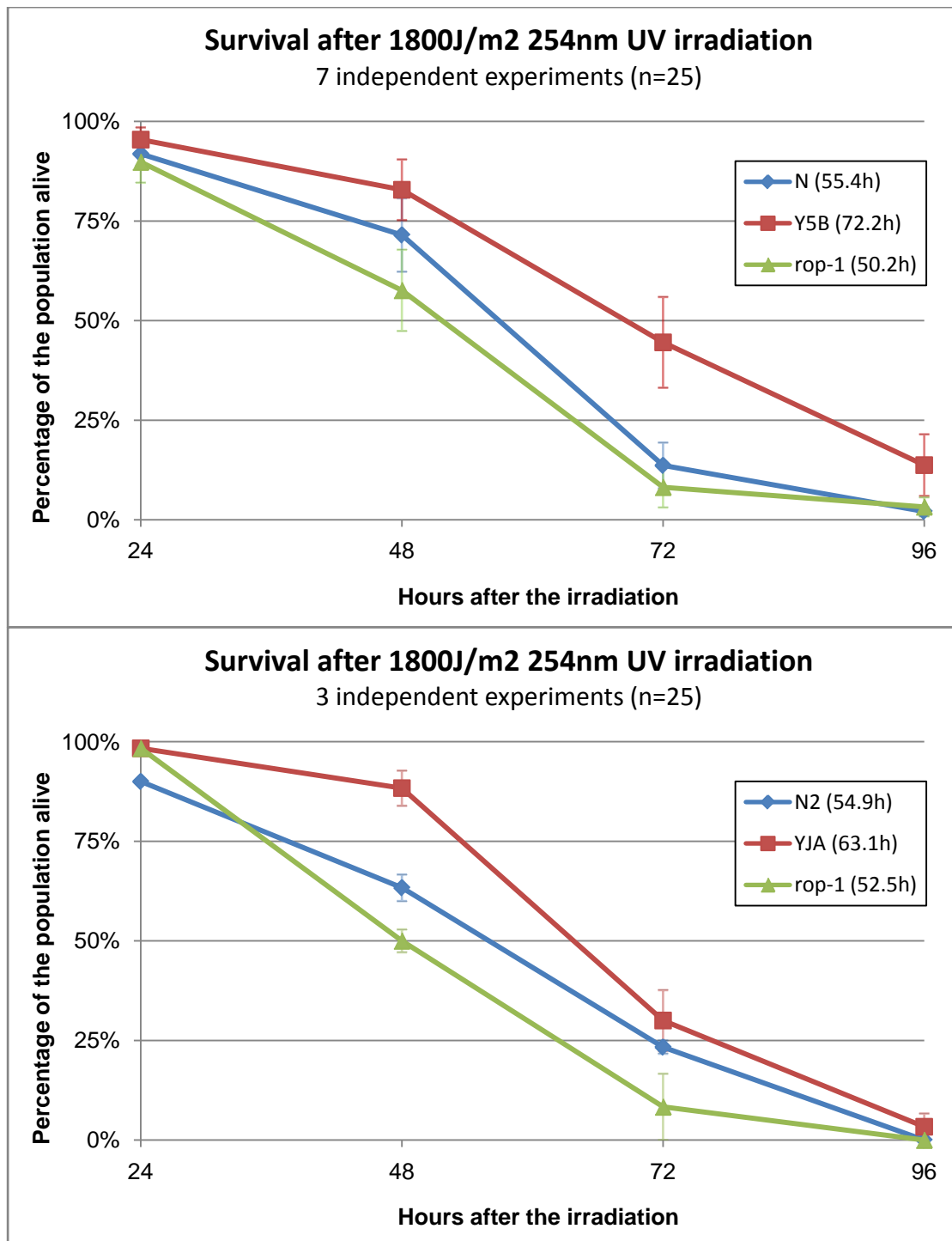
Figure 14: Survival after UV irradiation. 25 worms per strain and experiment were used, average life span after irradiation in parentheses. Worms were irradiated with 1.8kJ/m² at 254nm UV light and dead worms were counted every 24 hours. *Yrn-1(Y5B)* mutants (upper diagram) showed a significantly higher resistance to UV irradiation in 7 independent experiments (paired t test p=0.05). The experiments were confirmed with the *yrn-1(YJA)* mutant strain in 3 independent experiments resulting in a similar trend. *Rop-1* mutants show a lower survival rate than wild-type worms and this reduced resistance to UV irradiation is significant for the average life span of 55.2 hours for wild-type and 50.9 hours for *rop-1* worms in all 10 experiments from both series (paired t test p=0.05).

3.8 *Dauer* formation in the absence of Y RNA

A previous study demonstrated an involvement of the ROP-1 protein in formation of *dauer* larvae. It was shown that *rop-1* mutants do not readily form *dauer* larvae under starved and crowded conditions. Additionally it could be demonstrated that lack of ROP-1 dramatically enhances *dauer* formation together with *daf-2* alleles *e1370* and *m579*, but reduces *dauer* formation in combination with allele *m41* and *m596*. (Labbé et al. 2000)

We analyzed *dauer* larvae formation in *yrn-1* mutants. In contrast to the *rop-1* strain, *yrn-1* (*YJA* and *Y5B*) mutant worms are able to form *dauer* larvae in starved and crowded conditions and no difference in the disposition to do so was obvious, compared to wild-type worms. However as quantitative assays cannot be carried out under these conditions, *daf-2* alleles from two previously characterized allelic classes (Gems et al. 1998) *e1370* (class-I) as well as *m41* (class-II) were crossed into *yrn-1* (YJA) mutants. The *dauer* larvae formation assay was carried out according to Labbé et al. (2000) at 20°C and 22.5°C, respectively. Additionally to the *daf-2* single mutant and the *yrn-1;daf-2* double mutant, also the corresponding *rop-1;daf-2* double mutant was employed (Table 2, page 56). At 20°C *daf-2(e1370)* single mutant and the *daf-2(e1370);yrn-1(YJA)* double mutant produced very similar levels of *dauer* formation, while the *daf-2*(*e1370*);*rop-1* double mutant showed a more than ten times higher disposition to form *dauer* larvae. At 22.5°C the *daf-2*(*e1370*);*rop-1* double mutant formed twice as many *dauer* larvae compared to the *daf-2*(*e1370*) single mutant. Interestingly at this temperature *dauer* formation of the *daf-2*(*e1370*);*rop-1* and the *daf-2*(*e1370*);*yrn-1* double mutant, respectively, behaved very similar with only a slightly lower rate of *dauer* larvae formation in the latter.

Dauer formation of worms carrying the class-I *daf-2* allele *m41* was also analyzed in the *yrn-1* and *rop-1* background. At 20°C low *dauer* formation rates were observed for all three strains. Yet the *daf-2(m41)* single mutant showed a more than 10 times elevated *dauer* formation rate than the *daf-2(e1370)*;*rop-1* double mutant. Interestingly enough no *dauer* formation at all was observed in the *daf-2(m41);yrn-1* double mutant strain at 20°C. At 22.5°C the *daf-2(m41)* strain formed more than 86% *dauer* larvae on average while *dauer* formation was massively reduced by the absence of the ROP-1 protein but even stronger in the absence of the Y RNA.

In summary we could show that *yrn-1(YJA)* mutantion background negatively influence the *dauer* formation rate in a *daf-2(m41)* mutant. Thus it resembles the *rop-1* null allele in this respect - however, the impact of the *yrn-1* deletion is more severe. In the genetic background of the *daf-2(e1370)* allele, *yrn-1* deficiency positively affects *dauer* formation, but only at higher temperatures, while *rop-1* mutants show elevated *dauer* formation rates in this background independent of the temperature. Our results confirm previous observation of Labbé et al. (2000) concerning *dauer* formation in a *rop-1* mutant background.

	20°C			22,5°C		
Allele	Mean	±SEM	N	Mean	±SEM	N
daf-2(m41)	1.65%	±0.39%	2647 †	86.10%	±1.51%	2582 *
daf-2(m41);rop-1(pk93)	0.15%	±0.46%	2066 †	14.01%	±2.20%	2847 *
daf-2(m41);yrn-1(YJA)	0,00%	±0.00%	3180 †	2.21%	±0.54%	3670 *
daf-2(e1370)	1.26%	±0.24%	4093 §	40.48%	±2.96%	877 ‡
daf-2(e1370);rop-1(pk93)	20.17%	±2.36%	2520 §	82.32%	±2.99%	888 ‡
daf-2(e1370);yrn-1(YJA)	1.71%	±0.21%	3631 §	75.95%	±4.63%	1164 ‡

Table 2: *Dauer* formation rates of worms carrying class-I *daf-2* allele *m41* or class-II *daf-2* allele *e1370* alone or in the background of the *yrn-1*(YJA) or the *rop-1* null allele respectively.
† Values ± standard error was calculated from the percentage of *dauer* larva formation among progeny (complete broods) of 12 individual animals in 1 experiment.
§ Progeny of 13 individual animals in 2 independent experiments.
* Progeny of 20 individual animals in 2 independent experiments.
‡ Progeny of 21 individual animals in 3 independent experiments.

3.9 Expression of ROP-1 in absence of *yrn-1*

The Ro60 protein has been shown to influence the stability of Y RNAs *in vivo*. In *C. elegans* the levels of Y RNA were shown to be dramatically reduced in the absence of ROP-1 (Labbe et al. 1999b) and we could confirm these results (Figure 12, page 51). We wanted to find out if Y RNA deficiency has an effect on ROP-1 expression. Therefore protein extracts of wild-type as well as *yrn-1* and *rop-1* mutants (from 50 handpicked worms) were separated via SDS-PAGE. Immunoblotting using an anti-ROP-1 antibody showed that ROP-1 expression and stability is not affected in *yrn-1* mutants, while no signal was detectable in *rop-1* mutants (Figure 15, page 57). This indicates that the presence of the Y RNA is not essential for ROP-1 expression or stability.
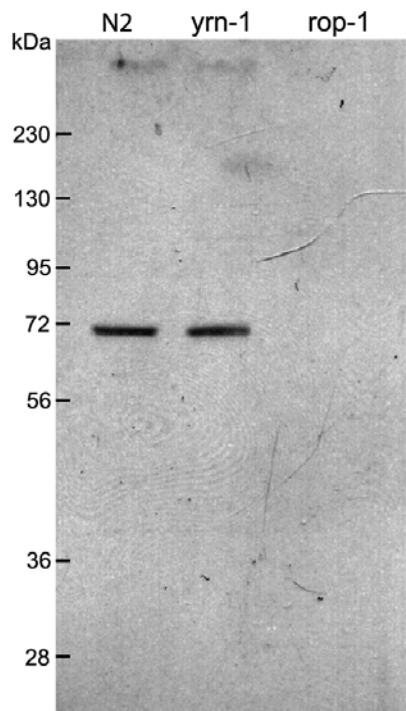
Figure 15: ROP-1 is stably expressed in Y RNA deficient worms. Adult worm protein extracts of 50 hand-picked wild-type (N2), *yrn-1* or *rop-1* mutant worms were fractionated by SDS-polyacrylamide gel electrophoresis (PAGE). Immunoblotting was carried out using a polyclonal anti-ROP-1 antibody.

3.10 Immunoprecipitation of ROP-1 in WT and *yrn-1* deletion strain

As the *Xenopus laevis* orthologue of ROP-1 was shown to possess an extensive RNA binding domain and the Y RNA was proposed to regulate access of other RNAs to this domain (Stein et al. 2005; Fuchs et al. 2006). We therefore wondered, if binding preferences of the ROP-1 protein for RNAs is altered in the absence of Y RNAs.

To address this question, we carried out a co-immunoprecipitation (co-IP) of ROP-1 from worm lysates of N2 and the *yrn-1(YJA)* deletion strain (Figure 16, page 58). A Y RNA band (105nt) appears in the ROP-1 IP from WT worms but is absent from the IP performed with *yrn-1* mutants. The Y RNA is also not visible if not enriched by ROP-1 IP in wild-type. Bands corresponding to 5.8S rRNA, 5S RNA, pre-tRNAs and tRNA are visible on the ethidiumbromide stained gel and apart from the pre-tRNAs, also in the N2 IP and *yrn-1* IP lanes. The mock IP sample was hundred times over-exposed for comparison, but only 5S and 5.8S bands are visible. Additionally there are several bands of unknown identity visible in both IP samples and two bands (k and l) only become visible if the Y RNA is missing. Counts on the autoradiograph of the different bands in N2 and *yrn-1* IP samples were measured and the local background was subtracted. The ratio for all visible bands in WT and *yrn-1* mutant was compared (Table 3, page 59). We also calculated a second ratio without taking highly

expressed ribosomal RNAs (5S rRNA and 5.8S RNA) and tRNA and the Y RNA in WT into account in order to perceive the changes of ROP-1 binding to low abundance targets. These results indicated a slight disposition of ROP-1 to bind higher molecular RNA targets in the absence of Y RNAs.

As we could not detect major changes in the RNA binding properties of ROP-1 in the absence of Y RNA, we did not further pursue these assays.
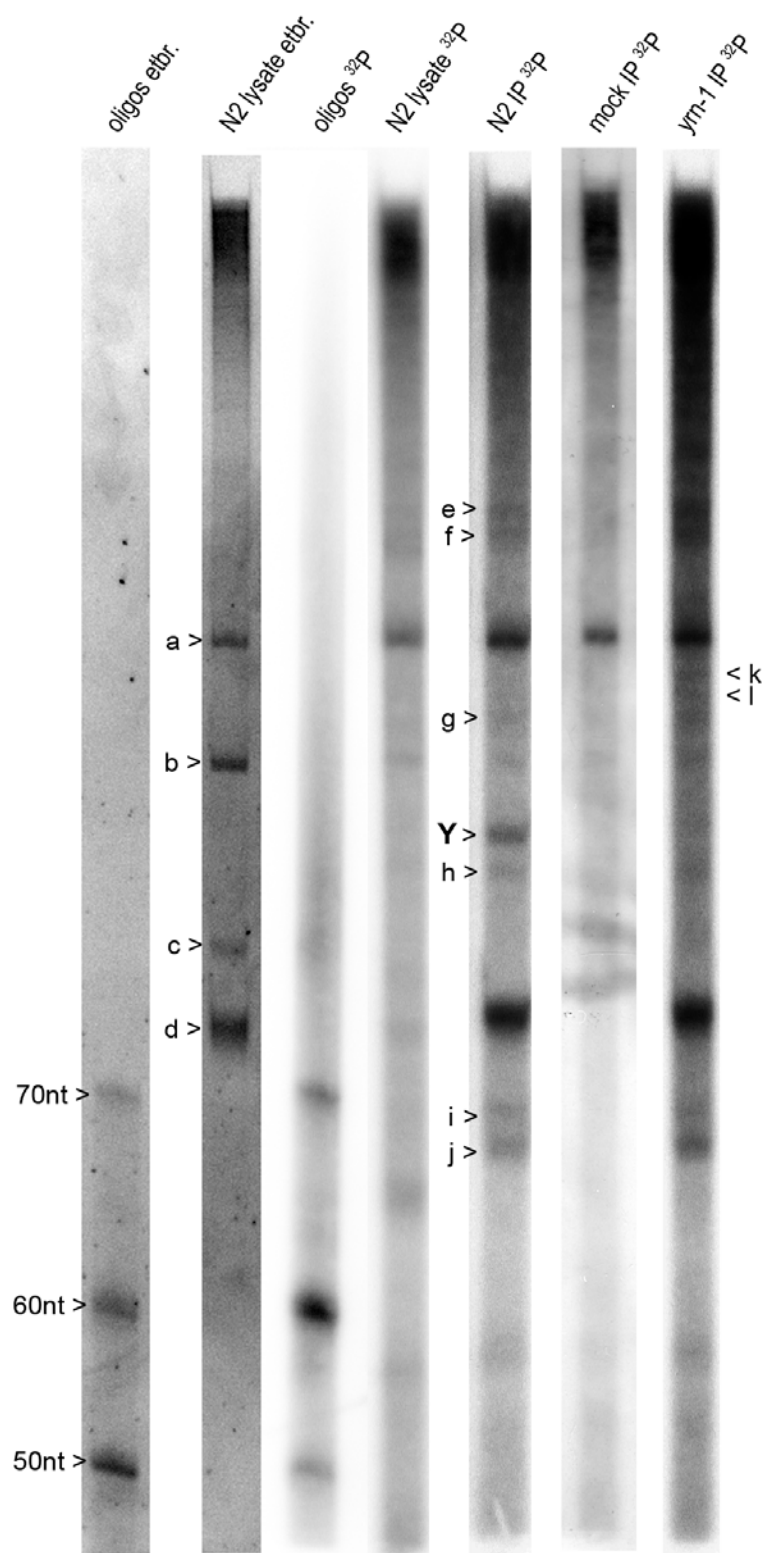

Figure 16: Analysis of RNAs co-immunoprecipitated by the anti-ROP-1 antibody. N2 total lysate as well as N2 IP, *yrn-1(Y5B)* IP and mock IP samples were used together with oligonucleotides to indicate RNA sizes. The first 2 lanes show ethidiumbromide staining of the total lysate sample and the oligonucleotides (50, 60 and 70nt). No signal was visible by ethidiumbromide staining in the IP lanes. The Y RNA band is indicated (Y) and is only visible in the labeled ROP-1 co-IP from N2 worms. The mock-IP was 10 times over-exposed, while the N2 lysate lane was exposed only a tenth of the time compared to N2 and *yrn-1* IP. Known bands are: a) 5.8S rRNA (154nt), b) 5S RNA (119nt), c) pre-tRNAs and d) tRNAs and intensity of all indicated bands (a-l) was measured (see Table 3).

Band (RNA species)	N2 α-ROP-1 IP	*Yrn-1* α-ROP-1 IP	Effect of *yrn-1* deficiency
e	0.04 (0.17)	0.06 (0.17)	↗ (=)
f	0.023 (0.11)	0.04 (0.11)	↗ (=)
a (5.8S rRNA)	0.28 (-)	0.27 (-)	=
k	-	0.07 (0.2)	new
l	-	0.07 (0.15)	new
g	0.05 (0.24)	0.05 (0.13)	= (↘)
b (5S RNA)	0.02 (-)	0.03 (-)	=
Y (Y RNA)	0.11 (-)	-	missing
h	0.04 (0.17)	0.03 (0.09)	= (↘)
d (tRNAs)	0.38 (-)	0.34 (-)	=
i	0.03 (0.14)	0.02 (0.04)	↘ (↘)
j	0.03 (0.17)	0.04 (0.1)	= (↘)

Table 3: Relative intensity of bands derived from the ROP-1 co-IP of N2 and *yrn-1* lysates (see Figure 16). Local background values were subtracted before calculation of ratios. The Ratios In parentheses were calculated without including ribosomal constituents (5.8S RNA; 5S RNA; tRNAs) and the Y RNA band in N2., The ratio for the Y RNA intensity is 0.33, if these RNAs are not taken into account.

3.11 RNAi screen for synthetic enhanced lethality and reduced fertility

Our previous experiments did not indicate a phenotype that would negatively influence the fitness of *yrn-1* knockout worms. As Y RNAs however are highly conserved and present in all animal cells an evolutionary advantage of animals expressing the native Y RNA could be expected. However the adverse effects of Y RNA depletion might not be obvious under laboratory conditions or possibly only occur in combination with the depletion of Y RNA interacting factors. We therefore carried out a conditional RNAi screen for enhanced lethality and reduced fertility in order to systematically identify synthetic genetic interactions between the Y RNA and other genes. We screened 2,937 RNAi feeding constructs from chromosome II and 2,692 from chromosome IV in wild-type and in the *yrn-1* mutant background. The RNAi clones were obtained from *Geneservice.co.uk* and are part of a *C. elegans* genome-wide RNAi library (Fraser et al. 2000; Kamath et al. 2003). Wild-type and *yrn-1* larval stage 1 worms were grown in liquid culture of bacteria expressing double stranded RNA until the F1 generation had hatched. Wild-type and *yrn-1* mutants were directly compared and scored for reduced fertility and enhanced lethality and the severity of the phenotype was categorized semi-quantitatively on a scale from 0 (wild-type offspring rate) to 3 (100% embryonic lethality [*emb*] or sterility [*ste*]) in N2 and *yrn-1* mutant background (according to Lehner et al. 2006). Twenty candidate

clones resulted in a more severe phenotype in the *yrn-1* mutant background of more than 2 points compared to wild-type (Table 4, page 60).

Interestingly, 45% of these candidates are believed to function in ribosome assembly and maturation. Another 20% of candidates are known or believed to interact with or modify nucleic acids, while a role in ribosome maturation has not been shown. Another group of 4 candidates (20%) are cytoskeleton constituents and the remaining three candidates do not fall in any of the above groups. Two of these candidates are mitochondrial proteins and one plays a role in the endosome. These results indicate a role for the Y RNA in ribosome biogenesis.

Gene	Orthologue	Possible Function
Ribosome biogenesis (=45%)		
F54C9.9 §	KRI1 (s.c)	A2 site cleavage in early 40S synthesis
Tag-151	TSR1 (s.c)	D site cleavage in late 40S synthesis
E02H1.1	Dim1 (s.c)	A1/A2 site cleavage & 3'small subunit rRNA dimethylation
R05H10.2	NOP4 (s.c)	Large subunit synthesis; 27S pre-rRNA stability, 35S precursor methylation
Pro-2	NOC2 (s.c)	Large subunit nucleolus to cytoplasm transport
Lsm-7 §	LSM7 (s.c.)	U3 snoRNA processing; A0 – A3 cleavage steps; rRNA precursor stability
K07H8.10	‡NCL-202 (h.s.)	Ribosomal protein transport; histone chaperoning in pol I transcription
T13H5.5 †	MRPS18B (h.s.)	Mitochondrial small subunit ribosomal protein
*C44E4.4	La/SS-B (h.s.)	3'TOP ribosomal protein translation; 5S rRNA, RNAse MRP stabilization
RNA binding and processing (=20%)		
Mrs-1	MES1 (s.c.)	methionyl-tRNA synthesis; intronless tRNA transport from nucleus to cytoplasm
F11A10.2	PRP11 (s.c.)	Spliceosome assembly
Tdp-1	HRP1 (s.c.)	Splicing factor; microRNA processing; apoptosis
B0035.11	LEO1	Transcription factor, histone methylation; Retrotransposition regulation
Cytoskeleton (=20%)		
Cap-2 §	CAP2 (s.c.)	Regulation of f-actin and dynactin cytoskeleton polymerization
Arp-1	ARP1 (h.s.)	Dynactin complex assembly; Vesicle transport via microtubules
Amph-1	RVS161 (s.c.)	Actin cytoskeleton polarization; endocytosis
Ssp-32	*Nematode spec.*	Component of the nematode specific major sperm protein cytoskeleton
Other functions		
C18E9.4 †	NDUFB3 (h.s.)	Oxidoreductase in mitochondrial electron transport chain
Gstk-1 †	GSTK1 (h.s.)	Detoxification in mitochondria and peroxisomes
Rab-7 §	RAB7 (h.s.)	GTPase in late endosome trafficking.

Table 4: Candidate clones from a conditional RNAi screen of genes located on chromosomes II and IV showing the strongest effect on fertility in *yrn-1(YJA)* mutant background compared to N2 wild-type in a conditional RNAi screen. First column: *C. elegans* gene name or ORF number. Second column: Gene name of the most closely related characterized orthologue in *Saccharomyces cerevisiae* (s.c.) or *Homo sapiens* (h.s.) if available. Third column: Putative function assigned to the candidate gene or the orthologue (from Wormbase.org; Yeastgenome.org and Uniprot.org)
* RNAi of C44E4.4 (*C. elegans* La orthologue) was not part of the library, but was cloned additionally and was included in validation experiments together with candidates derived from the screen.
§ These clones showed the strongest intensification of the sterility phenotype in the *yrn-1* mutant background.
† These candidates encode mitochondrial proteins.
‡ K07H8.10 is not a nucleolin orthologue but conserves an RRM domain that is homologous to 3 of the 4 Nucleolin RRM domains. A function in ribosome biogenesis is not certain.

3.12 RNAi candidates involved in ribosome assembly

Five of the nine candidate genes derived from the conditional RNAi screen which are involved with ribosome synthesis, play a role in early ribosome assembly and specifically in rRNA processing. Ribosomal RNA processing is a complex procedure and numerous steps, some of which are redundant, are carried out in the nucleolus and on the way through the nucleus to the cytoplasm. (A schematic view of *S. cerevisiae* rRNA processing and the roles RNAi candidate orthologues play in this process is depicted in Figure 17, page 64). The polycistronic 35S precursor a transcript of the nucleolar organizer region (NOR) tandem repeat is processed by several endonuclease and exonuclease cleavage steps. At the same time the transcript undergoes considerable covalent nucleotide modifications, which are guided by small nucleolar RNAs. One pathway, which leads to maturation of the 18S rRNA in the small 40S subunit, is functionally independent of the more complicated pathway which is involved in 60S large subunit 5.8S rRNA and 26S (or in yeast 25S) rRNA processing (reviewed in Fatica and Tollervey 2002).

Interestingly, however, our candidates which are functionally associated with early assembly or rRNA processing, act in different compartments of this procedure and the precursors, which were shown to accumulate upon their depletion, are diverse.

Three candidates (F54C9.9, *tag-151* and E02H1.1) or their yeast orthologues (Kri1p, Tsr1p, Dim1p), were shown to act in small subunit (SSU) synthesis and their depletion led to reduced 18S rRNA levels.

F54C9.9 encodes the orthologue of *S. cerevisiae* Kri1p, which is conserved among eukaryotes. Functionally it is an essential nucleolar protein required for 40S ribosome biogenesis, but not for the 60S subunit. A depletion of Kri1p in *S. cerevisiae* leads to increased 35S and 32S precursor accumulation, but to a reduced production of 18S rRNA and the 20S precursor. The A2 cleavage step was found to be impaired (Sasaki et al. 2000).

TAG-151 (F10G7.1) is an orthologue of *S. cerevisiae* Tsr1p (Twenty S rRNA accumulation). It locates to the nucleolus, acts in late small subunit synthesis and is required for the maturation of the 43S pre-ribosomal subunit – the immature small subunit containing the 20S rRNA precursor - and for its transport from the nucleus to the cytoplasm. Tsr1p is not involved in the assembly of the 60S subunit. In yeast

Tsr1p depletion leads to accumulation of the 35S precursor but moreover to a significant accumulation of the 20S precursor. Thus Tsr1p was shown to act in processing of 20S to 18S rRNA at site D in the cytoplasm (Gelperin et al. 2001).

The E02H1.1 gene product or its *S. cerevisiae* orthologue Dim1p, an adenine dimethylase, is involved in pre-rRNA cleavage at sites A1 and A2, but not the A0 site. This affects the synthesis of the 20S pre-rRNA and the mature 18S rRNA severely, while the 33S precursor accumulates. However, it was found that dim1p is also responsible for the dimethylation present at the 3' end of the small subunit rRNA – a modification conserved between bacteria and eukaryotes (Lafontaine et al. 1994; Lafontaine et al. 1995; Lafontaine et al. 1998).

Two additional candidates (R05H10.2 and *PRO-2*) which are orthologues of yeast Noc2p and Nop4p are defective in the large subunit synthesis. However, it has to be noted that Noc2p is rather involved in 60S subunit transport than in rRNA processing.

The R05H10.2 gene product or its *S. cerevisiae* orthologue Nop4p (alias Nop77p) is an RNA binding protein, as it contains four RNA recognition motifs (RRMs) including one non-canonical RRM. It was shown to be essential for the synthesis of yeast 25S (in *C. elegans* 26S) rRNA and 5.8S rRNA in the 60S large ribosomal subunit and depletion of Nop4p leads to accumulation of the 40S subunit. Either the processing of 27S pre-rRNA is deficient or rather the 27S pre-rRNA is unstable in Nop4 depleted *S. cerevisiae* cells. This could be related to a 35S rRNA methylation deficiency found in the absence of Nop4p (Berges et al. 1994; Sun and Woolford 1994; Sun and Woolford 1997).

The candidate gene *Pro-2* (C07E3.2) or its orthologue Noc2p in yeast encodes for a nucleolar protein Noc2p which is essential for 25S (in *C. elegans* 26S) rRNA and 5.8S rRNA production and thus 60S subunit synthesis. In a *S. cerevisiae* Noc2p depletion, mild a 35S pre-rRNA accumulation and reduced rates of 20S and 27S production were observed and connected to a deficiency in early processing steps (A0, A1, and A2). However, it was shown that Noc2p is not primarily involved in rRNA processing, but plays a role in 66S pre-ribosome transport from the nucleolus through the nucleus to the cytoplasm, where late assembly steps would take place. Therefore, accumulation of pre-rRNA is caused by a deficiency in disassembly and

recycling of nucleolar processing factors, which stay bound to the pre-ribosomal complex, due to the impaired export (Milkereit et al. 2001).

Highly conserved Sm-like proteins (including candidate LSM-7 - ZK593.7) - as related Sm-proteins - were shown to form heteromeric 6- to 7-membered rings. The Lsm2 – Lsm8 complex for instance was shown to stabilize spilceosomal U6 snRNA and function in splicing (Achsel et al. 1999; Mayes et al. 1999; Vidal et al. 1999). Another complex (Lsm1 – Lsm7) functions in mRNA decapping and mRNA decay (Bouveret et al. 2000; Tharun et al. 2000). Lsm proteins were also shown to be involved in pre-rRNA processing and additionally in processing of snoRNAs, which again play an important role in rRNA maturation (Kufel et al. 2003a; Kufel et al. 2003b). Depletion of Lsm proteins Lsm2 – Lsm8 (including candidate gene *lsm-7*) leads to 35S pre-rRNA accumulation and reduction of mature rRNAs, as early processing steps A0 – A2 are impaired, possibly due to lack of mature U3 snoRNA, which is essential for these steps. Additionally 5' – 3' exonuclease steps in 5.8S rRNA processing were deficient and intermediates of unguided 5' - 3' RNA degradation were observed. Interestingly these effects were severe when essential genes Lsm2 - 5 and Lsm8 were depleted, but comparably mild in Lsm6 and Lsm7 depletions, for which Lsm1 is possibly able to substitute (Kufel et al. 2003a). This would agree with our observations of viability of an *lsm-7* depletion in a wild-type background, in contrast to the synthetic phenotype observed in combination with a *yrn-1* mutation background.

A synthetic lethal phenotype was additionally observed with two RNAi clones (K07H8.10 and C44E4.4), whose role in ribosome biogenesis is less clearly defined and one candidate (T13H5.5) which encodes for mitochondrial ribosome protein S18b – a component of the 28S small mito-ribosomal subunit.

The K07H8.10 gene product contains an RRM domain that is homologous to three of the four human nucleolin (NCL) RRM domains. However, it is otherwise not related to NCL and the nucleolin orthologue in the worm is *cec-1.* Nucleolin was shown to function in several ribosome assembly related processes and bind Y RNAs (detailed description in chapter 1.1.3.5). An involvement of K07H8.10 in ribosome assembly is unsure, but binding to Y RNA might be possible via the conserved RRM.

ORF C44E4.4 is located on chromosome I and was not part of the original synthetic RNAi screen, which was limited to chromosomes II and IV. The open reading frame encodes an orthologue of human SS-B/La or *S. cerevisiae* LHP1. La was shown to bind mature Y RNAs and an indirect function in ribosome assembly via translational control of 5'-TOP-containing ribosomal protein mRNAs was shown (for a detailed description see chapter 1.1.3.1). However an interaction of La with Y RNA was not shown in *C. elegans* (Van Horn et al. 1995; Labbe et al. 1999a). We therefore decided to clone an RNAi construct for the La orthologue containing ORF C44E4.4 and to include it in our screen. We found a synthetic lethal phenotype in the *yrn-1* background compared to N2 worms, which indicates a genetic interaction between the *C. elegans* Y RNA and the La orthologue.
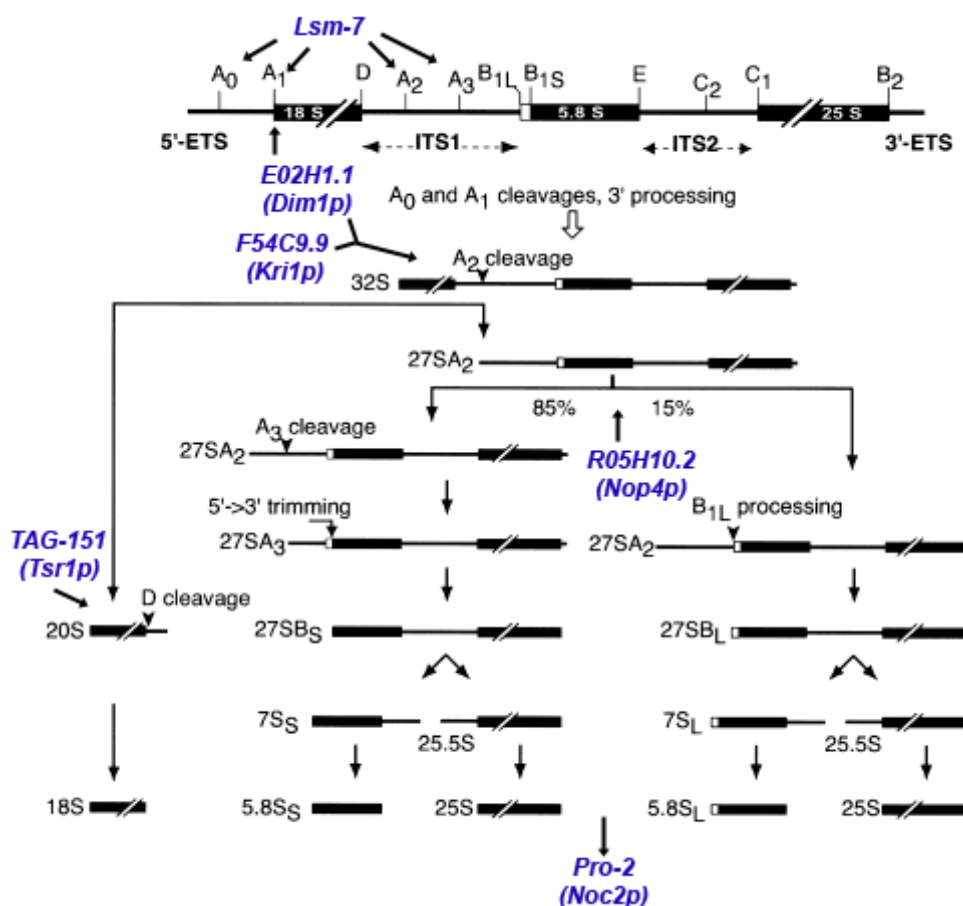

Figure 17: Ribosomal RNA processing in yeast. The 35S primary transcript is cleaved in U3 snoRNA dependent steps at sites A_0, A_1 and A_2 to release the 20S precursor which is transporter to the cytoplasm and further processed at site D to yield the mature small subunit 18S rRNA. The large subunit pathway is more complicated and partly redundant. Processing of a 27S precursor happens via two alternative branches, one of which involves processing by the RNA pol III transcript – the ribozyme RNAse MRP - in the nucleus to synthesize the mature large subunit 5.8S and 26S rRNAs. Candidates found in the RNAi screen that have yeast orthologues with characterized functions in this pathway are indicated in italic script (figure was taken from Fromont-Racine et al. 2003 and modified).

3.13 Other candidate genes found in the RNAi screen

Additionally to the candidates that act in ribosome assembly we found four candidates that are nucleic acid and/or processing proteins, while no function in ribosome assembly has been assigned to them:

MRS-1 (F58B3.5) or its yeast orthologue Mes1p is a cytoplasmic methionyl-tRNA synthetase and catalyzes the attachment of methionine to its cognate tRNA. It is therefore also required for protein biosynthesis, as the ribosomal assembly candidates (Chatton et al. 1987). Additionally Mes1p was also assigned a role in the transport of intronless tRNAs from the nucleus to the cytoplasm (Feng and Hopper 2002).

F11A10.2 or its yeast orthologue Prp11p is a subunit of the splicing factor 3a complex, required for spliceosome assembly (Chang et al. 1988; Vijayraghavan et al. 1989). Interestingly, PRP11 is a part of the U2 snRNP, while misfolded U2 snRNAs were shown to bind the Ro60 protein in mice (Ruby et al. 1993; Chen et al. 2003).

TDP-1 (F44G4.4), a human TAR DNA Binding Protein (TDBP or TDP-43) orthologue contains two RRM domains, structurally resembles a typical hnRNP protein family member. It was identified as a regulator of HIV-1 gene expression and has been reported to function in splicing. (Buratti et al. 2001) It has also been suggested to function in cellular processes such as microRNA biogenesis, apoptosis, and cell division. Possibly unrelated to its RNA related functions, mutated and hyper-phosphorylated TDP-43 has also been found to accumulate in the cytoplasm of neuronal cells of patients affected by some neurodegenerative diseases such as amyotrophic lateral sclerosis (reviewed in Buratti and Baralle 2008; Lagier-Tourenne and Cleveland 2009).

B0035.11 encodes for an orthologue of *S. cerevisiae* Leo1p, a component of the Paf1 complex, which associates with RNA polymerase II and is involved in histone methylation, but also plays a role in regulating Ty1 retrotransposition (Betz et al. 2002; Mueller and Jaehning 2002; Krogan et al. 2003; Nyswaner et al. 2008).

Additionally four candidates found in our screen are playing a role in the cytoskeleton assembly, of which two – CAP-2 and ARP-1 – interact in the dynactin complex:

CAP-2 (M106.5), an orthologue of yeast Cap2p and human CAPZ is a β-subunit of the capping protein heterodimer of Cap1p and Cap2p. It binds to the barbed ends of actin filaments such as F-actin but also dynactin, and prevents further polymerization. In *C. elegans* CAP-2 is involved in the establishment of the initial asymmetry in the embryo and is expressed in the cytoplasm of all embryonic cells (Amatruda et al. 1990; Waddle et al. 1993).

ARP-1 *(Y53F4B.22)* is an actin-related microtubule cytoskeletal protein located in the cytoplasm, a highly identical orthologue of human alpha-centractin ARP1. ARP1 is the major component of the dynactin complex - a small filament resembling F-actin - that binds to both microtubules and cytoplasmic dynein and allows for vesicle movement on microtubules. At least one molecule of CAPZ is additionally present in the dynactin complex. (Schafer et al. 1994; Blessing et al. 2004)

AMPH-1 (F58G6.1) is an Amphiphysin-like lipid raft protein and was found expressed in the gut and the nervous system in *C. elegans*. The yeast orthologue Rvs161p is a subunit of a heterodimer (Rvs161p and Rvs167p) that regulates endocytosis, polarization of the actin cytoskeleton, cell polarity, cell fusion and viability during starvation or osmotic stress (Lombardi and Riezman 2001; Gallop and McMahon 2005)

SSP-32 (F32B6.7), a major sperm domain containing protein that shows testis enhanced expression. Major sperm proteins (MSP) form a nematode specific cytoskeleton. There is neither structural nor sequence-specific homology to the actin cytoskeleton and in contrast to the latter MSP polymerizes into non-polar filaments. Interestingly yet MSP- and actin-based crawling motility is nearly indistinguishable at the phenotypic level (Tarr and Scott 2004).

The remaining three candidates cannot be categorized into one of the previous groups and do not share a common functional relation. C18E9.4 and *gstk-1* both encode mitochondrial proteins - a feature they share with the previously mentioned mito-ribosomal protein encoded by T13H5.5. The remaining candidate rab-7 encodes a small GTPase active in the endosome.

C18E9.4 encodes a conserved oxidoreductase, the orthologue of the human B3 subunit of the mitochondrial nicotinamide adenine dinucleotide (NADH)-ubiquinone dehydrogenase (NDUF) enzyme complex 1, the first complex in the electron transport chain at the mitochondrial inner membrane (Ton et al. 1997; Tsang and Lemire 2003) .

GSTK-1 (ZK1320.1), an orthologue of human GSTK1 is a member of the glutathione transferase kappa class superfamily of enzymes that function in cellular detoxification and locate to the mitochondrial inner membrane and to peroxisomes. GSTK1 assists in the conjugation of glutathione to many different hydrophobic compounds, thus facilitating their removal in peroxisomes, but also seems to help in detoxifying reactive oxygen species (ROS) generated by the respiratory chain in mitochondria (Jowsey et al. 2003; Morel et al. 2004) .

RAB-7 (W03C9.3) is a GTPase orthologous to human RAB7 and yeast YPT7. RAB-7 is located in the endosome and acts in early to late endosome trafficking as well as in the late endosome-lysosome membrane fusion. Accordingly *rab-7* is required for normal embryogenesis, locomotion, and body morphology. Human RAB7 was additionally shown to act in down-regulating nutrient transporters of the cell surface after withdrawal of growth factors and thus helps to initiate apoptosis (Edinger et al. 2003; Poteryaev et al. 2007).

3.14 Ribosome assembly is not severely affected in *yrn-1* (YJA) mutants

According to our results from the large conditional RNAi screen, we wanted to determine if the *yrn-1* deficiency has an effect on ribosome biogenesis: Our first aim in this respect was to study if defects in the nucleolar morphology were apparent in *yrn-1(YJA)* mutants. We therefore analyzed the expression of the common nucleolar marker fibrillarin, using an anti-fibrillarin antibody in cytology of dissected embryonic larvae. However, we were not able to observe any differences in the morphology of nucleoli in *yrn-1*(YJA) and *rop-1* mutants compared to wild-type worms (Figure 18, page 69).

As a next step, we wanted to analyze, if ribosome assembly is inhibited in *yrn-1* knockout worms. We therefore studied whether the proportion of ribosomal subunits was altered: Lysates of N2 and *yrn-1* worms were fractionated on continuous 10% to

50% sucrose gradients and the RNA content of the fractions was measured. We could not find any difference in the proportion of ribosomal subunits (Figure 19, page 70). Ribosomal subunits were mainly appearing in one major peak in their complexed form – the mature 80S ribosome. No accumulation of subunits represented by additional peaks was obvious.

To analyze, if accumulation of either of the mature ribosomal RNAs occurs, total RNA from N2, *yrn-1* (YJA) and *rop-1* mutants was separated on agarose gels. The ratio of 26S to 18S rRNA was measured after ethidiumbromide staining. The ratio of 26S rRNA to 18S rRNA turned out to be about 5% higher in *yrn-1*(YJA) and *rop-1* mutants. The average of 26S:18S rRNA ratios derived from 12 experiments - N2: 1.46 (SD ±0.16); *yrn-1* (YJA): 1.55 (SD ±0.23); *rop-1*: 1.53 (SD ±0.24). Although an accumulation of 5% observed in *yrn-1* mutants is rather small, however these results are statistically significant (paired t-test for *yrn-1(YJA)*: p=0.04).

Taken together our results do not show a major defect of nucleolar functions influencing the morphology of nucleoli, and we find that ribosomal subunits are present mainly complexed in mature 80S ribosomes. However we found a small but statistically significant accumulation of 26S rRNAs in *yrn-1* mutants, which could indicate a defect in 18S rRNA synthesis or in late protein related assembly of the large subunit. The accumulation of 5% might be too small to detect a similar accumulation of either subunit, taking into account the lower sensitivity of ribosomal subunit profiling.
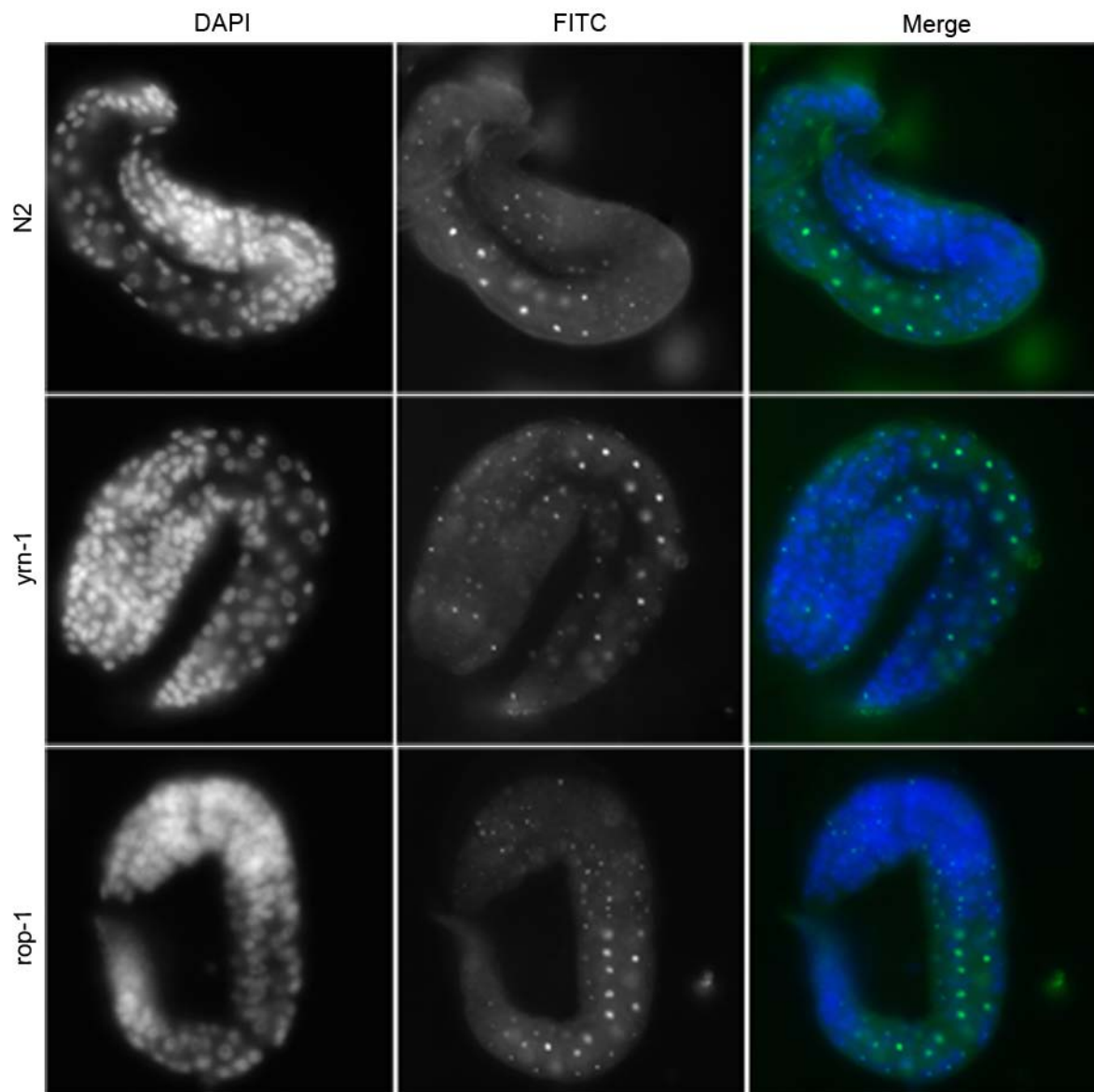
Figure 18: Anti-fibrillarin (FITC) and DAPI cytological staining of dissected *C. elegans* embryonic larvae of N2, *yrn-1* and *rop-1* strains to analyze the nucleolar morphology is shown.
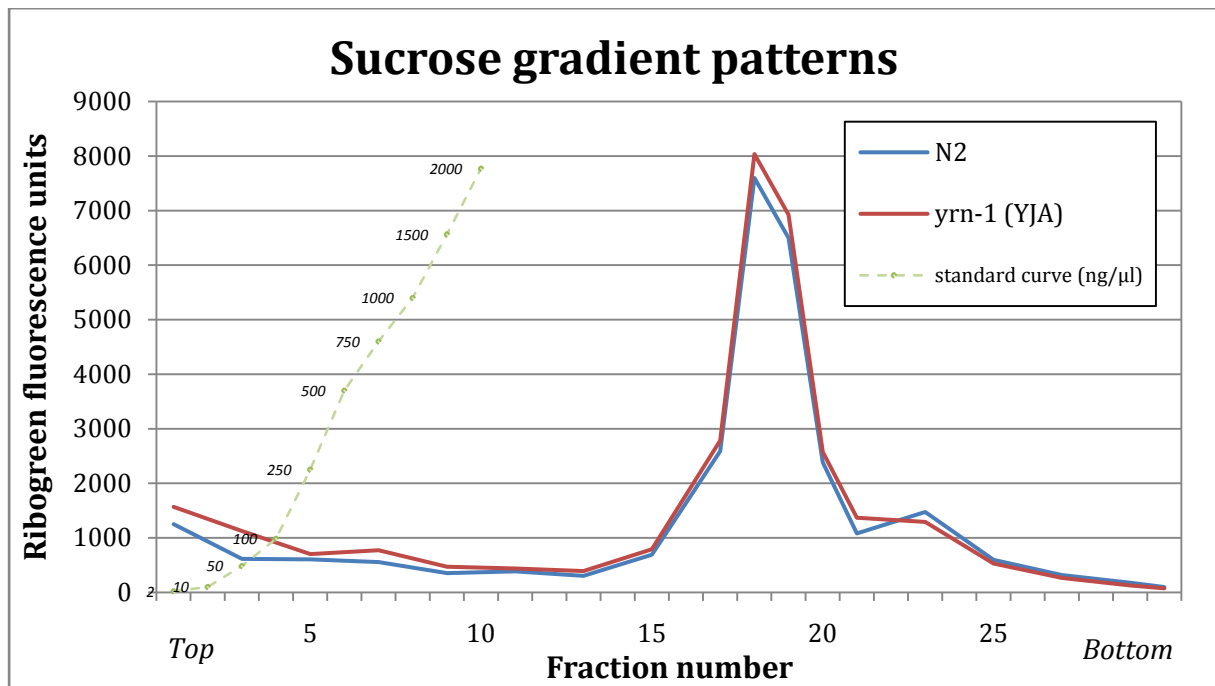
Figure 19: Sucrose gradient profiles of lysates from N2 and *yrn-1(YJA)* worms. Lysates were ultra-centrifuged on a continuous 10%-50% sucrose gradient. 1ml fractions from bottom were collected. 2µl of each sample were incubated with Ribogreen reagent before fluorescence measuring.

3.15 Effect of Y RNA depletion on ribosomal RNA processing

A major part of the candidate genes derived from our RNAi screen for reduced fertility, is playing a role in ribosome biogenesis. We could also observe a low, but statistically significant accumulation of the mature 26S rRNAs. We therefore wanted to establish if this accumulation might be caused by a defect in rRNA processing.

The *C. elegans* rRNA processing pathway has previously been analyzed in low detail (Saijou et al. 2004 and our figure 20). In order to establish, if rRNA processing is affected in the absence of the Y RNA, we hybridized northern blots from total RNA with probes of internally transcribed spacers (ITS) and externally transcribed spacers (ETS) (Figure 20, page 71). This allows the detection of the 35S pre-rRNA and the processed intermediate: the 20S or 27S rRNA precursor, respectively. Intensities of the 20S or 27S pre-rRNA bands and the 35S primary transcript were measured and a ratio was calculated (Figure 21, page 72). Experiments using probe 1 a 5'-ETS probe binding to the pre-rRNA primary transcript as well as to two 20S precursor intermediates (b and d), shows on average a 16% reduction in the 35S:20S pre-rRNA ratio compared to wild-type and accordingly an equal accumulation of the 20S rRNA precursor. In the same experiment *rop-1* mutants showed practically wild-type

values. Very similar results were obtained with Probe 2 another 20S pre-rRNA probe, which binds to the 5'-end of ITS1 and thus to the smaller 20S precursor intermediate b only. However, in the case of Probe 2 also the *rop-1* deficient strain shows a 35S:20S pre-rRNA ratio similar to WT. These results show a significant >15% accumulation of 20S rRNA precursor in the *yrn-1* strain (paired t-test for probe 2 p=0.03). We also tested large subunit rRNA processing using the 3'-ITS1 probe 3 and the ITS2 probe 4. While probe 3 is binding two 27S rRNA precursor fragments c and c' which include the 5.8S rRNA sequence, probe 4 is binding the smaller fragment c only. With probe 3 we saw a 6% accumulation of the 27S rRNA precursor in the *yrn-1* mutant strain compared to wild-type. A higher accumulation of the 27S precursor of 11% was observed using probe 3 with *rop-1* mutants compared to wild-type. Practically no difference to wild-type was observed using probe 4 in *yrn-1* and *rop-1* mutants.

Overall we observed a 15% accumulation of 20S rRNAs pre-cursors in the *yrn-1* knockout strain. The accumulation of 20S rRNA precursors is more severe and statistically significant compared the one of 27S precursors. These results together with data of a 26S rRNA accumulation in the *yrn-1* strain, indicate a defect in 20Spre-rRNA to 18S rRNA processing in the absence of Y RNA.
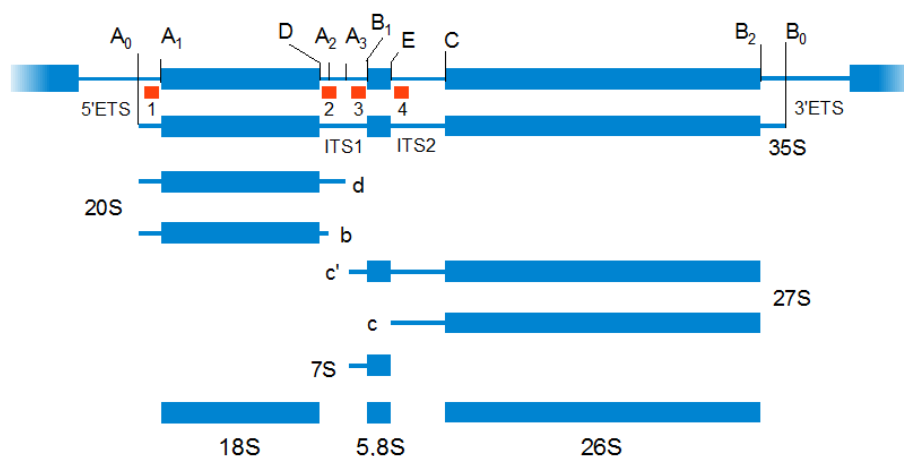

Figure 20: Schematic view of the *C. elegans* rDNA tandem repeat which serves as template for a polycistronic pre-ribosomal RNA transcript. Ribosomal RNA processing steps lead to mature 5.8S, 18S and 26S rRNAs. Probes 1 to 4, used for northern blot hybridization, are indicated in red refer to Figure 21 (modified from Saijou et al. 2004).

Mean ratio of rRNA pre-cursor bands

35S:20S - Values normalized to WT; ±SEM

Probe 1   Probe 2

■ N2   ■ yrn-1 (YJA)   ■ rop-1

35S:27S - Values normalized to WT; ±SEM
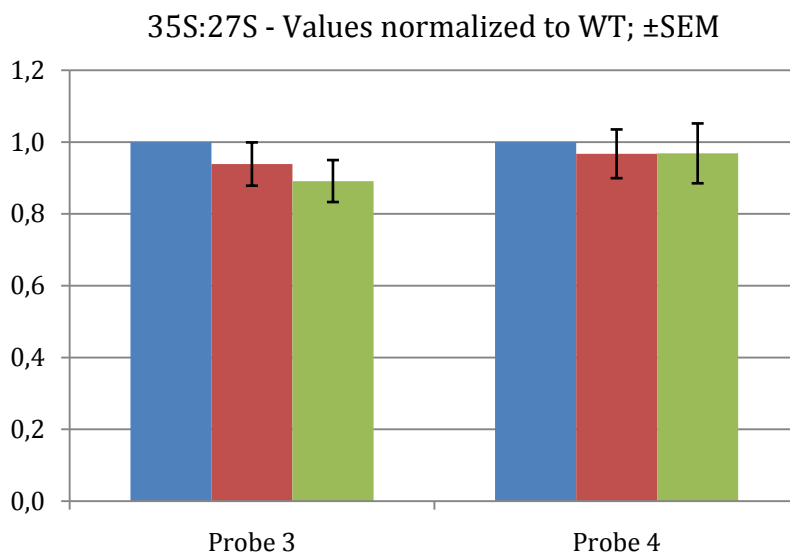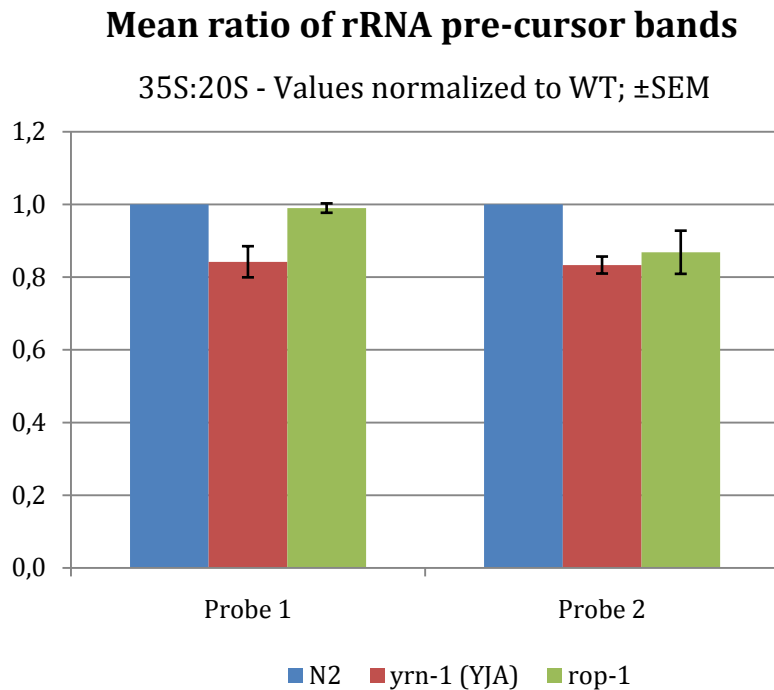

Probe 3   Probe 4

Figure 21: Analysis of rRNA processing. Ratios of the intensity of rRNA precursor bands are shown. Total RNA was northern blotted and hybridized to probes for ETS 1 (probe 1), ITS 1, (probes 2 and 3) or ITS 2 (probe 4). Probes are indicated in Figure 20. Mean values of the ratios of intensities of the 35S primary transcript to the 20S or the 27S rRNA precursor ±SEM were calculated from three (probes 1 and 3) or five (probes 2 and 4) independent experiments, respectively, and normalized to WT. The accumulation of 20S rRNA in the *yrn-1* mutant using probe 2 is statistically significant (paired t-test p=0.003)

3.16 Proportion of proteins in mature ribosomes

Ro60 together with the La protein has previously been connected with translational control of mRNAs encoding ribosomal proteins, which contain a terminal oligo-pyrimidine repeat in their 5'-UTRs in vertebrates. An unidentified RNA has been shown to assist Ro60 in this role and Y RNA was suggested as a candidate

(Pellizzoni et al. 1998). Also our synthetic lethality screen yielded many candidates involved in ribosome assembly. Interestingly, the majority of these candidates are playing a role in early ribosome assembly. As the ribosome has been shown to be a ribozyme, and ribosomal proteins arrange themselves around this catalytic RNA core, processes connected to ribosomal proteins are considered as late assembly.

It is possible that the increase of the severity of a phenotype in a conditional screen by a candidate gene is not caused by another deficiency in the same pathway, but rather in a closely related or dependent pathway. This combination of two minor phenotypes in parallel, but connected pathways, would lead to an amplification of the total phenotype, while depletion of two elements in the same pathway would rather lead to epistatic effects.

These considerations motivated us to analyze late ribosome assembly, even if the majority of our candidates from the RNAi screen play a role in early ribosome assembly. Extracts from N2 and *yrn-1* knockout worms were prepared and mature 80S ribosomes were isolated by ultracentrifugation on a continuous 10%-50% sucrose gradient and fractionation. The RNA content was measured and the peak fraction of each gradient was sent to our collaborator Knud Nierhaus at MPI Molecular Genetics, Berlin where the protein composition was analyzed by two dimensional PAGE (Figure 22, page 74). Proteins were separated by isoelectric focusing in the first dimension and by molecular weight in the second dimension and visualized by Coomassie staining. The total ribosomal protein composition proofs to be similar in WT and *yrn-1* mutants. However the expression of one very basic protein of a molecular weight above average appears nearly 40% reduced in the *yrn-1* sample on this gel. The identity of the protein is currently unknown, but bioinformatic comparison of *C. elegans* ribosomal proteins has indicated large subunit constituent RPL-15 (molecular weight 24.1kDa; isoelectric point at pH12.16) as a probable candidate. Interestingly, large subunit protein 15 orthologue (RPL15p) in yeast has been shown to interact with 5.8S rRNA. These results await further confirmation.
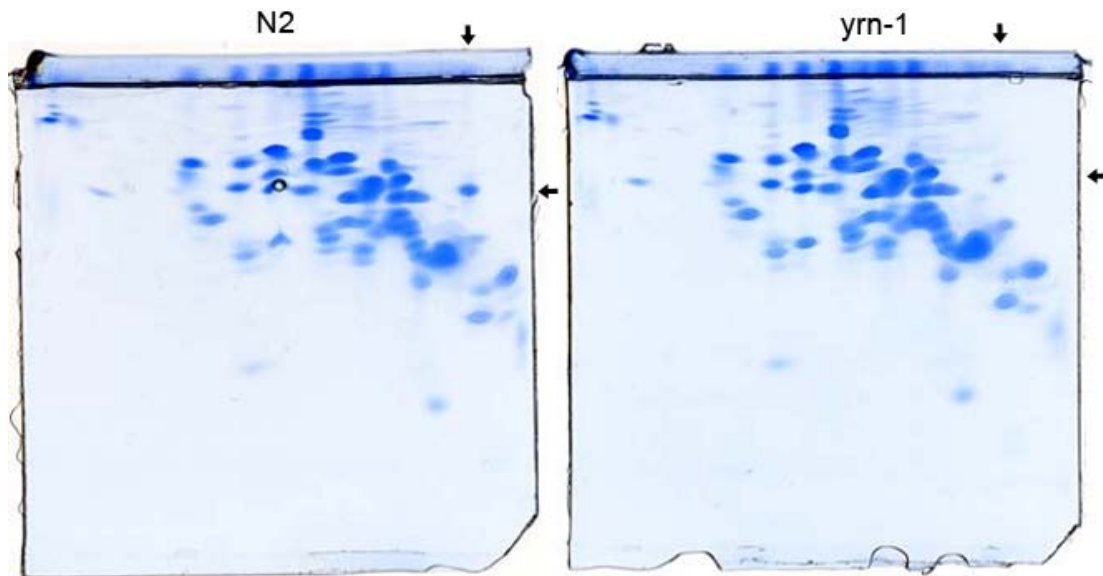
Figure 22 2D-PAGE of the mature 80S ribosome fraction. Proteins were separated by isoelectric focusing in the first dimension and by molecular weight in the second dimension and visualized by Coomassie staining. The protein spot in the upper right part of the gel indicated by arrows is about 40% reduced in the *yrn-1* mutant compared to wild-type.

4 Discussion

Y RNAs are a class of non-coding RNAs present in all animal cells and despite their high degree of conservation, only few functions have been attributed to them and these remain controversial. In order to obtain insight into the roles Y RNAs might play in eukaryotic cells, we constructed a knockout of the Y RNA in the nematode *C. elegans*. We characterized this strain (Y5B) together with a second Y RNA deletion strain (YJA) on the molecular level as well as concerning their phenotypes. As *C. elegans* was shown to contain only a single species of Y RNA, these stains represent the first complete knockout of Y RNA in a eukaryotic organism. As the Ro60 orthologue, ROP-1, is present in our *yrn-1* mutant strain, we could examine effects of Y RNA absence for the ROP-1 protein.

From the data obtained it can be concluded that Y RNA expression is not essential for viability or fertility of *C. elegans,* as both *yrn-1* mutant strains behaved wild-type under laboratory conditions. This is not surprising, as the same has been reported for a mutant of the *C. elegans* Y RNA binding protein ROP-1, in which Y RNA levels were found to be massively reduced (Labbe et al. 1999b).

Our observations make a requirement or even an involvement of Y RNA for *C. elegans* DNA replication as it has been reported for human cell free systems as well as human tissue culture cells very unlikely (Christov et al. 2006). DNA replication is a fundamental process and deficiencies in DNA replication are very likely to have obvious effects on development and fertility of a mutant. As no developmental phenotype can be observed in *yrn-1* mutants, we doubt that the *C. elegans* Y RNA is playing a role in DNA replication.

We were not able to detect a hypothetical second *C. elegans* Y RNA - termed CeN134 – which had been predicted by *in silico* analysis (Perreault et al. 2007). Analysis of CeN134 expression by northern blotting (of total RNA as well as anti-ROP-1 co-immunoprecipitated RNA) did not yield any signal. Yet, the *yrn-1* transcript was readily detectable on the same blots (data not shown). These findings support van Horn et al.'s (1995) results that there is only one single Y RNA species bound by ROP-1 in *C. elegans*, which is encoded by the *yrn-1* gene. Recent bioinformatic predictions, however, categorize CeN134 as one of 18 predicted nematode-specific

sbRNAs, representing a novel class of non-coding RNA pol III transcripts. Interestingly sbRNAs seem to be more related to human Y RNAs than to the *C. elegans yrn-1* gene product, concerning their structure and the presence of a conserved motif essential for human DNA replication (Stadler, PF personal communication). In this respect it is interesting that an inability of ROP-1 to bind human Y RNAs had previously been demonstrated (Van Horn et al. 1995).

Our experiments showed that the Y RNA is not essential for ROP-1 expression or stability. This is interesting, as in contrast, ROP-1 expression has been shown to be necessary for the stability of the Y RNA (Labbe et al. 1999b), as we were also able to confirm. We used the same antibody as van Horn et al. (1995) and could show that it decorates a single ~69kDa protein in samples of gravid adult worm extracts as previously reported. This band decorated by the antibody of van Horn et al (1995) was missing in the *rop-1* disruption strain (*MQ470)* analyzed by Labbé et al (1999b and 2000).

We tried to study the effect of *yrn-1* deficiency on the cellular localization of the ROP-1 protein in cytological experiments of dissected embryos. However, due to a massive background produced by the anti-ROP-1 antibody in cytological staining, no clear results could be obtained. Further experiments with Gfp-tagged ROP-1 protein in a *yrn-1;rop-1* double mutant, might help to overcome these obstacles.

Interestingly, we found both *yrn-1* mutant strains to feature a longer life span compared to wild-type after UVC irradiation. *Rop-1* mutants however died on average earlier then wild-type in these assays. Our findings concerning UV sensitivity of *rop-1* mutants agree with results published for a *Deinococcus radiodurans* strain in which the Ro60 orthologue RSR had been deleted (Chen et al. 2000) and with observations made in Ro60 knockout mice (Chen et al. 2003; Xue et al. 2003). To explain these observations, the reported higher sensitivity to UV irradiation of Ro60 deficient organisms and the proposed role for Ro60/ROP-1 in RNA quality control were combined with a theory, which defines protein:RNA and RNA:RNA crosslinking as a major consequence of UV irradiation (O'Brien and Wolin 1994; Labbe et al. 1999b; Wurtmann and Wolin 2009). It was hypothesized that newly synthesized incompletely

assembled RNAs may be especially susceptible to UV-irradiation-induced crosslinking. Ro60/ROP-1 had previously been shown to bind misfolded non-coding RNAs (O'Brien and Wolin 1994; Chen et al. 2003). Therefore, it might be possible, that after UV irradiation, Ro60/ROP-1 marks nascent RNAs that are misfolded due to crosslinking for treatment by chaperoning enzymes or for degradation.

Yet, we wondered, how our observations of a higher UV resistance of Y RNA deficient animals might fit into this model: In this model Y RNA would dissociate from Ro60/ROP-1 to allow binding of misfolded RNAs under stressful conditions. As Y RNA and Ro proteins exist complexed as Ro RNPs in the cell under default conditions, hard UVC irradiation might also induce crosslinks between ROP-1 and the bound Y RNAs in a considerable fraction of Ro RNPs. As a consequence Ro60/ROP-1 crosslinked to Y RNA would not be able to get released and as the binding site for misfolded RNAs is overlapping with the Y RNA binding site (Stein et al. 2005) these Ro proteins might not be able to fulfill their RNA quality control functions. Additionally Sim et al (2009) showed that dissociation from the Y RNA is also essential for translocation of Ro proteins to the nucleus after UV irradiation, where nascent or newly transcribed non-coding RNAs are located. In the situation of total absence of Y RNA – which we could show to have no effect on ROP-1 expression – a higher amount of free Ro protein, would possibly be available in the nucleus to carry out its RNA quality control function, as compared to the wild-type situation.

These speculations might indeed explain a higher resistance of Y RNA deficient worms to UVC irradiation. The relevance of this phenomenon for the *in vivo* situation, however, is unclear, as UVC irradiation, might not be a threat soil-living nematodes are frequently confronted with. Additionally it has to be noted that the UV doses used in these experiments were potent enough to completely inhibit the creation of viable offspring in all strains studied. Therefore the expanded life span of *yrn-1* mutants after UVC irradiation does not imply a gain of fitness for these worms.

Rop-1 mutants were shown to be deficient in *dauer* formation under starved and crowded conditions and *rop-1* genetically interacts with *daf-2* and *daf-7* in the *dauer* formation pathway (Labbe et al. 2000). While *daf-2* plays a role in the insulin

controlled branch of this pathway, *daf-7* is a key player in the parallel TGFβ branch (Figure 4, page 27). As Y RNA levels are massively reduced in the *rop-1* mutant a differentiation between ROP-1 and Y RNA related effects on the *dauer* formation pathway had previously not been possible. We therefore studied *dauer* formation in *yrn-1(YJA)* mutants and found that these worms are able to form *dauer* larvae under starved and crowded conditions. However, due to the population density necessary for the induction of *dauer* formation under these conditions, it was not possible to quantify their disposition to form *dauer* larvae. Accordingly we were not able to come to a definite conclusion about a possible effect of the absence of Y RNA on *dauer* formation under starved and crowded conditions. Hence we crossed the *yrn-1(YJA)* deletion mutant together with mutants carrying either of two *daf-2* alleles, onto which the *rop-1* mutation had been shown to have opposing effects (Labbe et al. 2000): The *rop-1* mutant background had been found to enhance *dauer* formation together with *daf-2* allele *e1370*, while it reduced *dauer* formation in combination with *daf-2* allele *m41*, as compared to *dauer* formation in the respective *daf-2* single mutants.

In our experiments we could verify the previously published results for the *rop-1* mutation background in general concerning *dauer* formation. We also observed that the *yrn-1* mutant background has similar influences as the *rop-1* null allele on the *dauer* formation of the two *daf-2* mutants. In the *daf-2(e1370)* mutant background the influence of Y RNA deficiency was temperature dependent, as *dauer* formation was enhanced at higher temperatures only. This stands in contrast to the *rop-1* mutation in the *daf-2(e1370)* background, which had a reinforcing impact on *dauer* formation at both temperatures tested.

Interestingly, when analyzing the second *daf-2* allele *(m41)* - whose *daf-c* phenotype had previously been shown to be reduced by the *rop-1* deficiency - we found a Y RNA dependent effect: We observed that the *yrn-1* mutation background caused an even lower disposition to form *dauer* larvae than the *rop1* null allele in *daf-2(m41)* mutants.

In summary, our results show a temperature dependent effect of the *yrn-1* null allele on the *dauer* formation in a *daf-2(e1370)* mutant. As RNA folding and RNA-protein binding are temperature dependent processes, this might indicate a role for the Y RNA for the DAF-2/ROP-1 interaction, which is influenced by the *e1370* mutation. Our data also demonstrate a stronger effect of the Y RNA deficiency than the of the

rop-1 mutation on *dauer* formation in the *daf-2(m41)* background. Especially as Y RNA levels are reduced but not abolished in the *rop-1* mutant, these results allow to speculate, if the Y RNA might not be the actual interactor with *DAF-2* at the ligand binding L1 domain, impaired by the *m41* mutation. In this case reduction of *dauer* formation in a *rop-1*;*daf*-2(m41) double mutant might in fact be caused by the reduced Y RNA expression in this mutant, as the *yrn-1* null allele causes an even stronger reduction of *dauer* formation compared to *rop-1* in this genetic background.

We analyzed possible influences of the Y RNA deficiency on the RNA binding properties of ROP-1 *in vivo*. However, we could not detect major changes in the ability of ROP-1 to bind other RNAs. We therefore were not able to observe consequences of Y RNA deficiency, which could be concluded from a model that implicates the Y RNA as a regulator of access for other RNAs to the extensive RNA-binding surface of Ro60/ROP-1 (Stein et al. 2005). In this case we would have anticipated seeing a dramatic increase of ROP-1 binding to other RNAs than Y RNA. On the other hand Ro60 was proposed to scavenge nascent non-coding RNAs, that are misfolded and to possibly assist in their degradation (Fuchs et al. 2006). Again the Y RNA was proposed to regulate this function. In this case a reduction of ROP-1 binding RNAs and possibly the appearance of degradation products would have been expected. As none of these events was observed in the ROP-1 IP experiment performed with *yrn-1* mutants, we did not further investigate this issue.

Since the phenotype of both strains mutant for *yrn-1* was not significantly different from wild-type, we carried out a large RNAi screen for enhanced lethality and reduced fertility in the *yrn-1(YJA)* deletion strain. We found that the major groups of candidate genes identified, are either involved in ribosome assembly, RNA binding/processing or cytoskeleton organization. Since no published data indicate a connection of Y RNA with the cytoskeleton, we did not analyze the cytoskeleton related genes any further. Another class of candidates found in our screen comprised several RNA binding proteins. To some extent it can be expected to find RNA-binding proteins to interact with a non-coding RNA. Also one of these candidates, MRS-1, functions in tRNA synthesis and therefore is part of the translational machinery and

functionally related with candidate genes involved in ribosome biogenesis. Since most candidates are involved in ribosome assembly we focused our attention on a possible role for the Y RNA in ribosome biogenesis.

Since the RNAi screen resulted in a high proportion of candidates involved in ribosome assembly, we decided to further investigate this process in the *yrn-1* mutation background. Immunofluorescence studies using an antibody to fibrillarin, a conserved nucleolar marker, did not indicate any morphological differences of nucleoli in *yrn-1* mutants. We could also not observe any accumulation of unpaired ribosomal subunits in the absence of Y RNA.

We next analyzed the protein composition of mature 80S ribosomes. We were interested if Y RNA deficiency might cause a change in the stoichiometry of ribosomal proteins. Sucrose gradient peak fractions from lysates of wild-type and *yrn-1* deficient worms were analyzed by our collaborator Knud Nierhaus, MPI Molecular Genetics, Berlin and a 40% reduction of an undefined basic ribosomal protein was found. This could indicate a possible role for the Y RNA in the expression of at least one ribosomal protein. However, these results wait for further verification.

We then analyzed the ratio of 18S: 26S rRNA in the *yrn-1* mutant and found a low, but statistically significant reduction of 18S rRNA compared to 26S rRNA. These results as well as data from the RNAi screen indicated an involvement of the Y RNA in ribosomal rRNA processing.

We therefore decided to investigate rRNA processing in more detail in search for a subtle deficiency, which would not lead to a phenotype under normal growth conditions. We studied processing of the 35S primary transcript to 20S rRNA and 27S rRNA precursors and wanted to see if accumulation of either of these precursors occurs in the *yrn-1* mutant. We observed a significant accumulation of the 20S pre-rRNA, while an accumulation of 27S pre-rRNA was only minor and not statistically significant. We therefore propose a deficiency in the downstream processing of the 20S pre-rRNA, possibly resulting in a low reduction of mature 18S rRNAs, which we were able to observe in previous experiments.

We found similar but not as severe effects on rRNA processing in a *rop-1* mutant background and further experiments should determine, if this might be caused by the strong reduction of Y RNA levels observed in this mutant.

Several small nucleolar RNAs have previously been shown to function in early cleavage steps of the primary 35S transcript, while the non-coding RNA pol III transcript RNAse MRP, a ribozyme, is active in the main branch of 27S large subunit pre-rRNAs processing in the nucleus. Late steps of the small subunit rRNA maturation including the 20S pre-rRNA to 18S rRNA cleavage step at site D are carried out in the cytoplasm, where also the majority of mature Y RNAs is located. Relatively little is known about the cleavage at site D and to date no RNA components have been found to be involved. Interestingly, the *C. elegans* small sub-unit maturation was found to be more complicated compared to other eukaryotic organisms, as it might involve an additional processing step prior to the D site cleavage. In this respect our results, which show a reduction of the 18S rRNA and an accumulation of the 20S pre-rRNA propose a function of non-coding Y RNAs in the fine tuning of ribosome synthesis especially in the late processing of the small subunit rRNA.

Taken together, the data obtained in the course of this thesis do not indicate the *C. elegans* Y RNA to be essential for viability and reproduction. However, they do suggest involvement of the Y RNA in cellular pathways including, stress response ribosome biogenesis and *dauer* larvae formation. Since, apart from the *dauer* formation pathway, these processes are of general nature, we can expect Y RNAs to play similar roles also in other higher eukaryotic organisms.

5 References

Achsel T, Brahms H, Kastner B, Bachi A, Wilm M, Luhrmann R. 1999. A doughnut-shaped heteromer of human Sm-like proteins binds to the 3'-end of U6 snRNA, thereby facilitating U4/U6 duplex formation in vitro. EMBO J 18(20): 5789-5802.

Alspaugh MA, Buchanan WW, Whaley K. 1978. Precipitating antibodies to cellular antigens in Sjogren's syndrome, rheumatoid arthritis, and other organ and nonorgan-specific autoimmune diseases. Ann Rheum Dis 37(3): 244-246.

Altman S. 2007. A view of RNase P. Mol Biosyst 3(9): 604-607.

Amatruda JF, Cannon JF, Tatchell K, Hug C, Cooper JA. 1990. Disruption of the actin cytoskeleton in yeast capping protein mutants. Nature 344(6264): 352-354.

Angelov D, Bondarenko VA, Almagro S, Menoni H, Mongelard F, Hans F, Mietton F, Studitsky VM, Hamiche A, Dimitrov S et al. 2006. Nucleolin is a histone chaperone with FACT-like activity and assists remodeling of nucleosomes. EMBO J 25(8): 1669-1679.

Barstead RJ, Kleiman L, Waterston RH. 1991. Cloning, sequencing, and mapping of an alpha-actinin gene from the nematode Caenorhabditis elegans. Cell Motil Cytoskeleton 20(1): 69-78.

Baugh LR, Sternberg PW. 2006. DAF-16/FOXO regulates transcription of cki-1/Cip/Kip and repression of lin-4 during C. elegans L1 arrest. Curr Biol 16(8): 780-785.

Belisova A, Semrad K, Mayer O, Kocian G, Waigmann E, Schroeder R, Steiner G. 2005. RNA chaperone activity of protein components of human Ro RNPs. RNA 11(7): 1084-1094.

Ben-Chetrit E, Chan EK, Sullivan KF, Tan EM. 1988. A 52-kD protein is a novel component of the SS-A/Ro antigenic particle. J Exp Med 167(5): 1560-1571.

Berezikov E, Bargmann CI, Plasterk RH. 2004. Homologous gene targeting in Caenorhabditis elegans by biolistic transformation. Nucleic Acids Res 32(4): e40.

Berges T, Petfalski E, Tollervey D, Hurt EC. 1994. Synthetic lethality with fibrillarin identifies NOP77p, a nucleolar protein required for pre-rRNA processing and modification. EMBO J 13(13): 3136-3148.

Betz JL, Chang M, Washburn TM, Porter SE, Mueller CL, Jaehning JA. 2002. Phenotypic analysis of Paf1/RNA polymerase II complex mutations reveals connections to cell cycle regulation, protein synthesis, and lipid and nucleic acid metabolism. Mol Genet Genomics 268(2): 272-285.

Blessing CA, Ugrinova GT, Goodson HV. 2004. Actin and ARPs: action in the nucleus. Trends Cell Biol 14(8): 435-442.

Boire G, Craft J. 1990. Human Ro ribonucleoprotein particles: characterization of native structure and stable association with the La polypeptide. J Clin Invest 85(4): 1182-1190.

Boire G, Gendron M, Monast N, Bastin B, Menard HA. 1995. Purification of antigenically intact Ro ribonucleoproteins; biochemical and immunological evidence that the 52-kD protein is not a Ro protein. Clin Exp Immunol 100(3): 489-498.

Bomsztyk K, Van Seuningen I, Suzuki H, Denisenko O, Ostrowski J. 1997. Diverse molecular interactions of the hnRNP K protein. FEBS Lett 403(2): 113-115.

Borer RA, Lehner CF, Eppenberger HM, Nigg EA. 1989. Major nucleolar proteins shuttle between nucleus and cytoplasm. Cell 56(3): 379-390.

Bouffard P, Barbar E, Briere F, Boire G. 2000. Interaction cloning and characterization of RoBPI, a novel protein binding to human Ro ribonucleoproteins. RNA 6(1): 66-78.

Bouffard P, Briere F, Wellinger RJ, Boire G. 1999. Identification of ribonucleoprotein (RNP)-specific protein interactions using a yeast RNP interaction trap assay (RITA). Biotechniques 27(4): 790-796.

Bouveret E, Rigaut G, Shevchenko A, Wilm M, Seraphin B. 2000. A Sm-like protein complex that participates in mRNA degradation. EMBO J 19(7): 1661-1671.

Bouvet P, Diaz JJ, Kindbeiter K, Madjar JJ, Amalric F. 1998. Nucleolin interacts with several ribosomal proteins through its RGG domain. J Biol Chem 273(30): 19025-19029.

Brenner S. 1974. The genetics of Caenorhabditis elegans. Genetics 77(1): 71-94.

Brown GE, Kolb AJ, Stanley WM, Jr. 1974. A general procedure for the preparation of highly active eukaryotic ribosomes and ribosomal subunits. Methods Enzymol 30(0): 368-387.

Brown T. 1994a. Analysis of RNA by Northern and Slot Blot Hybridization. In Current Protocols in Molecular Biology, Vol 1 (ed. FM Ausubel, R Brent, RE Kingston, DD Moore, JG Seidman, JA Smith, K Struhl). John Wiley & Sons, Inc.

-. 1994b. Hybridization Analysis of DNA Blots. In Current Protocols in Molecular Biology, Vol 1 (ed. FM Ausubel, R Brent, RE Kingston, DD Moore, JG Seidman, JA Smith, K Struhl). John Wiley & Sons, Inc.

Buratti E, Baralle FE. 2008. Multiple roles of TDP-43 in gene expression, splicing regulation, and human disease. Front Biosci 13: 867-878.

Buratti E, Dork T, Zuccato E, Pagani F, Romano M, Baralle FE. 2001. Nuclear factor TDP-43 and SR proteins promote in vitro and in vivo CFTR exon 9 skipping. EMBO J 20(7): 1774-1784.

Cardinali B, Carissimi C, Gravina P, Pierandrei-Amaldi P. 2003. La protein is associated with terminal oligopyrimidine mRNAs in actively translating polysomes. J Biol Chem 278(37): 35145-35151.

Cassada RC, Russell RL. 1975. The dauerlarva, a post-embryonic developmental variant of the nematode Caenorhabditis elegans. Dev Biol 46(2): 326-342.

Chang TH, Clark MW, Lustig AJ, Cusick ME, Abelson J. 1988. RNA11 protein is associated with the yeast spliceosome and is localized in the periphery of the cell nucleus. Mol Cell Biol 8(6): 2379-2393.

Chatton B, Winsor B, Boulanger Y, Fasiolo F. 1987. Cloning and characterization of the yeast methionyl-tRNA synthetase mutation mes1. J Biol Chem 262(31): 15094-15097.

Chen X, Quinn AM, Wolin SL. 2000. Ro ribonucleoproteins contribute to the resistance of Deinococcus radiodurans to ultraviolet irradiation. Genes Dev 14(7): 777-782.

Chen X, Smith JD, Shi H, Yang DD, Flavell RA, Wolin SL. 2003. The Ro autoantigen binds misfolded U2 small nuclear RNAs and assists mammalian cell survival after UV irradiation. Curr Biol 13(24): 2206-2211.

Chen X, Wolin SL. 2004. The Ro 60 kDa autoantigen: insights into cellular function and role in autoimmunity. J Mol Med 82(4): 232-239.

Chen X, Wurtmann EJ, Van Batavia J, Zybailov B, Washburn MP, Wolin SL. 2007. An ortholog of the Ro autoantigen functions in 23S rRNA maturation in D. radiodurans. Genes Dev 21(11): 1328-1339.

Christov CP, Gardiner TJ, Szuts D, Krude T. 2006. Functional requirement of noncoding Y RNAs for human chromosomal DNA replication. Mol Cell Biol 26(18): 6993-7004.

Christov CP, Trivier E, Krude T. 2008. Noncoding human Y RNAs are overexpressed in tumours and required for cell proliferation. Br J Cancer 98(5): 981-988.

Church GM, Gilbert W. 1984. Genomic sequencing. Proc Natl Acad Sci U S A 81(7): 1991-1995.

Crosio C, Boyl PP, Loreni F, Pierandrei-Amaldi P, Amaldi F. 2000. La protein has a positive effect on the translation of TOP mRNAs in vivo. Nucleic Acids Res 28(15): 2927-2934.

Deng W, Zhu X, Skogerbo G, Zhao Y, Fu Z, Wang Y, He H, Cai L, Sun H, Liu C et al. 2006. Organization of the Caenorhabditis elegans small non-coding transcriptome: genomic features, biogenesis, and expression. Genome Res 16(1): 20-29.

Edinger AL, Cinalli RM, Thompson CB. 2003. Rab7 prevents growth factor-independent survival by inhibiting cell-autonomous nutrient transporter expression. Dev Cell 5(4): 571-582.

Erard MS, Belenguer P, Caizergues-Ferrer M, Pantaloni A, Amalric F. 1988. A major nucleolar protein, nucleolin, induces chromatin decondensation by binding to histone H1. Eur J Biochem 175(3): 525-530.

Expert-Bezancon A, Le Caer JP, Marie J. 2002. Heterogeneous nuclear ribonucleoprotein (hnRNP) K is a component of an intronic splicing enhancer complex that activates the splicing of the alternative exon 6A from chicken beta-tropomyosin pre-mRNA. J Biol Chem 277(19): 16614-16623.

Fabini G, Raijmakers R, Hayer S, Fouraux MA, Pruijn GJ, Steiner G. 2001. The heterogeneous nuclear ribonucleoproteins I and K interact with a subset of the ro ribonucleoprotein-associated Y RNAs in vitro and in vivo. J Biol Chem 276(23): 20711-20718.

Fabini G, Rutjes SA, Zimmermann C, Pruijn GJ, Steiner G. 2000. Analysis of the molecular composition of Ro ribonucleoprotein complexes. Identification of novel Y RNA-binding proteins. Eur J Biochem 267(9): 2778-2789.

Farris AD, Koelsch G, Pruijn GJ, van Venrooij WJ, Harley JB. 1999. Conserved features of Y RNAs revealed by automated phylogenetic secondary structure analysis. Nucleic Acids Res 27(4): 1070-1078.

Fatica A, Tollervey D. 2002. Making ribosomes. Curr Opin Cell Biol 14(3): 313-318.

Feinberg AP, Vogelstein B. 1983. A technique for radiolabeling DNA restriction endonuclease fragments to high specific activity. Anal Biochem 132(1): 6-13.

Feng W, Hopper AK. 2002. A Los1p-independent pathway for nuclear export of intronless tRNAs in Saccharomycescerevisiae. Proc Natl Acad Sci U S A 99(8): 5412-5417.

Fielenbach N, Antebi A. 2008. C. elegans dauer formation and the molecular basis of plasticity. Genes Dev 22(16): 2149-2165.

Fouraux MA, Bouvet P, Verkaart S, van Venrooij WJ, Pruijn GJ. 2002. Nucleolin associates with a subset of the human Ro ribonucleoprotein complexes. J Mol Biol 320(3): 475-488.

Fraser AG, Kamath RS, Zipperlen P, Martinez-Campos M, Sohrmann M, Ahringer J. 2000. Functional genomic analysis of C. elegans chromosome I by systematic RNA interference. Nature 408(6810): 325-330.

Fromont-Racine M, Senger B, Saveanu C, Fasiolo F. 2003. Ribosome assembly in eukaryotes. Gene 313: 17-42.

Fuchs G, Stein AJ, Fu C, Reinisch KM, Wolin SL. 2006. Structural and biochemical basis for misfolded RNA recognition by the Ro autoantigen. Nat Struct Mol Biol 13(11): 1002-1009.

Gallagher SR, Smith JA. 1993. Electrophoretic Separation of Proteins. In Current Protocols in Molecular Biology, Vol Volume 2 (ed. FM Ausubel, R Brent, RE Kingston, DD Moore, JG Seidman, JA Smith, K Struhl). John Wiley & Sons, Inc.

Gallop JL, McMahon HT. 2005. BAR domains and membrane curvature: bringing your curves to the BAR. Biochem Soc Symp(72): 223-231.

Gardiner TJ, Christov CP, Langley AR, Krude T. An evolutionarily conserved motif of vertebrate Y RNAs is essential and sufficient for chromosomal DNA replication in human cell extracts. RNA: in press.

Gelperin D, Horton L, Beckman J, Hensold J, Lemmon SK. 2001. Bms1p, a novel GTP-binding protein, and the related Tsr1p are required for distinct steps of 40S ribosome biogenesis in yeast. RNA 7(9): 1268-1283.

Gems D, Sutton AJ, Sundermeyer ML, Albert PS, King KV, Edgley ML, Larsen PL, Riddle DL. 1998. Two pleiotropic classes of daf-2 mutation affect larval arrest, adult behavior, reproduction and longevity in Caenorhabditis elegans. Genetics 150(1): 129-155.

Gendron M, Roberge D, Boire G. 2001. Heterogeneity of human Ro ribonucleoproteins (RNPS): nuclear retention of Ro RNPS containing the human hY5 RNA in human and mouse cells. Clin Exp Immunol 125(1): 162-168.

Ghetti A, Pinol-Roma S, Michael WM, Morandi C, Dreyfuss G. 1992. hnRNP I, the polypyrimidine tract-binding protein: distinct nuclear localization and association with hnRNAs. Nucleic Acids Res 20(14): 3671-3678.

Ginisty H, Amalric F, Bouvet P. 1998. Nucleolin functions in the first step of ribosomal RNA processing. EMBO J 17(5): 1476-1486.

Golden JW, Riddle DL. 1982. A pheromone influences larval development in the nematode Caenorhabditis elegans. Science 218(4572): 578-580.

Green CD, Long KS, Shi H, Wolin SL. 1998. Binding of the 60-kDa Ro autoantigen to Y RNAs: evidence for recognition in the major groove of a conserved helix. RNA 4(7): 750-765.

Grimm C, Lund E, Dahlberg JE. 1997. In vivo selection of RNAs that localize in the nucleus. EMBO J 16(4): 793-806.

Gwizdek C, Ossareh-Nazari B, Brownawell AM, Doglio A, Bertrand E, Macara IG, Dargemont C. 2003. Exportin-5 mediates nuclear export of minihelix-containing RNAs. J Biol Chem 278(8): 5505-5508.

Hamilton TL, Stoneley M, Spriggs KA, Bushell M. 2006. TOPs and their regulation. Biochem Soc Trans 34(Pt 1): 12-16.

Harmon CE, Deng JS, Peebles CL, Tan EM. 1984. The importance of tissue substrate in the SS-A/Ro antigen-antibody system. Arthritis Rheum 27(2): 166-173.

Hastings ML, Allemand E, Duelli DM, Myers MP, Krainer AR. 2007. Control of pre-mRNA splicing by the general splicing factors PUF60 and U2AF65. PLoS ONE 2(6): e538.

Hendrick JP, Wolin SL, Rinke J, Lerner MR, Steitz JA. 1981. Ro small cytoplasmic ribonucleoproteins are a subclass of La ribonucleoproteins: further characterization of the Ro and La small ribonucleoproteins from uninfected mammalian cells. Mol Cell Biol 1(12): 1138-1149.

Hogg JR, Collins K. 2007. Human Y5 RNA specializes a Ro ribonucleoprotein for 5S ribosomal RNA quality control. Genes Dev 21(23): 3067-3072.

Hu PJ. 2007. Dauer. WormBook: 1-19.

Hubbard SR, Wei L, Ellis L, Hendrickson WA. 1994. Crystal structure of the tyrosine kinase domain of the human insulin receptor. Nature 372(6508): 746-754.

Intine RV, Dundr M, Vassilev A, Schwartz E, Zhao Y, Depamphilis ML, Maraia RJ. 2004. Nonphosphorylated human La antigen interacts with nucleolin at nucleolar sites involved in rRNA biogenesis. Mol Cell Biol 24(24): 10894-10904.

Intine RV, Tenenbaum SA, Sakulich AL, Keene JD, Maraia RJ. 2003. Differential phosphorylation and subcellular localization of La RNPs associated with precursor tRNAs and translation-related mRNAs. Mol Cell 12(5): 1301-1307.

Itoh Y, Reichlin M. 1991. Ro/SS-A antigen in human platelets. Different distributions of the isoforms of Ro/SS-A protein and the Ro/SS-A-binding RNA. Arthritis Rheum 34(7): 888-893.

Izumi RE, Valdez B, Banerjee R, Srivastava M, Dasgupta A. 2001. Nucleolin stimulates viral internal ribosome entry site-mediated translation. Virus Res 76(1): 17-29.

Jantsch V, Pasierbek P, Mueller MM, Schweizer D, Jantsch M, Loidl J. 2004. Targeted gene knockout reveals a role in meiotic recombination for ZHP-3, a Zip3-related protein in Caenorhabditis elegans. Mol Cell Biol 24(18): 7998-8006.

Jowsey IR, Thomson RE, Orton TC, Elcombe CR, Hayes JD. 2003. Biochemical and genetic characterization of a murine class Kappa glutathione S-transferase. Biochem J 373(Pt 2): 559-569.

Kamath RS, Fraser AG, Dong Y, Poulin G, Durbin R, Gotta M, Kanapin A, Le Bot N, Moreno S, Sohrmann M et al. 2003. Systematic functional analysis of the Caenorhabditis elegans genome using RNAi. Nature 421(6920): 231-237.

Kato N, Hoshino H, Harada F. 1982. Nucleotide sequence of 4.5S RNA (C8 or hY5) from HeLa cells. Biochem Biophys Res Commun 108(1): 363-370.

Kim JH, Hahm B, Kim YK, Choi M, Jang SK. 2000. Protein-protein interaction among hnRNPs shuttling between nucleus and cytoplasm. J Mol Biol 298(3): 395-405.

Knobel KM, Davis WS, Jorgensen EM, Bastiani MJ. 2001. UNC-119 suppresses axon branching in C. elegans. Development 128(20): 4079-4092.

Krause M. 1995. Techniques for analyzing transcription and translation. In Caenorhabditis elegans: Modern Biological Analysis of an Organism, Vol 48 (ed. H Epstein, D Shakes), pp. 513-529. Academic Press, San Diego, CA.

Krogan NJ, Dover J, Wood A, Schneider J, Heidt J, Boateng MA, Dean K, Ryan OW, Golshani A, Johnston M et al. 2003. The Paf1 complex is required for histone H3 methylation by COMPASS and Dot1p: linking transcriptional elongation to histone methylation. Mol Cell 11(3): 721-729.

Kufel J, Allmang C, Petfalski E, Beggs J, Tollervey D. 2003a. Lsm Proteins are required for normal processing and stability of ribosomal RNAs. J Biol Chem 278(4): 2147-2156.

Kufel J, Allmang C, Verdone L, Beggs J, Tollervey D. 2003b. A complex pathway for 3' processing of the yeast U3 snoRNA. Nucleic Acids Res 31(23): 6788-6797.

Labbe JC, Burgess J, Rokeach LA, Hekimi S. 2000. ROP-1, an RNA quality-control pathway component, affects Caenorhabditis elegans dauer formation. Proc Natl Acad Sci U S A 97(24): 13233-13238.

Labbe JC, Hekimi S, Rokeach LA. 1999a. Assessing the function of the Ro ribonucleoprotein complex using Caenorhabditis elegans as a biological tool. Biochem Cell Biol 77(4): 349-354.

-. 1999b. The levels of the RoRNP-associated Y RNA are dependent upon the presence of ROP-1, the Caenorhabditis elegans Ro60 protein. Genetics 151(1): 143-150.

Labbe JC, Jannatipour M, Rokeach LA. 1995. The Caenorhabditis elegans rop-1 gene encodes the homologue of the human 60-kDa Ro autoantigen. Gene 167(1-2): 227-231.

Lafontaine D, Delcour J, Glasser AL, Desgres J, Vandenhaute J. 1994. The DIM1 gene responsible for the conserved m6(2)Am6(2)A dimethylation in the 3'-terminal loop of 18 S rRNA is essential in yeast. J Mol Biol 241(3): 492-497.

Lafontaine D, Vandenhaute J, Tollervey D. 1995. The 18S rRNA dimethylase Dim1p is required for pre-ribosomal RNA processing in yeast. Genes Dev 9(20): 2470-2481.

Lafontaine DL, Preiss T, Tollervey D. 1998. Yeast 18S rRNA dimethylase Dim1p: a quality control mechanism in ribosome synthesis? Mol Cell Biol 18(4): 2360-2370.

Lagier-Tourenne C, Cleveland DW. 2009. Rethinking ALS: the FUS about TDP-43. Cell 136(6): 1001-1004.

Lehner B, Tischler J, Fraser AG. 2006. RNAi screens in Caenorhabditis elegans in a 96-well liquid format and their application to the systematic identification of genetic interactions. Nat Protoc 1(3): 1617-1620.

Lerner MR, Boyle JA, Hardin JA, Steitz JA. 1981. Two novel classes of small ribonucleoproteins detected by antibodies associated with lupus erythematosus. Science 211(4480): 400-402.

Liu J, Kouzine F, Nie Z, Chung HJ, Elisha-Feil Z, Weber A, Zhao K, Levens D. 2006. The FUSE/FBP/FIR/TFIIH system is a molecular machine programming a pulse of c-myc expression. EMBO J 25(10): 2119-2130.

Lombardi R, Riezman H. 2001. Rvs161p and Rvs167p, the two yeast amphiphysin homologs, function together in vivo. J Biol Chem 276(8): 6016-6022.

Lopez-Robles E, Herrera-Esparza R, Avalos-Diaz E. 1986. Cellular localization of the Ro/SS-A antigen. Clin Rheumatol 5(1): 33-38.

Lygerou Z, Allmang C, Tollervey D, Seraphin B. 1996. Accurate processing of a eukaryotic precursor ribosomal RNA by ribonuclease MRP in vitro. Science 272(5259): 268-270.

Maduro M, Pilgrim D. 1995. Identification and cloning of unc-119, a gene expressed in the Caenorhabditis elegans nervous system. Genetics 141(3): 977-988.

Mamula MJ, O'Brien CA, Harley JB, Hardin JA. 1989a. The Ro ribonucleoprotein particle: induction of autoantibodies and the detection of Ro RNAs among species. Clin Immunol Immunopathol 52(3): 435-446.

Mamula MJ, Silverman ED, Laxer RM, Bentur L, Isacovics B, Hardin JA. 1989b. Human monoclonal anti-La antibodies. The La protein resides on a subset of Ro particles. J Immunol 143(9): 2923-2928.

Maraia R, Sakulich AL, Brinkmann E, Green ED. 1996. Gene encoding human Ro-associated autoantigen Y5 RNA. Nucleic Acids Res 24(18): 3552-3559.

Matera AG, Frey MR, Margelot K, Wolin SL. 1995. A perinucleolar compartment contains several RNA polymerase III transcripts as well as the polypyrimidine tract-binding protein, hnRNP I. J Cell Biol 129(5): 1181-1193.

Mayes AE, Verdone L, Legrain P, Beggs JD. 1999. Characterization of Sm-like proteins in yeast and their association with U6 snRNA. EMBO J 18(15): 4321-4331.

McCauliffe DP, Zappi E, Lieu TS, Michalak M, Sontheimer RD, Capra JD. 1990. A human Ro/SS-A autoantigen is the homologue of calreticulin and is highly homologous with onchocercal RAL-1 antigen and an aplysia "memory molecule". J Clin Invest 86(1): 332-335.

Meerovitch K, Svitkin YV, Lee HS, Lejbkowicz F, Kenan DJ, Chan EK, Agol VI, Keene JD, Sonenberg N. 1993. La autoantigen enhances and corrects aberrant translation of poliovirus RNA in reticulocyte lysate. J Virol 67(7): 3798-3807.

Michael WM, Eder PS, Dreyfuss G. 1997. The K nuclear shuttling domain: a novel signal for nuclear import and nuclear export in the hnRNP K protein. EMBO J 16(12): 3587-3598.

Milkereit P, Gadal O, Podtelejnikov A, Trumtel S, Gas N, Petfalski E, Tollervey D, Mann M, Hurt E, Tschochner H. 2001. Maturation and intranuclear transport of pre-ribosomes requires Noc proteins. Cell 105(4): 499-509.

Morel F, Rauch C, Petit E, Piton A, Theret N, Coles B, Guillouzo A. 2004. Gene and protein characterization of the human glutathione S-transferase kappa and evidence for a peroxisomal localization. J Biol Chem 279(16): 16246-16253.

Mosig A, Guofeng M, Stadler BM, Stadler PF. 2007. Evolution of the vertebrate Y RNA cluster. Theory Biosci 126(1): 9-14.

Mueller CL, Jaehning JA. 2002. Ctr9, Rtf1, and Leo1 are components of the Paf1/RNA polymerase II complex. Mol Cell Biol 22(7): 1971-1980.

Nyswaner KM, Checkley MA, Yi M, Stephens RM, Garfinkel DJ. 2008. Chromatin-associated genes protect the yeast genome from Ty1 insertional mutagenesis. Genetics 178(1): 197-214.

O'Brien CA, Harley JB. 1990. A subset of hY RNAs is associated with erythrocyte Ro ribonucleoproteins. EMBO J 9(11): 3683-3689.

O'Brien CA, Margelot K, Wolin SL. 1993. Xenopus Ro ribonucleoproteins: members of an evolutionarily conserved class of cytoplasmic ribonucleoproteins. Proc Natl Acad Sci U S A 90(15): 7250-7254.

O'Brien CA, Wolin SL. 1994. A possible role for the 60-kD Ro autoantigen in a discard pathway for defective 5S rRNA precursors. Genes Dev 8(23): 2891-2903.

Ostrowski J, Kawata Y, Schullery DS, Denisenko ON, Bomsztyk K. 2003. Transient recruitment of the hnRNP K protein to inducibly transcribed gene loci. Nucleic Acids Res 31(14): 3954-3962.

Page-McCaw PS, Amonlirdviman K, Sharp PA. 1999. PUF60: a novel U2AF65-related splicing activity. RNA 5(12): 1548-1560.

Patel DS, Garza-Garcia A, Nanji M, McElwee JJ, Ackerman D, Driscoll PC, Gems D. 2008. Clustering of genetically defined allele classes in the Caenorhabditis elegans DAF-2 insulin/IGF-1 receptor. Genetics 178(2): 931-946.

Peek R, Pruijn GJ, van der Kemp AJ, van Venrooij WJ. 1993. Subcellular distribution of Ro ribonucleoprotein complexes and their constituents. J Cell Sci 106 (Pt 3): 929-935.

Peek R, Pruijn GJ, Van Venrooij WJ. 1996. Interaction of the La (SS-B) autoantigen with small ribosomal subunits. Eur J Biochem 236(2): 649-655.

Pellizzoni L, Cardinali B, Lin-Marq N, Mercanti D, Pierandrei-Amaldi P. 1996. A Xenopus laevis homologue of the La autoantigen binds the pyrimidine tract of the 5' UTR of ribosomal protein mRNAs in vitro: implication of a protein factor in complex formation. J Mol Biol 259(5): 904-915.

Pellizzoni L, Lotti F, Maras B, Pierandrei-Amaldi P. 1997. Cellular nucleic acid binding protein binds a conserved region of the 5' UTR of Xenopus laevis ribosomal protein mRNAs. J Mol Biol 267(2): 264-275.

Pellizzoni L, Lotti F, Rutjes SA, Pierandrei-Amaldi P. 1998. Involvement of the Xenopus laevis Ro60 autoantigen in the alternative interaction of La and CNBP proteins with the 5'UTR of L4 ribosomal protein mRNA. J Mol Biol 281(4): 593-608.

Perreault J, Noel JF, Briere F, Cousineau B, Lucier JF, Perreault JP, Boire G. 2005. Retropseudogenes derived from the human Ro/SS-A autoantigen-associated hY RNAs. Nucleic Acids Res 33(6): 2032-2041.

Perreault J, Perreault JP, Boire G. 2007. Ro-associated Y RNAs in metazoans: evolution and diversification. Mol Biol Evol 24(8): 1678-1689.

Pinol-Roma S, Dreyfuss G. 1992. Shuttling of pre-mRNA binding proteins between nucleus and cytoplasm. Nature 355(6362): 730-732.

Poteryaev D, Fares H, Bowerman B, Spang A. 2007. Caenorhabditis elegans SAND-1 is essential for RAB-7 function in endosomal traffic. EMBO J 26(2): 301-312.

Praitis V, Casey E, Collar D, Austin J. 2001. Creation of low-copy integrated transgenic lines in Caenorhabditis elegans. Genetics 157(3): 1217-1226.

Pruijn GJ, Simons FH, van Venrooij WJ. 1997. Intracellular localization and nucleocytoplasmic transport of Ro RNP components. Eur J Cell Biol 74(2): 123-132.

Pruijn GJ, Slobbe RL, van Venrooij WJ. 1991. Analysis of protein--RNA interactions within Ro ribonucleoprotein complexes. Nucleic Acids Res 19(19): 5173-5180.

Rader MD, O'Brien C, Liu YS, Harley JB, Reichlin M. 1989. Heterogeneity of the Ro/SSA antigen. Different molecular forms in lymphocytes and red blood cells. J Clin Invest 83(4): 1293-1298.

Rajkowitsch L, Chen D, Stampfl S, Semrad K, Waldsich C, Mayer O, Jantsch MF, Konrat R, Blasi U, Schroeder R. 2007. RNA chaperones, RNA annealers and RNA helicases. RNA Biol 4(3): 118-130.

Ramesh A, Savva CG, Holzenburg A, Sacchettini JC. 2007. Crystal structure of Rsr, an ortholog of the antigenic Ro protein, links conformational flexibility to RNA binding activity. J Biol Chem 282(20): 14960-14967.

Reiner R, Ben-Asouli Y, Krilovetzky I, Jarrous N. 2006. A role for the catalytic ribonucleoprotein RNase P in RNA polymerase III transcription. Genes Dev 20(12): 1621-1635.

Reinisch KM, Wolin SL. 2007. Emerging themes in non-coding RNA quality control. Curr Opin Struct Biol 17(2): 209-214.

Rickards B, Flint SJ, Cole MD, LeRoy G. 2007. Nucleolin is required for RNA polymerase I transcription in vivo. Mol Cell Biol 27(3): 937-948.

Riddle D, Albert P. 1997. Genetic and Environmental Regulation of Dauer Larva Development. In C elegans II, Vol 33 (ed. D Riddle, T Blumenthal, B Meyer, J Priess), pp. 739–768. COLD SPRING HARBOR LABORATORY PRESS, Plainview, NY.

Ruby SW, Chang TH, Abelson J. 1993. Four yeast spliceosomal proteins (PRP5, PRP9, PRP11, and PRP21) interact to promote U2 snRNP binding to pre-mRNA. Genes Dev 7(10): 1909-1925.

Rutjes SA, Lund E, van der Heijden A, Grimm C, van Venrooij WJ, Pruijn GJ. 2001. Identification of a novel cis-acting RNA element involved in nuclear export of hY RNAs. RNA 7(5): 741-752.

Rutjes SA, van der Heijden A, Utz PJ, van Venrooij WJ, Pruijn GJ. 1999. Rapid nucleolytic degradation of the small cytoplasmic Y RNAs during apoptosis. J Biol Chem 274(35): 24799-24807.

Saijou E, Fujiwara T, Suzaki T, Inoue K, Sakamoto H. 2004. RBD-1, a nucleolar RNA-binding protein, is essential for Caenorhabditis elegans early development through 18S ribosomal RNA processing. Nucleic Acids Res 32(3): 1028-1036.

Sasaki T, Toh EA, Kikuchi Y. 2000. Yeast Krr1p physically and functionally interacts with a novel essential Kri1p, and both proteins are required for 40S ribosome biogenesis in the nucleolus. Mol Cell Biol 20(21): 7971-7979.

Schafer DA, Gill SR, Cooper JA, Heuser JE, Schroer TA. 1994. Ultrastructural analysis of the dynactin complex: an actin-related protein is a component of a filament that resembles F-actin. J Cell Biol 126(2): 403-412.

Shi H, O'Brien CA, Van Horn DJ, Wolin SL. 1996. A misfolded form of 5S rRNA is complexed with the Ro and La autoantigens. RNA 2(8): 769-784.

Sim S, Weinberg DE, Fuchs G, Choi K, Chung J, Wolin SL. 2009. The subcellular distribution of an RNA quality control protein, the Ro autoantigen, is regulated by noncoding Y RNA binding. Mol Biol Cell 20(5): 1555-1564.

Simons FH, Broers FJ, Van Venrooij WJ, Pruijn GJ. 1996a. Characterization of cis-acting signals for nuclear import and retention of the La (SS-B) autoantigen. Exp Cell Res 224(2): 224-236.

Simons FH, Pruijn GJ, van Venrooij WJ. 1994. Analysis of the intracellular localization and assembly of Ro ribonucleoprotein particles by microinjection into Xenopus laevis oocytes. J Cell Biol 125(5): 981-988.

Simons FH, Rutjes SA, van Venrooij WJ, Pruijn GJ. 1996b. The interactions with Ro60 and La differentially affect nuclear export of hY1 RNA. RNA 2(3): 264-273.

Slobbe RL, Pluk W, van Venrooij WJ, Pruijn GJ. 1992. Ro ribonucleoprotein assembly in vitro. Identification of RNA-protein and protein-protein interactions. J Mol Biol 227(2): 361-366.

Southern EM. 1975. Detection of specific sequences among DNA fragments separated by gel electrophoresis. J Mol Biol 98(3): 503-517.

Springer TA. 1994. Immunoprecipitation. In Current Protocols in Molecular Biology, Vol 1 (ed. FM Ausubel, R Brent, RE Kingston, DD Moore, JG Seidman, JA Smith, K Struhl). John Wiley & Sons, Inc.

Stefano JE. 1984. Purified lupus antigen La recognizes an oligouridylate stretch common to the 3' termini of RNA polymerase III transcripts. Cell 36(1): 145-154.

Stein AJ, Fuchs G, Fu C, Wolin SL, Reinisch KM. 2005. Structural insights into RNA quality control: the Ro autoantigen binds misfolded RNAs via its central cavity. Cell 121(4): 529-539.

Steitz JA, Berg C, Hendrick JP, La Branche-Chabot H, Metspalu A, Rinke J, Yario T. 1988. A 5S rRNA/L5 complex is a precursor to ribosome assembly in mammalian cells. J Cell Biol 106(3): 545-556.

Stinton LM, Fritzler MJ. 2007. A clinical approach to autoantibody testing in systemic autoimmune rheumatic disorders. Autoimmun Rev 7(1): 77-84.

Sun C, Woolford JL, Jr. 1994. The yeast NOP4 gene product is an essential nucleolar protein required for pre-rRNA processing and accumulation of 60S ribosomal subunits. EMBO J 13(13): 3127-3135.

-. 1997. The yeast nucleolar protein Nop4p contains four RNA recognition motifs necessary for ribosome biogenesis. J Biol Chem 272(40): 25345-25352.

Svitkin YV, Pause A, Sonenberg N. 1994. La autoantigen alleviates translational repression by the 5' leader sequence of the human immunodeficiency virus type 1 mRNA. J Virol 68(11): 7001-7007.

Tarr DE, Scott AL. 2004. MSP domain proteins show enhanced expression in male germ line cells. Mol Biochem Parasitol 137(1): 87-98.

Teunissen SW, Kruithof MJ, Farris AD, Harley JB, Venrooij WJ, Pruijn GJ. 2000. Conserved features of Y RNAs: a comparison of experimentally derived secondary structures. Nucleic Acids Res 28(2): 610-619.

Tharun S, He W, Mayes AE, Lennertz P, Beggs JD, Parker R. 2000. Yeast Sm-like proteins function in mRNA decapping and decay. Nature 404(6777): 515-518.

Tillmar L, Welsh N. 2002. Hypoxia may increase rat insulin mRNA levels by promoting binding of the polypyrimidine tract-binding protein (PTB) to the pyrimidine-rich insulin mRNA 3'-untranslated region. Mol Med 8(5): 263-272.

Timmons L, Fire A. 1998. Specific interference by ingested dsRNA. Nature 395(6705): 854.

Ton C, Hwang DM, Dempsey AA, Liew CC. 1997. Identification and primary structure of five human NADH-ubiquinone oxidoreductase subunits. Biochem Biophys Res Commun 241(2): 589-594.

Tsang WY, Lemire BD. 2003. The role of mitochondria in the life of the nematode, Caenorhabditis elegans. Biochim Biophys Acta 1638(2): 91-105.

Van Horn DJ, Eisenberg D, O'Brien CA, Wolin SL. 1995. Caenorhabditis elegans embryos contain only one major species of Ro RNP. RNA 1(3): 293-303.

Vidal VP, Verdone L, Mayes AE, Beggs JD. 1999. Characterization of U6 snRNA-protein interactions. RNA 5(11): 1470-1481.

Vijayraghavan U, Company M, Abelson J. 1989. Isolation and characterization of pre-mRNA splicing mutants of Saccharomyces cerevisiae. Genes Dev 3(8): 1206-1216.

von Muhlen CA, Tan EM. 1995. Autoantibodies in the diagnosis of systemic rheumatic diseases. Semin Arthritis Rheum 24(5): 323-358.

Von Stetina SE, Watson JD, Fox RM, Olszewski KL, Spencer WC, Roy PJ, Miller DM, 3rd. 2007. Cell-specific microarray profiling experiments reveal a comprehensive picture of gene expression in the C. elegans nervous system. Genome Biol 8(7): R135.

Waddle JA, Cooper JA, Waterston RH. 1993. The alpha and beta subunits of nematode actin capping protein function in yeast. Mol Biol Cell 4(9): 907-917.

Wang D, Buyon JP, Zhu W, Chan EK. 1999. Defining a novel 75-kDa phosphoprotein associated with SS-A/Ro and identification of distinct human autoantibodies. J Clin Invest 104(9): 1265-1275.

Welsh GI, Leney SE, Lloyd-Lewis B, Wherlock M, Lindsay AJ, McCaffrey MW, Tavare JM. 2007. Rip11 is a Rab11- and AS160-RabGAP-binding protein required for insulin-stimulated glucose uptake in adipocytes. J Cell Sci 120(Pt 23): 4197-4208.

Williams BD, Schrank B, Huynh C, Shownkeen R, Waterston RH. 1992. A genetic mapping system in Caenorhabditis elegans based on polymorphic sequence-tagged sites. Genetics 131(3): 609-624.

Wilm T, Demel P, Koop HU, Schnabel H, Schnabel R. 1999. Ballistic transformation of Caenorhabditis elegans. Gene 229(1-2): 31-35.

Wolin SL, Cedervall T. 2002. The La protein. Annu Rev Biochem 71: 375-403.

Wolin SL, Steitz JA. 1983. Genes for two small cytoplasmic Ro RNAs are adjacent and appear to be single-copy in the human genome. Cell 32(3): 735-744.

-. 1984. The Ro small cytoplasmic ribonucleoproteins: identification of the antigenic protein and its binding site on the Ro RNAs. Proc Natl Acad Sci U S A 81(7): 1996-2000.

Wolin SL, Wurtmann EJ. 2006. Molecular chaperones and quality control in noncoding RNA biogenesis. Cold Spring Harb Symp Quant Biol 71: 505-511.

Wurtmann EJ, Wolin SL. 2009. RNA under attack: cellular handling of RNA damage. Crit Rev Biochem Mol Biol 44(1): 34-49.

Xia PZ, Fritz KA, Geoghegan WD, Jordon RE. 1987. The particulate (speckled-like thread) nuclear staining pattern: species and cellular distribution of Ro/SSA antigen. J Clin Lab Immunol 22(3): 101-105.

Xue D, Shi H, Smith JD, Chen X, Noe DA, Cedervall T, Yang DD, Eynon E, Brash DE, Kashgarian M et al. 2003. A lupus-like syndrome develops in mice lacking the Ro 60-kDa protein, a major lupus autoantigen. Proc Natl Acad Sci U S A 100(13): 7503-7508.

Electronic sources:

WormAtlas Altun, Z. F. and Hall, D. H. (ed.s). 2002-2006. http://www.wormatlas.org

WormBase web site, http://www.wormbase.org, release WS201, April 2009

Wormbook web site, http://www.wormbook.org

The following figures were taken from or are based on external publications:
Figure 1: Structure of the *Xenopus laevis* Ro60 protein (Reinisch and Wolin 2007)
Figure 2: structure Prediction of the Y RNAs (Van Horn et al. 1995)
Figure 3: The *C. elegans* Life cycle (http://www.wormatlas.org)
Figure 4: A) The *C. elegans Dauer* pathway (Von Stetina et al. 2007)
Figure 4: B) Structure model of *DAF-2* (Patel et al. 2008)
Figure 6: Genetic locus (WormBase web site, http://www.wormbase.org)
Figure 17: *S. cerevisiae* rRNA processing (Fromont-Racine et al. 2003)
Figure 20: *C. elegans* rRNA processing (Saijou et al. 2004)

6 Acknowledgements

Danksagung

Für die Unterstützung von meinen Betreuern Dr. Günter Steiner und Dr. Michael Jantsch sowie von Dr. Verena Jantsch möchte ich mich an dieser Stelle bedanken. Durch sie wurde dieses Projekt und somit meine Dissertation erst ermöglicht.

Ich bedanke mich darüber hinaus bei meinen Eltern für die Ermöglichung meines Studiums. Erst durch ihre finanzielle Hilfe war es mir möglich ein Studium zu beginnen.

Darüber hinaus bedanke ich mich beim FWF, MFPL, der Universität Wien und der Medizinischen Universität Wien sowie dem AMS für die abwechslungsreiche finanzielle Unterstützung meiner Dissertation.

Vielen Dank besonders auch an Dr. Alexandra Penkner für etwa 300g extra-puren 3,7-Dihydro-1,3,7-trimethyl-1H-purine-2,6-diones, welches in den letzten Jahren gemeinsam konsumiert wurde, sowie für Tipps und Tricks bei vielen Experimenten.

I am also especially grateful to Dr. Lois Tang who never was at loss for yet another juicy story, and thus definitely made lab routine more bearable…

Bei all meinen „Biologenfreunden" und weiteren Kollegen aus dem Frog lab und dem Worm lab sowie dem Department für Chromosomenbiologie möchte ich mich bedanken. Es war (fast immer) eine lustige Zeit.

Zuletzt möchte ich mich bei meiner Freundin Silke Frank bedanken. Sie stand mir während der ganzen Zeit zur Seite und hat mich jederzeit unterstützt. Und über die reine Anwesenheit durch meinen Sohn Nikolas bin ich sehr dankbar. Er hatte in den letzten acht Monaten immer ein wohltuendes Lächeln für mich bereit und hat mir in den Endzügen, wenn auch für ihn unbewusst, sehr geholfen.

7 Abstract

Members of the family of non-coding Y RNAs, which are highly conserved in their structure, have been found in all animal cells. Y RNAs are present in up to four different variants in vertebrate cells and they are always bound by a homologue of the Ro60 autoantigen, forming cytoplasmic Ro ribonucleoprotein complexes (Ro RNPs). In the nematode *Caenorhabditis elegans* only one unique Y RNA species, encoded by the gene *yrn-1,* is present and binding the Ro60 orthologue ROP-1. In order to gain insight into the functions of Y RNAs, we generated a knockout of *yrn-1* and find that worms deficient for this gene do not show a reproductive or developmental phenotype under laboratory conditions. However, these worms exhibit a higher resistance to UVC irradiation and we could observe an effect on the formation of stress-resistant *dauer* larvae in the absence of Y RNA. We carried out a conditional RNAi screen for synthetically enhanced lethality or reduced fertility in the *yrn-1* mutant background. A large fraction of candidates derived from this screen are involved in ribosome biogenesis. Analysis of rRNA processing and ribosomal protein composition, indicate a role for the *C. elegans* Y RNA in ribosome assembly - especially in a late cleavage step of small subunit rRNA processing. Taken together, although Y RNAs do not seem to be essential for development and reproduction, the data obtained, suggest that Y RNAs are involved in several important cellular pathways, including stress response and ribosome synthesis.

8 Zusammenfassung

Mitglieder der Gruppe der nicht-proteincodierende Y RNS Moleküle sind hochkonserviert in ihrer Sekundärstruktur und wurden in allen untersuchten tierischen Zellen gefunden. Y RNS Moleküle sind in bis zu vier verschiedenen Varianten in Wirbeltierzellen vorhanden und sind immer an ein dem Ro60 Autoantigen homologes Protein gebunden. Die beiden bilden dabei einen zytoplasmatischen Komplex aus, welcher Ro Ribonukleoprotein (Ro RNP) genannt wird. Im Fadenwurm *Caenorhabditis elegans* wurde nur eine einzelne Sorte von Y RNS Molekülen gefunden, welche das Produkt eines einzelnen Genes (*yrn-1)* ist. *C. elegans* Y RNS Moleküle binden das dem Ro60 homologe Protein ROP-1. Um mehr über die Funktionen der Y RNS zu erfahren, haben wir einen knockout des *yrn-1* Gens konstruiert und konnten beobachten, dass Würmer, welche keine Y RNS exprimieren, unter Laborbedingungen keinen auffälligen Phänotyp bezüglich ihrer Vermehrung oder Entwicklung zeigen. Jedoch sind diese Würmer resistenter gegenüber Ultravioletter Strahlung im hochenergetischen Bereich. Zusätzlich konnten wir einen Effekt auf die Bildung von stress-resistenten *Dauer*-Larven bei diesen Würmern beobachten. Wir führten an *yrn-1* Mutanten eine genetische Auslese mit inhibitorischer RNS durch und suchten nach Genen, welche konditionell in diesem Mutationshintergrund erhöhte Sterblichkeit oder verringerte Fruchtbarkeit auslösen. Ein Großteil der Kandidaten, die wir dabei fanden, spielt bei der Synthese von Ribosomen eine Rolle. Daher analysierten wir die Prozessierung der ribosomalen RNS und die Proteinzusammensetzung der Ribosomen. Wir beobachteten, dass die Y RNS bei der Herstellung von Ribosomen eine Rolle spielt und zwar im Speziellen bei einem späten Prozessierungsschritt der ribosomalen RNS der kleinen ribosomalen Untereinheit. Zusammenfassend scheint die Y RNS nicht für Entwicklung oder Reproduktion notwendig zu sein. Unsere Daten zeigen aber, dass sie in verschiedenen zellulären Abläufen, wie der Stressbewältigung oder der Synthese von Ribosomen eine Rolle spielt.

9 Curriculum Vitae

Full name: **Michael Matthias Müller**.

Date of Birth: 4th March 1978.

Nationality: Austrian.

Education

since 08/2004   PhD student in Genetics at the Department of Chromosome Biology, Max F. Perutz Laboratories, Vienna, Austria.

05/ 2003   Master Degree in Science with Honours in Genetics from the University of Vienna (2003).

2002 – 2003   Diploma thesis at the Institute of Botany, University of Vienna. Title: The role of sumoylation in *C. elegans* meiosis.

2000 – 2001   Courses in Molecular and Cellular Biology at the Institute of Biomedical and Life Sciences, University of Glasgow, UK. via the ERASMUS exchange programme.

2000 – 2003   Honours course in Genetics at the Institute of Microbiology and Genetics, University of Vienna.

1997 – 2000   Undergraduate course in Biology at the Faculty of Science, University of Vienna.

06/ 1996   Matura at Bundesgymnasium Vöcklabruck, Austria.

Scientific Publications

Jantsch V, Pasierbek P, Mueller MM, Schweizer D, Jantsch M, Loidl J. Targeted gene knockout reveals a role in meiotic recombination for ZHP-3, a Zip3-related protein in *Caenorhabditis elegans.* Molecular and Cellular Biology 2004 Sep; 24(18):7998-8006.

Scientific Presentations

Poster presentation at the European Worm Meeting 2006, Hersonissos, Greece.

Poster presentation at the 11th annual meeting of the RNA Society, 2006, Seattle, USA.

Poster presentation at the 13th annual meeting of the RNA Society, 2008, Berlin, Germany.